Brain and gaze based wheelchair navigation enhancement

Hachem Amine Lamti

University of Toulon University of Sfax

Doctoral Thesis

Brain and gaze based wheelchair navigation enhancement

Author: Hachem Amine LAMTI

A thesis submitted in fulfilment of the requirements
for the degree of Doctor of Philosophy

in Automatic, signal, productics and robotics discipline

Laboratoire de la biomodelisation et ingénierie du handicap
Research Group on Intelligent Machines
University of Toulon
University of Sfax

In presence of the jury:

Pr. Adel M. ALIMI	Thesis director (University of Sfax)
Dr. Mohamed M. BEN KHELIFA	Thesis co-supervisor (University of Toulon)
Pr. François CABESTAING	Thesis reviewer (University of Lille)
Pr. Farhat FNAIECH	Thesis reviewer (University of Tunis)
Pr. Philippe GORCE	Thesis director (University of Toulon)
Dr. Nadine VIGOUROUX	Research director, IRIT/CNRS

09 December 2013

Declaration of Authorship

I, Hachem Amine LAMTI, declare that this thesis titled, 'Brain and gaze based wheelchair navigation enhancement' and the work presented in it are my own. I confirm that:

- This work was done wholly or mainly while in candidature for a research degree at this University.
- Where any part of this thesis has previously been submitted for a degree or any other qualification at this University or any other institution, this has been clearly stated.
- Where I have consulted the published work of others, this is always clearly attributed.
- Where I have quoted from the work of others, the source is always given. With the exception of such quotations, this thesis is entirely my own work.
- I have acknowledged all main sources of help.
- Where the thesis is based on work done by myself jointly with others, I have made clear exactly what was done by others and what I have contributed myself.

Signed: _____

Date: _____

"I do not know what I may appear to the world, but to myself I seem to have been only like a boy playing on the seashore, and diverting myself in now and then finding a smoother pebble or a prettier shell than ordinary, whilst the great ocean of truth lay all undiscovered before me."

Isaac NEWTON

UNIVERSITY OF TOULON and UNIVERSITY OF SFAX

Abstract

University of Toulon
University of Sfax

Doctor of Philosophy

Brain and gaze based wheelchair navigation enhancement

by Hachem Amine LAMTI

The Brain Eyes WHEELchair Interface (BEWHEELI) project aims at proposing a new alternative for severely disabled people (example palsy and Locked-In patients) to command their wheelchairs. It's built on two major blocks: the command block which ensures the migration from the use of joystick to the gaze/brain automated command (including the intermediate phase of gaze/joystick command). The security block deals with the wheelchair control by assessing human factors mainly emotions and mental fatigue through its impact on brainwave patterns. In the former, four emotions were induced and implemented (relaxation, nervousness, excitement and stress) in three navigation scenarios where the introduction of the detection block was assessed. The next step consists on evaluating the impact the mental fatigue can have on two sources of control : Positive 300 (P300) and Steady State Visual Evocked Potentials (SSVEP). Those are treated individually and combined be the mean of evidential theory reasoning to build up a fatigue detection block. At the end a fuzzy logic based decision system was introduced to combine emotional and fatigue blocks that triggers to three navigation modes : manual, semi-autonomous and autonomous that reflect physical abilities of the users to command their wheelchairs.

Acknowledgements

I would like to express my special appreciation and thanks to my supervisors professor Philippe GORCE, professor Adel M. ALIMI and doctor Mohamed Moncef BEN KHELIFA you have been a tremendous mentor for me. I would like to thank you for encouraging my research and for allowing me to grow as a research scientist. Your advice on both research as well as on my career have been priceless and this project is subscribed under those eight years of collaboration between Handibio and Regim since 2004. I would also like to thank my committee members, professor François CABESTAING, professor Farhat FNAIECH, doctor Nadine VIGOUROUX for serving as my committee members even at hardship. I also want to thank you for letting my defense be an enjoyable moment, and for your brilliant comments and suggestions, thanks to you.

A special thanks to my family. Words cannot express how grateful I am to my mother Dalila, and father Rached for all of the sacrifices that you've made on my behalf. Your prayer for me was what sustained me thus far. I would also like to thank all of my friends who supported me in writing, and incented me to strive towards my goal. At the end I would like express appreciation to my beloved wife Emna MASMOUDI who spent sleepless nights with and was always my support in the moments when there was no one to answer my queries.

Contents

List of Figures

List of Tables

Introduction

Nowadays, in the field of technical assistance, every proposed system should be designed in order to ensure the required user's needs. Tests in real world provide us with pertinent indications regarding the adaptation of the user to a new assistance technique. However, those are not really cost effective and present the drawback of being user specific. In other words, it should be ensured that users can accept and appropriate that technique without causing secondary effects such as tiredness, fatigue and lack of concentration... For disabled or elderly persons with heavily reduced physical and/or mental abilities steering powered wheelchairs by means of a conventional joystick is hardly possible. For these people, special control devices (e.g. button pads or sip-puff devices) have been developed. Due to the reduced command set such input devices provide, their use is time-consuming and tiring, leading to significantly reduced acceptance among the user group. Many approaches to increase wheelchairs' usability by introducing assistive and autonomous functionalities exist [1] [2]. Though, most of these are not suited for severely disabled people due to the reduced information provided via special input devices. Furthermore, many approaches require knowledge about the environment to be able to provide support. To enable convenient and dependable support, an approach is needed, that retrieves additional information about the wheelchair driver, without raising the workload imposed on the user [3]. The development and evaluation of multimodal human-computer interfaces (HCIs) has been on the agenda of many researchers for some time. The idea of implementing "natural" ways of communicating with machines is certainly promising, even more so when combining various communication modalities in a way that humans normally do when interacting with each other [4]. However, usability studies and evaluations of HCIs with able-bodied users have shown that this group is rather proficient and, in fact, efficient, in using established standard HCIs such as computer keyboards. Performance, e.g. text typing speed, and user satisfaction are usually much higher for standard devices than for alternative HCIs, such as gaze-operated virtual keyboards - even after training. For handicapped user groups, however, the situation is different. Handicapped people rely on alternative methods to interact or communicate with their environment and, specifically, with technical devices. For

example, those with immobility in their upper or lower limbs are potential users of gaze interfaces. Another group, locked-in patients, can only communicate with their environment via a brain and/or gaze. With many different such special groups that all require their own interaction interfaces or a combination thereof, specifically adapted to their special needs and individual capabilities, these users are amongst the main target groups for the development of novel multi-modal human-computer interfaces. Most novel HCI methods were only developed recently and, to date, little effort has been made to combine these methods in multi-modal interfaces for special-needs groups. Our contribution is to put in place a Brain-Eyes based interface that could help severely disabled controlling a wheelchair and assist him. The idea is to integrate some other parameters based on human factors that can enhance navigation performances; emotions and mental fatigue. those were merely suggested by doctors ans specialists as they are the origin of many navigation accidents. Consequently, parameters emotions and mental fatigue are investigated more. For the former, many studies show that emotion can have an impact on navigation. Take for example car driving, many accidents occur due to wrong decision made by the driver that originates from the fact that he was nervous, stressed or very excited... the same case could be applied for wheelchair navigation where the most important factor is the user's safety. In this context, emotion induction will be used in order to investigate the user reaction during navigation and the influence of such an approach in enhancing navigation. Another parameter that can influence very much navigation is mental levels of fatigue. This latter can influence concentration and can be the cause of too much problems. Exhaustion, tiredness... and other situations of fatigue should be accounted for, in order to enhance navigation. This also will be treated as an influence study will be taken to investigate the impact of mental fatigue on Positive300 (P300) and Steady State Visual Evoked Potential (SSVEP). This project is divided into three chapters described as follows: In the first chapter, projects that target wheelchair navigation enhancement based on shared paradigms are presented and detailed. from those, we conclude the importance of the integration of emotions and mental fatigue as to propose an anticipative architecture for wheelchair navigation. As the problem is to assign and measure them, their influence on ElectroEncephaloGraphy (EEG) technology is investigated. It's undeniable that integration of human factors is main goal of this project, but a long term objective can be set; the latter is to combine between gaze and brain as input modalities. In fact, an overview on available projects show that the use of brain or gaze individually was on the agenda but not the combination between both. In Appendix A, a comparison between a gaze based-interface and a combined one were compared in order to proof that the concept can be original. In the second chapter, emotion will be introduced as a factor of wheelchair navigation enhancement. For this purpose many steps were to follow: starting by the setup of emotion induction protocol in order to induce four emotions: relaxation, excitement,

nerve and sadness, those will be introduced as velocity moderator; if the system can detect one of these emotions, it will try to decrease velocity of the wheelchair. To be noticed, a simulation environment will be used and the virtual navigation will be ensured through the wheelchair itself. In the third chapter, mental fatigue will be studied too. For this purpose, two brain sources of control will be used which are P300 and SSVEP. The idea is to study each modality separately, determine the most correlated parameters with fatigue ratings, classify them using classification algorithms and fuse between both modalities before a second classification. The results will be compared. The final session, will be devoted to a general conclusion, in which the shortages of the project will be exposed yielding to some outcomes that could be treated in future works.

Chapter 1

BEWHEELI project : Why, where and when

1.1 Introduction

Disabled or elderly persons with heavily reduced physical and/or mental abilities find it hardly possible to control a powered wheelchair using conventional joystick. For these persons, shared paradigms were introduced to enhance navigation security; it consists of giving the user more or less control on a need basis [5]. Many studies incorporated this paradigm in order to conceive a suitable wheelchair according to the subject pathology. In this section some related works will be explained as those of Vander poorten et al. [6], Peinado et al. [7] and Ren et al. [8]. These projects centered the navigation enhancement on modifying the wheelchair system either by adding new on board sensors such as GPS, cameras... either by assessing user's performance by the mean of motor activities such as haptic feedbacks which is still centered on the wheelchair system and holds a delayed aspect; the wheelchair corrective behavior is generated after that the user commits an error during navigation. In the present project, the proposed shared control is rather centered on human factors and holds an anticipatory aspect; through human factor, the wheelchair anticipates the next action to do. To the best of our knowledge, the proposal of anticipatory human factors-based wheelchair navigation is not so many. In fact, during the exchange with experts, doctors, occupational therapist and psychologists, many human factors could influence wheelchair navigation such as mental fatigue and emotions.

From clinical perspective [9], severely disabled people are exposed to several forms of negative emotions that can influence their navigation performance. The most common forms are the followings: stress, excitement and nervousness which will be exposed later.

another parameter that could be very influent on navigation performance is mental fatigue: As far as it has some influence on cerebral activities, the latter shows specific perturbation on its ElectroEncephalographie (EEG) patterns, which can influence its role as a source of control. We investigate in this project two common sources of control namely: P300 and SSVEP.

This section is divided into three major parts. In the first one, an overview about shared paradigms based projects is exposed. In the second part, emotion, fatigue and its correlations with Electroencephalographie (EEG) patterns will be explained. While the main goal of this project is to integrate emotions and fatigue to control wheelchair actions, a long term goal can be set. The latter is to fully command a wheelchair by the mean of combination between gaze and brain. The idea seems to be quite interesting as many projects focused only on the use of either gaze or brain separately but not by combining them. The proposed command/control architecture will be explained as well as the different materials used to setup a simulation environment needed to assess subjects performances.

1.2 Related works

The concept of shared paradigm consists on sharing the control between the wheelchair and its driver. Naturally, this approach requires personalization: each wheelchair user has different skills and needs and it is hard to know a priori from diagnosis how much assistance must be provided. Consequently, several approaches are proposed to ensure the navigation safety.

1.2.1 Haptic Obstacle Avoidance for Intuitive Powered Wheelchair Navigation

Vander poorten et al. [6] describes how through haptic feedback a fast 'bilateral' communication channel is established between wheelchair controller and user and how this can lead to more intuitive and safer wheelchair navigation; By setting up a fast, bilateral communication channel between the user and the wheelchair controller, control can be shared deeper and problems such as mode confusion can be avoided [10]. The user can directly negotiate with the wheelchair controller over the haptic channel and is given the final word, as he/she can overrule unwanted wheelchair actions. A novel haptic collision avoidance scheme is proposed to demonstrate the potential of this new technology which is based on the rendering of a local map from onboard sensors. Within this environment, a set of circular collision-free paths is calculated with circular paths corresponding to a

certain combination of wheelchair linear and rotational velocities (v, w). A path is then drawn starting from the wheelchair's local coordinate system and runs until it reaches obstacles (see Figure 1.1).

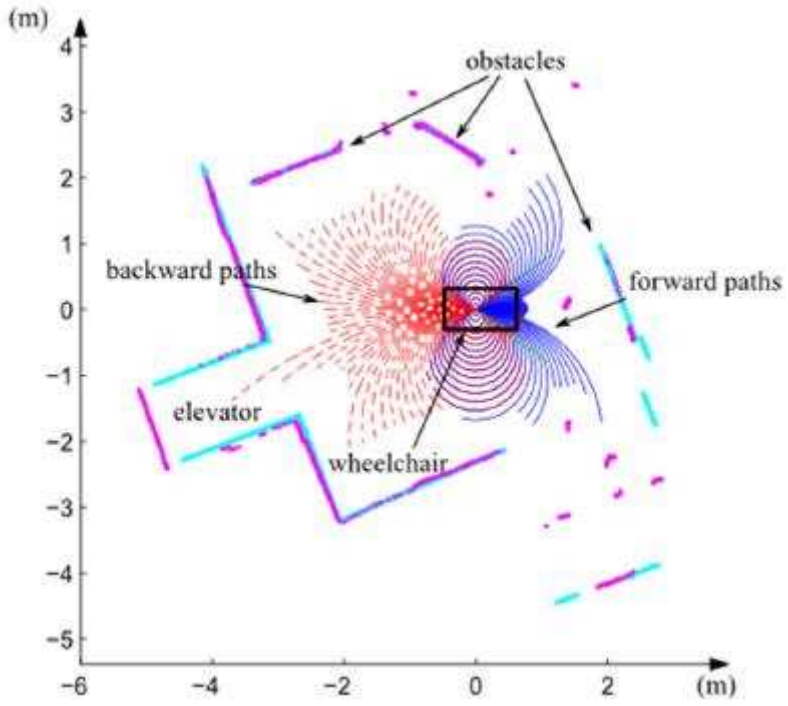

FIGURE 1.1: Environment and obstacles encoding [6]

Based on the previous operation, a haptic collision and obstacle avoidance algorithm was set up. for the former, When approaching an obstacle along a certain circular path, the repulsive force will push the joystick and tries to move it towards the origin along a straight line with constant angle. As a result the wheelchair will be slowed down along the same circular path. If tuned well the wheelchair should come to a rest in front of the obstacle. Haptic obstacle avoidance actively redirects the wheelchair towards circular paths with longer collision-free lengths. In addition to a radial force component that slows the wheelchair down nearing objects, the scheme foresees a tangential force component that bends wheelchair motion towards longer collision-free paths. To validate their approach, some first experiments were conducted with the haptic obstacle avoidance scheme. With cardboard boxes an artificial environment was built that represented an elevator. The user was asked to manoeuvre the wheelchair backwards inside this elevator beginning from a fixed start position solely using the haptic guidance and without looking backwards. While performing such a manoeuver without looking backwards was close to impossible if no haptic guidance was present, thanks to the haptic guidance the user managed to successfully drive into the elevator in 6 of the 10 times. Although some more experiments need to be done, those results are quite encouraging.

1.2.2 GPS and fuzzy logic map matching for wheelchair navigation

Ming Ren et al. [8], suggest that an essential process in wheelchair navigation is matching the position obtained from GPS or other sensors on a sidewalk network. This process of map matching in turn assists in making decisions under uncertainty. However, GPS-based wheelchair navigation systems have difficulties in tracking wheelchairs in urban areas due to poor satellite availability. To overcome this, a fuzzy logic-based algorithm is applied to effectively perform matching wheelchair movements on sidewalks. Fuzzy logic, based on fuzzy reasoning concepts, in many circumstances can take noisy and imprecise input to yield numerically accurate output. To validate its reliability, experiments were carried on. Map-matching GPS points on a map is twofold: (1) identification of the correct segment and (2) determination of the vehicle location on the selected segment. In this algorithm, a three-stage process was used for finding the correct segment. The process has the following steps: (1) the initial map-matching process, (2) the subsequent map-matching process along a segment, and (3) the renewed map matching across an intersection. The flowchart of the fuzzy logic maps-matching process can be found in the figure (1.2)

In order to validate the fuzzy logic map-matching algorithm, the process of fuzzy logic map matching is implemented and tested on a sidewalk network. To test performances of the map matching in terms of accuracy and consuming time, further analysis is done by matching GPS points on three routes. The map-matching performances on three chosen routes are presented in Table 1.1. Testing results show that both positioning systems and the density of the sidewalk network affect the accuracy of this map-matching algorithm.

TABLE 1.1: Performances of experiments

Example	GPS points	mismatched points	Correct identification (%)	Computation time (s)
Route 1	682	85	87.5	5.485
Route 2	1.516	87	94.3	12.93
Route 3	933	53	94.3	7.828

The accuracy in the experiments is mainly influenced by failure in differentiating two sides of a road by only using stand-alone GPS data, so the experimental performance was not as good as those reported by other studies [11], Most mismatched points occur on sidewalks of narrow roads due to GPS accuracy limitation. Moreover, wheelchairs are hardly equipped with more than one sensor, which makes it impossible to create additional fuzzy logic rules to help matching. With regard to the time performance, this fuzzy logic map-matching algorithm performs reasonably well to meet the demand of real-time navigation, based on the average computation time.

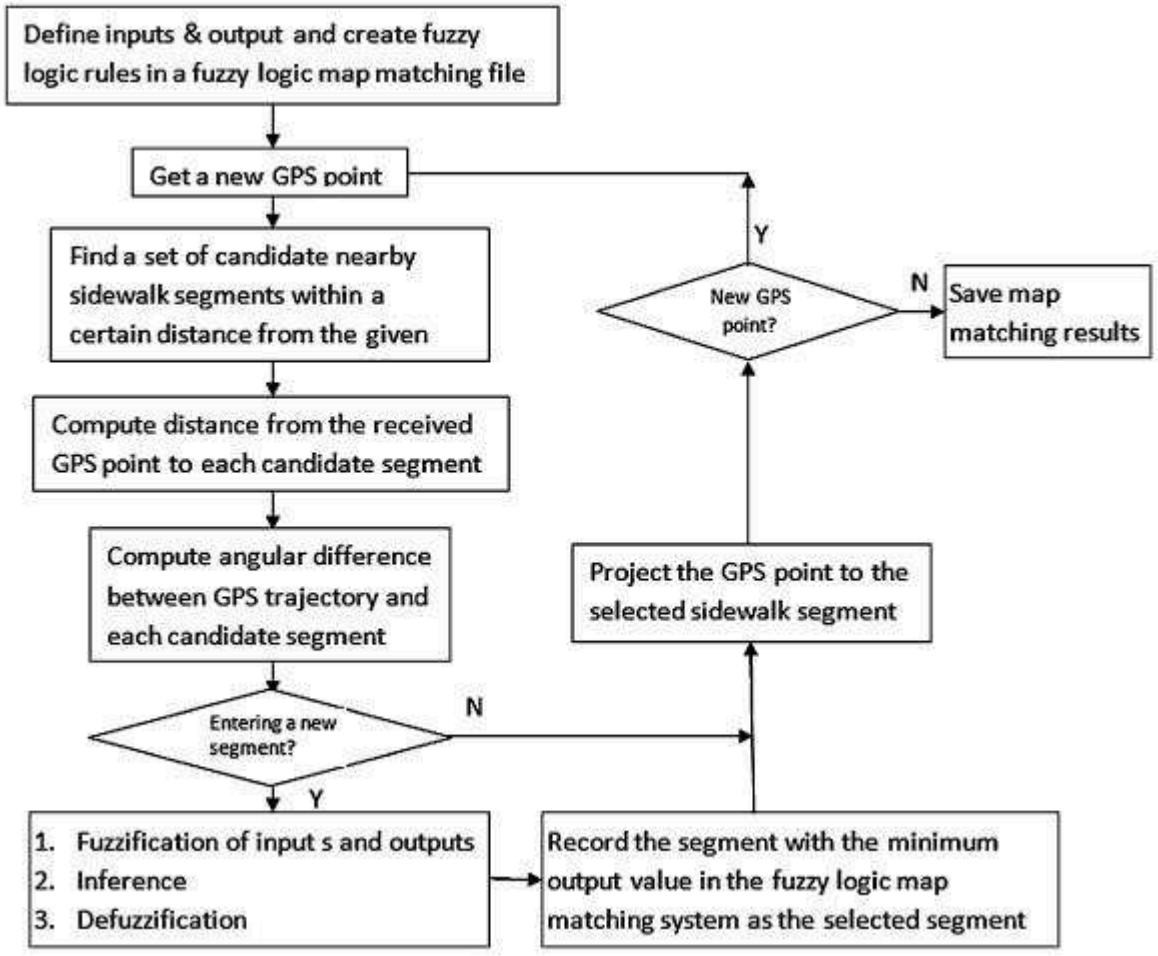

FIGURE 1.2: Flowchart of the fuzzy logic maps-matching process [8]

1.2.3 Navigation skills based profiling for collaborative wheelchair control

Peinado et al. [7] present a new approach to proactive collaborative wheelchair control. The system is based on estimating how much help the person needs at each situation and providing just the correct amount. This is achieved by combining robot and human control commands in a reactive fashion after weighting them by their respective local efficiency. Consequently, the better the person drives, the more control he/she is awarded with. In order to predict how much help users may need in advance rather than waiting for them to decrease in efficiency, their skills to deal with each situation are estimated with respect to a baseline driver profile to increase assistance when needed. Situations are characterized at reactive level to keep a reduced set. At reactive level, any situation has to be characterized only within the range of the agent's sensors. For navigation,complex scenario can be reduced to a set of relatively simple situations that is complete, i.e. fully describes all possible obstacle configurations, and robot and goal

locations; and is exclusive. Using a binary decision tree they obtain the regions highlighted in (Figure 1.3): High Safety or Low Safety Goal in Region (HSGR and LSGR) if the goal is in line of view, High Safety Wide or Narrow Region (HSWR and HSNR), if obstacles around are not too close and Low Safety 1 side and 2 sides (LS1 and LS2), if obstacles are close on one or both sides of the mobile. These situations are represented in Figure (Figure 1.3), where the area considered as Low Safety area around the robot is printed in yellow, the area free of obstacles of the robot is printed in green, obstacles are printed in black and the goal to reach in red.

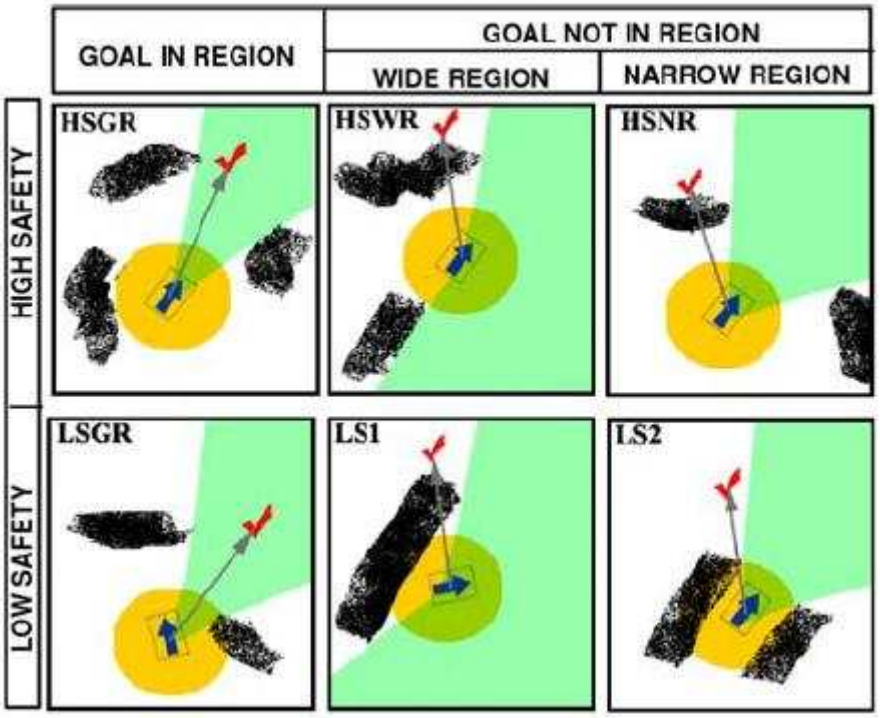

FIGURE 1.3: Generic prototypes for all possible navigation situations [7]

Assuming that any location of the environment belongs to one of these classes, a user can be profiled by estimating how well he/she solves each of these situations. If someone is able to solve all 6 situations with a reasonable efficiency, it will validate the efficiency to deal with any complex environment and does not require much help. As the word 'reasonable' still not defined yet, a series of experiments took place by gathering driving data from around 80 people, including more than 70 persons with physical and/or cognitive disabilities, and classified the situations they faced while driving into the commented 6 classes. In order to check the proposed model, subjects were told to navigate using their wheelchairs in a standard compliant home for people with disabilities. Results show that collaborative control fills in for skills that users may not have and increases the efficiency of residual ones. They also prove that prediction based modulation improves

performance in remaining skills. Future work will focus on correlating low level profile data with high level reasoning techniques via a hybrid control architecture.

1.2.4 Discussion

As it may be concluded, the way we can enhance wheelchair navigation are different and can target many levels : either low level (by adding new sensors such as infrared, GPS ...) or even high level (by proposing intelligent algorithms based on navigation skills) which is undeniably very efficient. However, these approaches need to be more tuned as the wheelchair proceeds to its corrective behavior after assessing the subject's performance during navigation. This particular point can be, in some cases, dangerous as our main objective is ensure a better security for wheelchair drivers. In fact during navigation, as the type of error committed cannot be predicted, this latter could lead to fatal accidents. It's explaind by the fact that these systems lack an anticipative behavior that could modify the wheelchair parameters : example decreasing velocity in order to prevent a misbehavior could occur. During our talks with doctors, experts, occupational therapist and psychologists, they stated that many human factors have a direct effect on the navigation performance. Among them, mental fatigue and emotions are the most influent. However, these two parameters are not easy to cope with, as they need much more investigations. In the next section, we will focus on their relationship with ElectroEncephaloGraphy (EEG) patterns.

1.3 Emotion, mental fatigue and EEG technology

The use of human factors such as emotions and mental fatigue to enhance wheelchair navigation can be very interesting if these parameters are well studied. the way to measure and quantify them remains a real challenge. On the other hand, EEG technology was widely used in many fields that ranges from video games to wheelchair navigation commands. It's also known that many projects reported the correlation between emotions and fatigue and EEG patterns. In the following, we will deal with those components as to understand the relationship between them.

1.3.1 EEG technology and Brain-Computer interfaces

The advances of recent years in the field of human-machine interfaces based on the use of brain activity (called: BCI for Brain Computer Interface) have opened up new opportunities. From the EEG (electroencephalograph) technology, we get to quantify

certain mental states (consciousness, unconsciousness, concentration, relaxation ...) in the preamble as specific EEG patterns detected following a distribution of a number of electrodes following 10-20 defined by the standard system [12]. The 10-20 system or International 10-20 system is an internationally recognized method to describe and apply the location of scalp electrodes in the context of an EEG test or experiment. This method was developed to ensure standardized reproducibility so that subject studies can be compared over time and subjects could be compared to each other. This system is based on the relationship between the location of the electrode and the underlying area of the cerebral cortex. The "10" and "20" refer to the fact that the actual distance between adjacent electrodes is 10% or 20% of the front-back or left-right distance from the skull. Each site has a letter to identify the lobe and a number to identify the hemisphere location. The letters F, T, C, P and O stand for frontal, temporal, central, parietal and occipital, respectively. Note that there is no central lobe, the letter "C" is only used for identification purposes only. A "Z" (zero) refers to an electrode positioned on the center line. Even numbers (2, 4, 6 and 8) refer to electrode positions on the right hemisphere, while the odd numbers (1, 3, 5 and 7) refer to those of the left hemisphere. Two anatomical landmarks are used for positioning the essential EEG electrodes: first, the nasion is the point between the forehead and nose, secondly, the inion which is the lowest point of the skull at the back of the head and is normally indicated by a prominent bump.

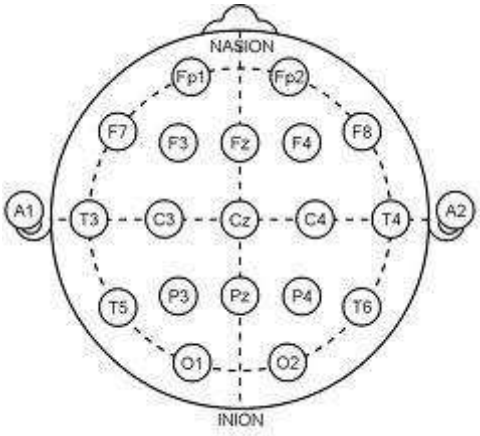

FIGURE 1.4: Sensors distribution according to the 10-20 system

BCI makes persons communicate with external world only by thinking without relying on muscular or nervous activity [13]. (Figure 1.5) illustrates the functionality of a BCI starting by monitoring the user's brain activity which is conveyed into brain signals processed to obtain features grouped into vector called "feature vector". The mapping of the latter, results into commands to be executed by the system, and can be used in two different ways, namely:

• Active BCI allows the user to perform "direct" orders obtained from the relative detection of "mental states" to motor movements (e.g. imagine a movement of the right hand without realizing it physically); it may well translate into commands to control the properties of the system.

• Passive BCI : it is based on recognizing specific mental states of the user as wakefulness, relaxation, nervousness[14] ... to provide support systems to improve the safety of users (e.g. switch to autopilot if a state of stress of the user is detected ...).

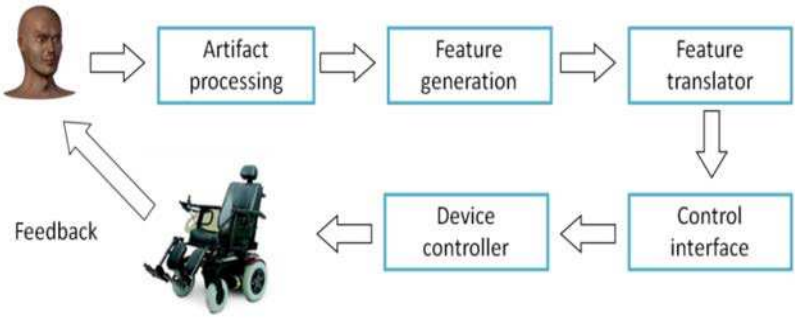

FIGURE 1.5: Functional model of BCI

In EEG, user's mental activities appear as distinctive patterns. Recognized by BCI, those are mapped into commands which are associated with certain actions. The current field of applications of EEG-based BCI systems is very wide and ranges from wheelchair navigation, evaluation of Brain-Computer Interface to categorize human emotional response [15], assessment of cognitive loads [16] to neurofeedback training for children with attention deficit disorders [17]. From the many researches that cited BCI as a source of control, the most known are listed below:

• ERD/ERS: from the primary sensorimotor cortex, originate Mu (8-12Hz) and Beta rhythms which are more prominent when a person is not engaged in processing sensorimotor inputs (such as processing a coming sound) or producing motor outputs (moving hand, etc). An Event Related Desynchronization (ERD) is the term to describe the desychronization in Beta and Mu rhythms that occurs when person is engaged into a voluntary movement. It occurs in the contralateral rolandic region about 2 seconds prior to the onset of the movement. Similarly, after the end of the movement, the power of Beta and Mu increases considerably resulting in an Event Related Synchronization (ERS). The imagination of such motor movements illicit the same EEG patterns [18]. In BCI, the use of such a technique to imagine moving left/right or both hands is widely used to perform action commands using algorithms that take the power of Beta and Mu rhythms as inputs.

• P300: The use of infrequent visual, auditory or somatosensory stimuli evokes a positive peak over the parietal cortex at about 300 ms after the stimulus presentation. This is referred as P300. The way to induce such a phenomenon is proceeded by presenting a matrix of stimuli and request from the user to choose one of them. A P300 appears when the highlighted choice appears. Knowing the user's choice is very important in BCI in order to execute corresponding action.

• Steady State Visual Evoked Potentials (SSVEP): when presented with a repetitive stimulus at a rate > 5 Hz, a continuous oscillatory response is elicited in the visual cortex. This is termed as SSVEP which is present at occipital sites. To detect the user's choice, stimuli must be presented with different frequencies and by matching oscillations to the focused stimulus; the system should be able to intercept the needed action. During the last decade, BCI applications became more and more prominent especially that it could offer two ways of control mainly active and passive where systems are adapted to the user's mental state [19].

1.3.2 Mental fatigue, P300 and SSVEP

Performing a cognitively demanding task for an extended period of time induces a state that is labeled mental fatigue [20]. The latter is a common in everyday life and becomes clear in compromised task performance, subjective feelings of tiredness, and the accompanying unwillingness for further mental effort [21]. However, it is not well understood scientifically because it is a complex multidimensional phenomenon: It includes changes in motivational, mood, and cognitive processes [22]. Mental fatigue has been found to result in a reduced goal-directed attention [23], a decreased effectiveness in selective attention [24] and an increased difficulty in dividing attention [25]. As far as mental fatigue has some influence on cerebral activities, the latter shows specific perturbation on its EEG patterns, which can influence its role as a source of control. We investigate in this chapter two common sources of control namely: P300 and SSVEP. The use of infrequent visual, auditory or somatosensory stimuli evokes a positive peak over the parietal cortex at about 300 ms after the stimulus presentation. This is referred as P300. The way to induce such a phenomenon is proceeded by presenting a matrix of stimuli and request from the user to choose one of them. A P300 appears when the highlighted choice appears. Knowing the user's choice is very important in BCI in order to execute corresponding action. The P300 response is elicited by the "oddball" paradigm, in which repeated stimuli are presented to the user, and there is a specific target stimuli that rarely occurs among the more common non-target stimuli. Each time the target stimulus is presented to the user, the P300 response appears in the EEG signals. Although the P300 response is known to occur with different forms of stimuli,

such as auditory stimuli [26], these experiments only use visual stimuli. A typical P300 is characterized by the following parameters (see Figure 1.6):

• Maximum amplitude: the maximum magnitude of the generated pick it varies depending on the sensor and the region where the P300 occurred.

• Minimum amplitude: the minimum magnitude reached before that the signal stabilizes.

• Latency: the time that separates the onset time of the stimulus and the appearance of the P300. Usually, this value is approximately 300 ms.

• Period: the needed time for the EEG signal to stabilize after reaching its P300 maximum and minimum amplitudes.

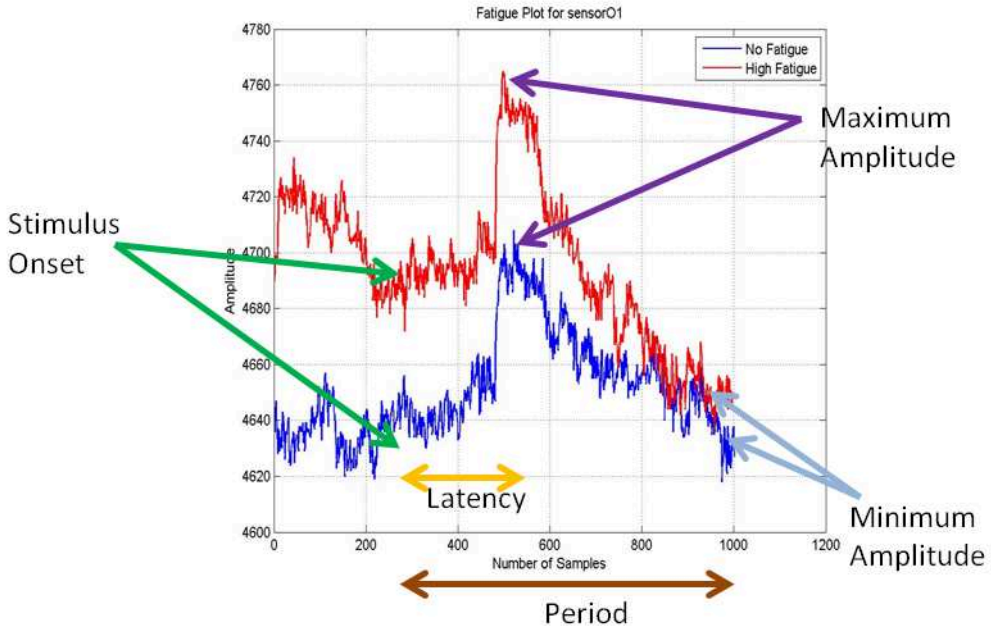

FIGURE 1.6: P300 parameters (maximum, minimum amplitudes, latency and period)

Steady-state Visual Evoked Potential (SSVEP) is a brain response to visual stimulus that flashes with certain pattern. When the retina is excited by a visual stimulus presented at frequencies ranging from 3,5 Hz to 75 Hz [27], a continuous or oscillatory response is generated by the brain. The latter appears at the same or multiple frequency of the visual stimulus. SSVEP-based BCI uses lights that flash at various frequencies. These systems can be used for remotely controlled devices such as wheelchairs which can be useful for severely disabled people [28]. We study SSVEP's because of the excellent signal-to-noise ratio and relative immunity to artifacts, SSVEP's also provide a means to characterize preferred frequencies of neocortical dynamic processes, SSVEP is generated by stationary localized sources and distributed sources that exhibit characteristics of wave phenomena. SSVEP-based BCIs have the advantages of better accuracy, high

information rate and short even no training time is required [29]. Yet it suffers from many drawbacks, such as risk of high fatigue and can induce seizure in photosensitive people. In SSVEP-based BCI, many issues should be raised such as:

• Robustness: misclassification, errors can be very annoying and in some cases very crucial especially in a wheelchair navigation context. This is why high accuracy is needed.

• Safety: flashing rate/pattern, size and color of the stimulus is very influent. It can cause an adverse effect, such as seizure, high fatigue [30]. The best chosen frequency ranges between 9 Hz and 15 Hz, with the use of white color and circular shape [31].

• Classification algorithms: most SSVEP algorithms were developed in frequency domain with the use of Welch method to extract features for classification. Those algorithms are generally based on the first or even the second harmonics of the presentation frequency [32]. However, some others argue that EEG signal may contain important information about the flashing stimulus as well as the enhancement of the classification algorithm [33].

There has been a number of published works in the domain of fatigue influence on P300. Of these studies, [34] examined the effects of mental fatigue on planning and preparation for future actions, using a task switching paradigm. Fatigue was induced by "time on task," with subjects performing a switch task continuously for 2 hours. Subjects had to alternate between tasks on every second trial, so that a new task set was required on every second trial.

A clear post stimulus parietal negativity was observed on repetition trials, which reduced with time on task. This attention-related component was less pronounced in switch trials; instead, ERPs elicited in switch trials showed a clear frontal negativity. This negativity was also diminished by time on task. ERP differences between repetition and switch trials became smaller with increasing time on task. [35] measured multichannel EEG spectra during a continuous mental arithmetic task and created statistical learning models of cognitive fatigue for single subjects.

Subjects viewed 4-digit problems on a computer, solved the problems, and pressed keys to respond (inter-trial interval = 1 s). Subjects performed until either they felt exhausted or three hours had elapsed. Response times (RT); amplitudes of ERP components N1, P2, and P300, readiness potentials; and power of frontal theta and parietal alpha rhythms were examined for change as a function of time. They used 30-channel EEG frequency spectra to model the effects of time in single subjects using a kernel partial least squares (KPLS) classifier [36]. They concluded that a KPLS classifier of

multichannel spectral measures provides a highly accurate model of EEG-fatigue relationships and is suitable for on-line applications to neurological monitoring.

1.3.3 Emotions

Emotions consist of multiple components that may include intentions, action tendencies, appraisals, other cognitions, central and peripheral changes in physiology, and subjective feelings. Emotions are not directly observable, but are inferred from expressive behavior, self-report, physiological indicators, and context [37]. Emotions are classified into discrete and dimensional models. Discrete emotions could be divided into: Basic set (core set) and secondary set depending on the action tendencies [38], [39]. Some other theories argue that emotions could be better measured as differing in degree on dimensions. The well known dimensional models are the pleasure-arousal (pleasure for pleasantness to a given emotional state and arousal for physiological activation) [40] and the approach-avoidance (tendencies to approach or avoid the stimuli) [41]. Note that pleasure-arousal dimension is used in this project in line with many researches. To elicit emotions, many standard strategies such as films, pictures, sound and odors were adopted. Other methods like autobiographic recall and social interactions are also used. It requested that the behavior of others would affect our own emotional state. Little work in computer tried to induce emotions. For example, in MIT Media Lab, Picard, Healey and Vyzas [42] used pictures to induce a set of emotions including happiness, sadness, anger, fear, disgust, surprise, neutrality, etc. In addition, [43] used the results found by Gross and Levenson [44] to induce sadness, anger, surprise, fear, frustration, and fun. As it was already mentioned, emotions play a fundamental role in cognitive processes; Estrada Isen, and Young [45] found that positive emotions can increase intrinsic motivation. In order to measure emotions, the used methods are either objective or subjective. The subjective methods consist of questionnaire, adjective checklists and pictorial tools such as Activation-Deactivation Check List (AD-ACL) Positive and Negative Affect Schedule (PANAS) and Self Assessment Mankini (SAM). Objective methods use physiological manifestations derived from emotions such as brainwave activity, heart rate, facial expression, vocal properties and others. In chapter 2, three forms of negative emotions will be discussed as they were the most suggested by experts to have the highest impact on disable subjects : stress, nervousness and excitement.

1.4 Gaze/brain based wheelchair command

As it was said before, commanding a wheelchair by the mean of gaze and brain together reveals to be one of our long term objective. In fact, projects dealing with wheelchair

command with the combination of those two modalities weren't so many. This is because manipulation of gaze or brain alone isn't a simple task. Moreover, each modality has its own drawbacks that scientific community was sckeptic regarding their reliability. In this section, we will present some projects based on gaze or brain to command wheelchairs.

1.4.1 Gaze based wheelchair command

Wheelesly project : The project WHEELESLY, Yanco et al.[46] proposed a semi-automatic wheelchair named Wheelesly that receives commands from a GUI (Graphical User Interface). These commands are predefined by the points of view of the user so that it can provide support solutions for the disabled and are distributed as shown in the Figure 1.7:

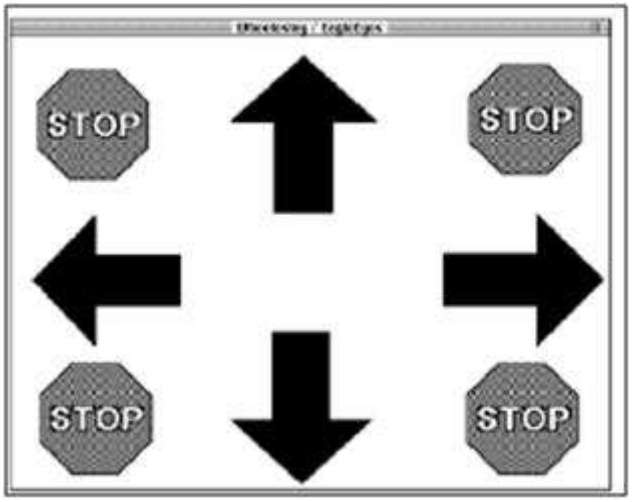

FIGURE 1.7: Wheelesly GUI commands [46]

The interface is divided into four zones of commands that are respectively: forward (right arrow), decrease (down arrow), turn right (right arrow) and turn left (left arrow). For support of the chair, it must merge the order information with the state of the environment in which it navigates (example obstacle avoidance, wall ...) This can affect the speed of rotation and translation which can either increase or decrease depending on the case.

Despite the success of this interface and the originality of its use during that period, it is not always sure this can be the perfect choice for the user who must spend much time staring at buttons with which he must control the chair that makes its control very tedious in long-term and opposes the idea that the solution must be natural relative to the user and should not ask an additional workload for navigation.

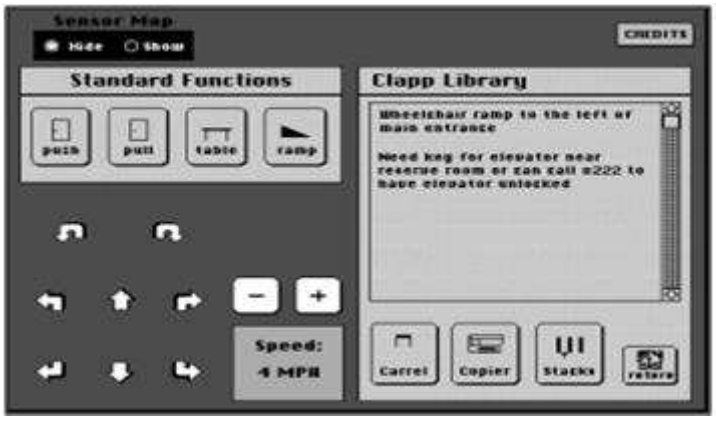

FIGURE 1.8: Assistance module of the Wheelesly interface [46]

Chern project : Lin et al. [47] proposed an improved control wheelchair solution. A calibration algorithm is used to estimate the gaze direction in real time with a relatively low-cost architecture.

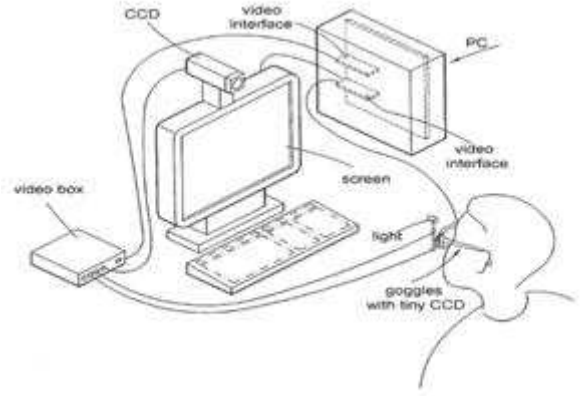

FIGURE 1.9: Framework Architecture [47]

The tracking system uses a camera to look for capturing images of the eye movement and seeks the pupil for an image processing program. For improving the brightness of the image, CCD cameras and a small lamp were used. The results are then transmitted to the controller of the wheelchair using a USB-RS232 converter. Thereafter, the procedure is to define thresholding areas $Thres\_Foreward, Thres\_Backward, Thres\_Right, Thres\_Left$ which correspond to the forward command, backward, turn right, turn left at a constant speed and preset as well as the stop command. The pseudo code of this application can be translated in the table below:

Once the user exceeds a definite increment for each area, the command is sent to the chair (appointed by Robot in the algorithm). This project was tested with subjects and showed good results especially for navigation time and system efficiency.

TABLE 1.2: The method of counting and judgment where sm, sn: the coordinates after transformation; Fwd_cnt: the times of gazing at the forward region; Aft_cnt: the times of gazing at the backward region; R_Turn_cnt: the times of gazing at the right region; L_Turn_cnt: the times of gazing at the left region; $Right\_X, Left\_X, Up\_Y, Down\_Y$: the coordinates of the nine command zones.

Region	Algorithm

Left Region	$If(sm \leq Left\_X \&\& Up\_Y \leq sn \leq Down\_Y)$
	{
	L_Turn_cnt++;
	Fwd_cnt=0;
	Aft_cnt=0;
	L_Turn_cnt=0;
	}

Right Region	$If(Right\_X \leq sm \&\& Up\_Y \leq sn \leq Down\_Y)$
	{
	R_Turn_cnt++;
	Fwd_cnt=0;
	Aft_cnt=0;
	L_Turn_cnt=0;
	}

Other Regions	R_Turn_cnt=0; Fwd_cnt=0; Aft_cnt=0; L_Turn_cnt=0;

Bartolein project : This work [48] intends to present a new way to ease wheelchair control for severely disabled users via gaze control and estimating the intended motion direction. They also focused on how to distinguish between relevant and non relevant gaze behavior so they can improve safety in wheelchair navigation. It's important to know that, according to physiological findings, there is a strong relationship between

humans gaze and locomotion: eye and head movements anticipate users actions and indicating where the person intends to go but it's not a general case because, when being distracted by environmental changes or searching on it, persons don't have any intension for directional changes. Based on these statements and self recorded gaze data from test persons, a set of gaze patterns has been determined. To generate suitable wheelchair motions, two steps were followed:

• A Hidden Markov Model was put in place to estimate through a gaze observation sequence the most probable gaze state listed above

• Knowing the accordant direction, a translational and rotational velocity will be transmitted to the wheelchair to initiate its motion.

The system takes into consideration people with differences into gaze behavior like for example asymmetries for looking left and right by training the HMM parameters to their individual gaze and this was done by the mean of Baum-Welch algorithm. The wheelchair motion state was designed using an FSM based on gaze states and combined to a Sip/Puff system states which are "up", "down" and "neutral".

FIGURE 1.10: Navigation framework

1.4.2 Brain based wheelchair command

The use of a system controlled by brain has the advantage of producing no muscle activity as the movement of the arms or even eye movements. This point was operated in many projects that use the brainwaves as a source of control. From those we can state :

BCW project : Puanhvuan et al. [49] proposed a prototype of Brain Controlled Wheelchair (BCW) that allows the persons with severe disabilities to practically control the electric wheelchair in their home environment. The combination of EEG signal between P300 phenomenon and eyes-blink artifact were used as a hybrid BCW system. Furthermore, this hybrid BCW can be operated in automatic navigation and normal control mode. These two modes delivered 4 destination commands in automatic navigation control and 4 direction commands (forward, backward, turn left and turn right) in normal control mode. These commands were selected via P300 processing system. The different pattern of eyes blinking was used for fast stop, on/off P300 system, and mode changing command (2 times, 3 times and 4 times of eyes-blinking respectively). The result show that the prototype BCW can be operated both automatic navigation and brain control mode with safe by 2 times confirmation of P300 command. Without assistant, user can operate this system by them self via defined different pattern of eyes blinking command. 100% accuracy can be achieved in eyes-blinking detection algorithm and 95% averaged accuracy with the transfer rate of 3.52command/minute was achieved by P300 detection algorithm.

Toyota project : In 2009, Toyota [50] proposed A new signal processing technology for BCI application. Features used in this project are

• Commands for smooth left and right turns and forward motion of the wheelchair are processed every 125 milliseconds by analyzing brain waves using signal processing technology.

• Brain-wave analysis data are displayed on a screen in real time, giving neuro-feedback to the driver for efficient operation.

• This technology is expected to be useful in the field of rehabilitation, and for physical and psychological support of wheelchair drivers.

The system merges between blind signal separation and space-time-frequency filtering technology to allow brain-wave analysis in as little as 125 ms, as compared to several seconds required by conventional methods. Brain-wave analysis results are displayed on a panel so quickly that drivers do not sense any delay. The system has the capacity to adjust itself to the characteristics of each individual driver, and thereby is able to improve the efficiency with which it senses the driver's commands. Thus the driver is able to get the system to learn his/her commands (forward/right/left) quickly and efficiently. The new system has succeeded in having drivers correctly give commands to their wheelchairs. An accuracy rate of 95% was achieved.

FIGURE 1.11: Toyota project to command a wheelchair using EEG [50]

Muller project : Muller et al. [51] proposed the integration of two systems: a brain-computer interface (BCI) based on steady-state visual evoked potentials (SSVEPs) and an autonomous robotic wheelchair, with the former being used to command the latter. The signals used in this work come from individuals who are visually stimulated. The stimuli are black-and-white checkerboards, like stripes, flickering at different frequencies. Four experiments were performed for the BCI development. For all experiments, the volunteers were asked to watch a stimulation screen with a central stripe or to watch a stimulation screen with four stripes presented simultaneously, one at each side, one at the top and one at the bottom. The EEG signal analysis consists of two steps: feature extraction, performed using a statistic test, and classification, performed by a rule-based classifier. This kind of classifier obtains good results in a short time and does not demand any training. The result is a system with high classification rate (up to 96%), high information transfer rate (ITR) (up to 101.66 bits/min), and processing time of about 120 ms for each incremental analysis. Each frequency value can be associated to a user command or a user feeling. The user, who is seated on the wheelchair, can thus choose a specific place to move to. Upon such choice, the control system onboard the wheelchair generates reference paths with low risk of collision, connecting the current position to the chosen one.

Discussion : Although these efforts, the design of gaze-based systems has to consider unintentional fixations and sporadic dwellings on objects that typically occur during visual search or when people are engaged in demanding mental activity [52]: This problem is called "The Midas Touch": to understand better let's imagine that one can control a

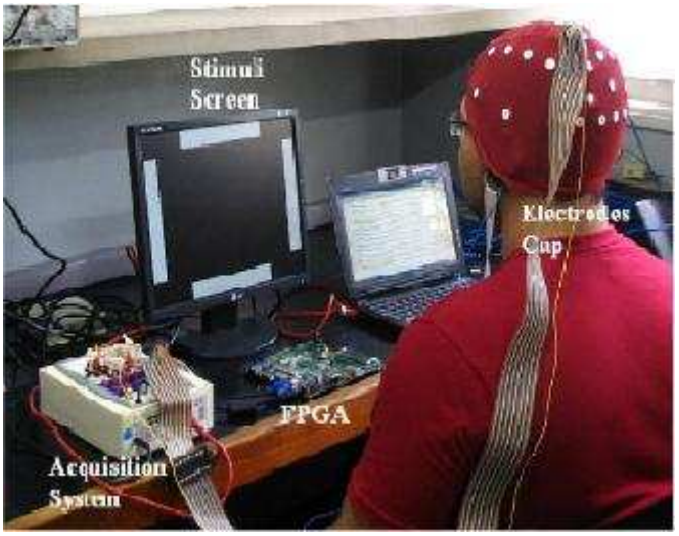

FIGURE 1.12: Signal acquisition with four stripes simultaneously presented [51]

mouse move and clicks on computer using gaze. While this is successful when simulating the mouse move, it's impossible to simulate the click one. Some solutions have been proposed such as blinking, but their innate nature is a big obstacle that even makes it impossible to use such a system: in fact we do not know when to blink eyes since we are not able to control it. Another used method is the dwell-time: the user can activate the needed object by fixing it for certain duration. The challenge consists on choosing the adequate time that ensures the best trade-off between speed and precision. If duration is too short, the system could fall easily into many command errors and conflicts. In the other hand, experienced users can find it very embarrassing that can cause many other problems on itself. A proposed enhancement consists on using adaptive algorithms in a way that the dwell-time decreases proportionally to the increase of the familiarity of the user with the system but the same problem has to be considered: how to differentiate between looking at a button to activate it or just because its text is not very clear. This is explained by the fact that the perfect relation between gaze duration and user intention is impossible to find and it will be beneficial to replace this way by a more direct one [53].

In the other hand, using BCI to command wheelchairs can be very efficient especially that users aren't engaged to produce any muscular efforts but only relying on brain as a source of control. Also, the use of ERD/ERS, P300 and SSVEP by the mean of different techniques made it even more practical as well as the emergence of portable EEG headgears will often contribute to the success of such a technology. However, the complexity of the brain as an organ makes those tasks very difficult and though, in situations where security is very important as it is for wheelchair navigations, reliablity of such a technology alone is questionnable. Another point, even we stated that in

Toyota project classification rate is up to 96%, the used headgear is bulky and invasive enough to cause dissatisfaction for disabled users. Finally, it's important to state that, brainwave signals are very sensitive to artifacts especially eyes movements which can make the navigation task harder. Combining both modalities (Brain and gaze), could bring solutions to problems stated before. The idea is to combine gaze, as a selection module, with the brain as a validation source : this means that brainwave signals will be considered as a binary trigger (ON/OFF) and consequently, avoiding further processing.

1.5 The BEWHEELI project setup

The Brain Eyes WHEELchair Interface (BEWHEELI) aims at proposing new modality to command/control a powered wheelchair. Since the main objective is to enhance navigation security by integrating emotions and mental fatigue, a simulation environment must be prepared that can bear with :

• Inducing emotions, mental fatigue, P300 and SSVEP : by simulating situations inspired from reality, emotions can be triggered and induced as well as mental fatigue. Also by introducing multiple artifacts such as visual stimuli and flickering pictures, P300 and SSVEP can be handled and measured. Finally correlation studies can be held to assess the relationship between parameters and environmental artifacts or within parameters themselves

• Assessing user's performance : In order to validate approaches, it's important to have an idea about the user's performance. This includes, number of obstacles that the wheelchair can hit during navigation, time needed to accomplish tasks, path stability that can be deduced by comparing subject's followed path with an optimal one, and even psychological phenomena such as gaze dwell time or agglomerations which can reflect human satisfaction or dissatisfaction.

It can be stated that this project is divided into short and long term objectives. While the former is the integration of emotion and fatigue as to control wheelchair parameters, the long term objective targets the command block of our architecture; in fact, many projects tried to command wheelchairs either by gaze or by brain individually. However, combining both modalities wasn't common yet. The proposed architecture takes into consideration the combination process to command the powered wheelchair. In this section, the used materials to set up the simulation platfrom is presented. Next, the BEWHEELI architecture will be explained.

1.5.1 Materials used for environmental setup

The experimental environment consists of many components. Those can be divided into hardware and software.

Hardware framework : As the experiment targets wheelchair navigation, the use of a wheelchair is crucial and for this purpose, an Invacare Storm 3G Ranger X branded wheelchair is used. Equipped with joystick, encoders were added to its wheels so the wheelchair velocity can be digitized and treated. Those can be useful to control a virtual world projected on a 180 degrees panoramic screen to help the immersion of the user in the world. As to calculate his points of gaze (POG), an ASL EyeTrac 6 branded eye tracker was placed in front of the user with 60Hz sampling frequency to record the subject's gaze sequence. A specific algorithm was used for system calibration and for dividing the screen into command zones. Alternatively, the Emotiv Epoc with 16 sensors and 128Hz sampling frequency headgear is added to record brainwave activity.

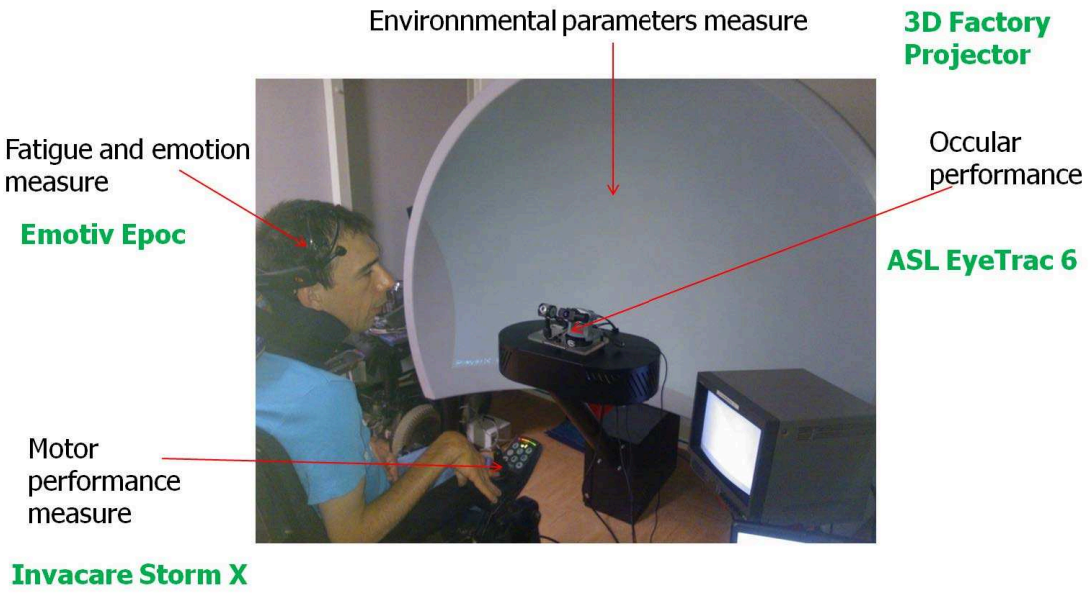

FIGURE 1.13: Experimental platform

Virtual world : The virtual world was developed using Reality Factory engine [54]. The latter is used to develop video games, was adapted to our series of experiments. For example, a virtual maze was conceived and presented for subjects (see Figure 2.12) formed by several rooms, each of which dealing with specific artifacts in order to induce specific emotions and mental fatigue as well as assessing subjects performance during navigation. The use of simulators is very important. Thanks to it, we can set up new

cases that can induce physiological phenomena such as P300, SSVEP, emotions and fatigue by inserting sepcial artifacts such as lights, stimuli and variating parameters like obstacles ammount, type and velocity. Those can help us to grant deeper investigations and have an idea about correlations between different parameters before proceeding to real world situations.

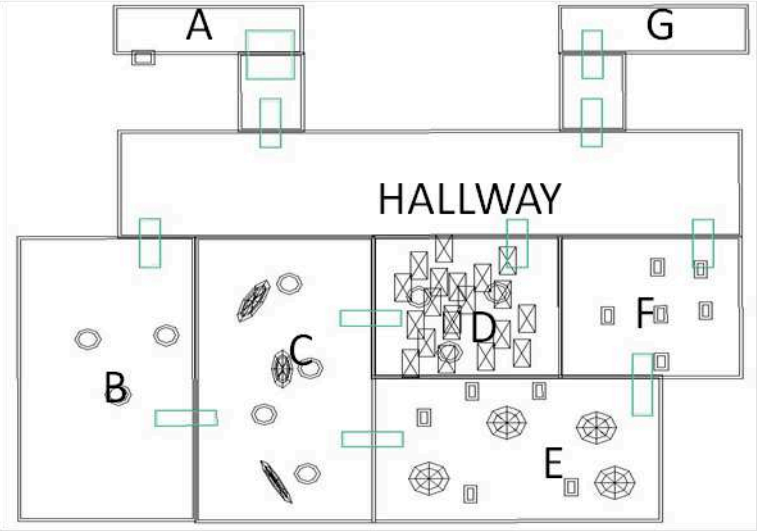

FIGURE 1.14: The plan of the navigation maze with rooms labeled from A to G

1.5.2 System framework

In order to send commands to the wheelchair, gaze and brain wave signals should be processed separately from gaze sequence and thanks to EOG technology, horizontal and vertical coordinates are processed using infrared and high speed cameras. From gaze concentrations, the command selector module (CSM) detects the selected command (which must be confirmed with the Merging Module) and map it into left, right, forward, backward or idle. In parallel, brainwave signals are also processed through EEG technology. The latter outputs instead of raw signals (electric potentials amplified and filtered from artifacts) the five standards EEG bands mainly: delta (up to 4 Hz), theta (4Hz-8Hz), alpha (8Hz-13Hz) beta (13Hz-30Hz) and gamma (30Hz-100Hz). Each of which is more prominent in different situations (e.g. delta band is more prominent when sleepy, alpha when conscious...). Also these bands perform some patterns related to particular actions (example the system can detect if the user wants to move his right or left hand through particular command pattern). Those signals are then sent to both Mental State detection module (MSDM) and command detector one. Mental State detection module (MSDM) is a system dedicated to map raw brainwave signals into mental states: relaxed, stressed... which play an important role in detecting the specific command for

binary switch (example: the "go" command can have a different brain patterns according to the user's mental state). Also, it influences the velocity mapper module (VMM) which changes angular and linear velocities according to the user's mental state. The second most important module is the command detection (CDM) one. Through raw brainwave signals the system detects specific EEG patterns related to certain command (turn left/right, move...). To be noted this specific command should be filtered from other EEG patterns that could be manifested in similar fluctuations. Another module named merging module (MM) helps to merge between the selected command by the CSM and the CDM to send angular and linear velocities of the wheelchair otherwise, the system should be inhibited and a loop back is sent to the CSM. The last module used is the velocity mapper (VMM). This module is activated once a confirmation command is received from the previous module with information identifying the confirmed command (turning left/turning right...). Another input that should be passed to this module is the user mental state; in fact the wheelchair velocity should be adapted to the user's state (example: angular and linear velocity should decrease when the user is sleepy or stressed or anxious.) Finally upon velocities reception, the wheelchair could initiate its motion. This includes two databases interacting with different module and could be enhanced through feedbacks and adaptive trainings.

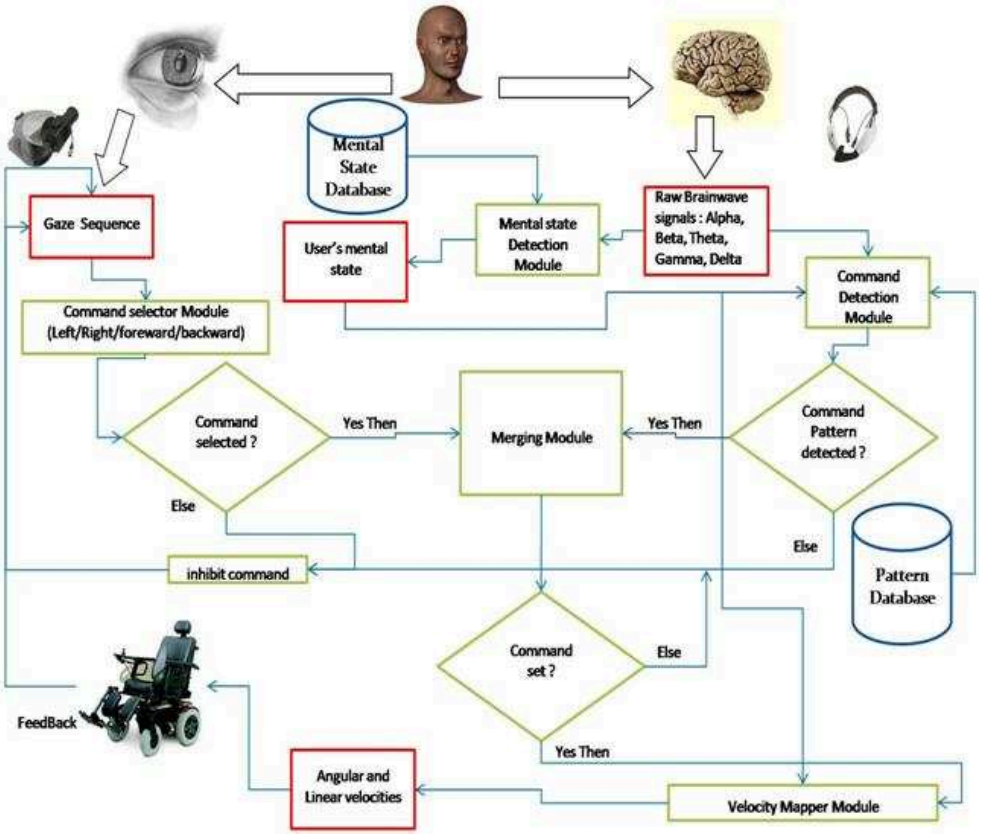

FIGURE 1.15: BEWHEELI project framework description

With the integration of emotion and fatigue blocks, a simplified framework could be presented as follows :

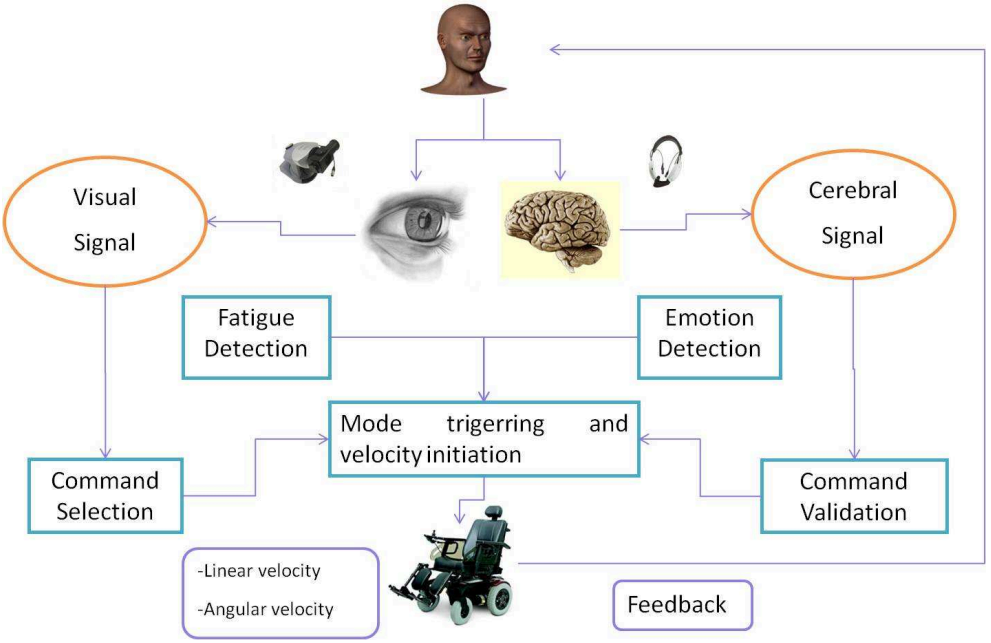

FIGURE 1.16: BEWHEELI project framework emotion and fatigue integrations

In this figure, emotion and fatigue blocks have the role of controlling the wheelchair parameters (such as velocity). Its importance relies on the fact that safety enhancements depend on the efficiency of the detection of disturbing emotions or high fatigue level that can influence navigation performance. The details of the processing of those two blocks will be given in the next chapters as a treatment must be done in order to induce and measure them. By setting up a reference database, one can attribute a specific profile to each studied emotion or fatigue level.

1.6 Conclusion

In this section, we presented some projects that used shared paradigm to enhance wheelchair navigation. Noticing the corrective behavior of the latter and the lack of anticipative aspect, human factors integration were proposed namely emotions and mental fatigue. Before its integration, a study was taken to assess its impact on EEG patterns with proposed models and the way they are measured. the next step was to set up an experimental environment that can puts together EEG headgear, EOG camera and panoramic projector with powered wheelchair to prepare a series of experiments that can induce different studied phenomena and measure the user performance in each situation. In the following chapters, emotions and mental fatigue will be investigated more.

Emotions induction protocol will discussed and implemented in simulated navigation scenarios to check whether it can really bring some ameliorations on user's performance or it's not really reliable especially with the lack of maturity of EEG technology.

Chapter 2

Emotion integration in the service of wheelchair control

2.1 Introduction

The detection of emotions is very important in a way that it could be integrated for two purposes: first, it could be a basis for EEG command patterns to be detected (example: when performing a motor imagery task, the EEG pattern manifestation depends on the user mental state). Second, in order to enhance wheelchair navigation, its velocity should be enslaved to the user's emotions (example: when performing a motor imagery task, the EEG pattern manifestation depends on the user mental state). Second, in order to enhance wheelchair navigation, its velocity should be enslaved to the user's emotions (example, it should decrease if the user is frustrated...). But it's still not evident that emotions can bring the expected results and especially that EEG reliablity in this context is still not proved yet and that measuring emotions also rises a lot of challenges. This section is divided into three major parts. In the first part, the framework used to induce emotions is exposed. In the second part, emotion induction experiment, techniques used for extraction, selection and detection of features are explained with comparison of different techniques used. In the third part, the integration of emotions as a velocity controller, as well as, the experiment employed to assess navigation performance are described with results and discussion of different measures found. Finally, a conclusion will introduce the next section of the project which is the investigation of mental fatigue.

2.2 System framework

The system framework (Figure 2.1) involves two major parts: the inputs and the outputs. The inputs are formed by raw signals issued from EEG, ElectroOcculoGraphy (EOG) and joystick. Those are filtered, sampled and processed depending on the modality used. In the current study, we focus most on EEG activity in order to extract emotions. The methodology used for emotion detection is illustrated in Figure 2.2 and all techniques needed for the latter are further explained in appendix B; the features extracted from bandwave signals are the Power mean (Pm) and the Root mean square (Rms) by adopting two different techniques: the Welch method and wavelets. With the huge quantity of data in the extracted features due to the crossing of many parameters (bandwave per time per sensor per subject) a selection phase is needed. For this purpose, Principal Component Analysis (PCA) and Genetic Algorithm (GA) were applied. At the classification phase, three techniques were compared: Linear Discriminate Analysis (LDA), Multi Layer Perceptron (MLP) and Support Vector Machine (SVM). Before the application of different techniques on the raw data, a reference database was setup containing temporal profile of each studied emotion class for different subject samples. We assume that the studied emotions are situated in separated quadrants in valence-arousal model. In this case, each combination of valence and arousal rates results in one emotion class. The second hypothesis assumes that cerebral activity during visualization period match the given rating in the valence-arousal scale and in this way; one can attribute a temporal profile to each chosen emotion. Meanwhile, the Points of Gaze (POG) extracted from EOG camera were processed and classified to estimate the user's direction choice: left or right. A calibration algorithm, based on nine-point visualization, is used to estimate points of gaze. These are used as inputs in the classification algorithm which splits the screen on three quadrants (Right/Idle/Left), by calculating the maximum fluctuation of the eye gaze. Finally, right and left commands are sent to the Reference Velocity Calculation module. If the navigation direction is controlled by the user's gaze, forward and backward commands are calculated according to the joystick angle; in fact, an embedded cursor, can convert the joystick angle to an analogical signal needed for the wheelchair wheels to move forward or backward. The three described signals constitute the inputs of the Reference Velocity Bloc. The latter uses a special algorithm to calculate reference angular and linear velocity based on the rotation angle, raw linear velocity and the user's emotion. This algorithm will be detailed later, as it takes into consideration the emotional part; if the latter is detected; braking command is sent to the raw angular and linear velocities so that the wheelchair stops moving. After obtaining the reference velocities, those are compared to the real ones provided by a coupler mounted on the wheels, and processed by an analog digital converter. Next to the correction, those are transmitted to the wheelchair actuators and in parallel to the virtual world projection.

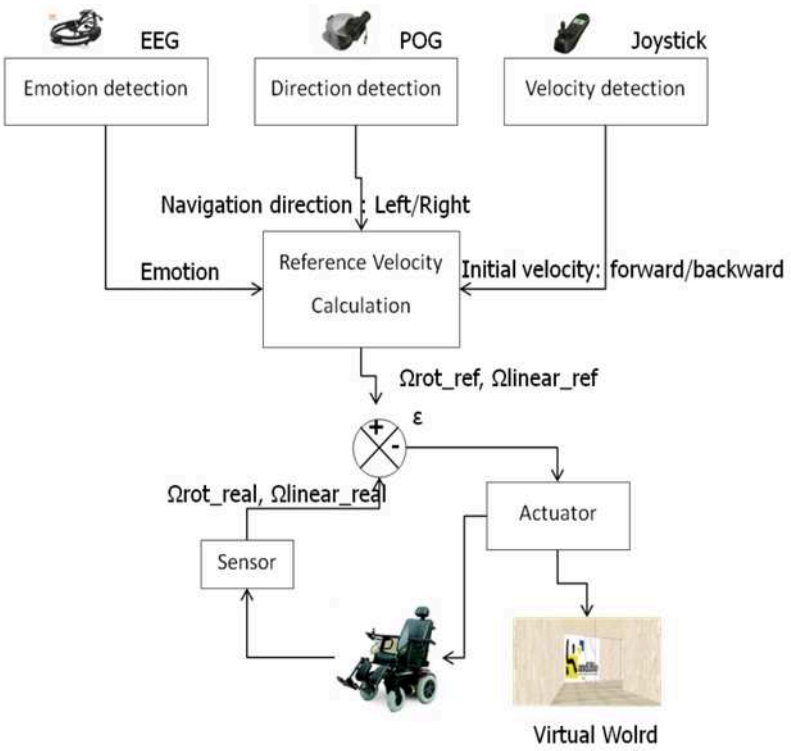

FIGURE 2.1: System framework: the illustration of the use of emotions as velocity modulator.

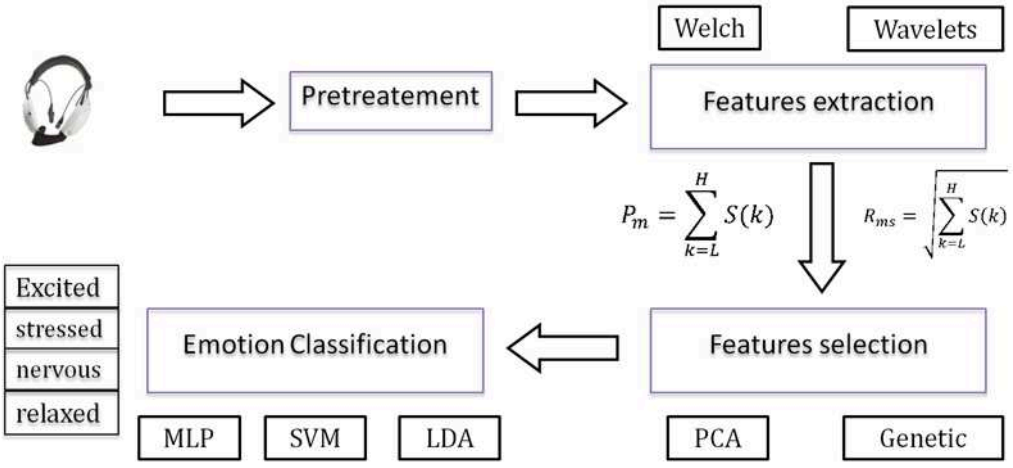

FIGURE 2.2: Emotion detection methodology

2.3 Experimental setup for emotion detection

Our experience consists on measuring the emotional states of the persons when viewing and listening to audio/video sequences. This will supply a reference database in order to assign to each emotion class a temporal EEG data profile and thus applying different techniques offline before implementing an online emotion detection module. Consequently, the authenticity of the collected emotions must be checked. This will be done by comparing emotions distribution with the valence/arousal common distribution which is considered as our ground-truth. In this case, the association between signal features and emotion is deduced from the correlation between the EEG activity in each second with the rate given by the subject at the end of the experiment. Five factors that can influence recordings are defined: subject-elicited vs. event-elicited, laboratory setting vs. real world, focus on expression vs. feeling of the emotion, openly-recorded vs. hidden recording and emotion-purpose vs. other purpose. The following protocol description addresses those five factors.

2.3.1 Participants

40 healthy subjects participated in the experience. They were aged from 22 to 55 years old. Their vision was normal or corrected to be normal. Before the implementation of the experimental equipments, the subjects signed a consent form and answered a questionnaire to analyze their normal states and verify if they consume medicines or exciting drinks such as coffee and tea, this means that the experiment is openly recorded.

2.3.2 Procedure

Once in the experimental room, the experimenter explained to the participant that this study aims to measure his emotional state with regards to the audio/video sequences. Each experience is based on these following steps. In the first stage, the experimenter asks the participant to complete a form containing his personal information (gender, age, left/right handed, alcohol/coffee/tea consumption, etc). In fact, several studies [55] showed the influence of the sex and the age of the human on his emotional state. In the second stage, the experimenter asks the participant to choose four audio/video sequences to measure his emotional state in different situations such as excitement, nervousness, relaxation and stress. After the preparation of the chosen sequences, the experimenter sets the EEG headgear on the scalp of the participant. Before beginning the recording, he must be sure of the good quality of the recorded signals. In the third stage, the participant watches the four sequences one by one (Figure 2.3).

FIGURE 2.3: Participant in experimental room

The duration of each sequence is limited to 63 seconds with the first three seconds considered as a baseline. A period of one minute separates the current session to the next one. After every test, the experimenter asks him to self-assess his emotional state from the dimensional model consisted of two manikin scales (Self Assessment Manikin, SAM) representing two dimensions arousal and valence [56]. The dimension of valence ranges from two poles negative/bad and positive/good, whereas the arousal dimension spans between the two poles sleepy/calm for very low arousal and aroused/excited for very high arousal. In the third stage the participant should fill in, each of the two scales, and indicates his levels of valence and arousal by choosing two numbers between one and nine. (Figure 2.4) depicts the two SAM scales.

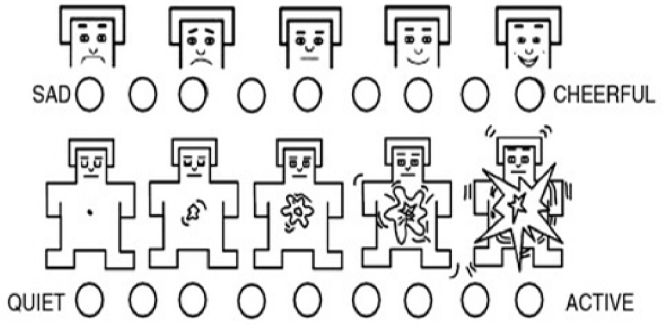

FIGURE 2.4: SAM-Scales for valence and arousal

2.3.3 Subjective rating analysis

Stimuli were selected to induce emotions in the four quadrants of the valence-arousal space (Low Arousal Low Valence, High Arousal Low Valence, Low Arousal High Valence, and High Arousal High Valence). (Figure 2.5) summarizes the distribution of the mean ratings of different users according to the induced emotion. Emotions choice was made

intentionally in a way that each studied emotion belongs to only one quadrant (and though, the combination of valence and arousal rates results in only one emotion class). The purpose is to avoid the overlap between emotions on the same quadrant. It can be seen that the results are well within those found in the literature.

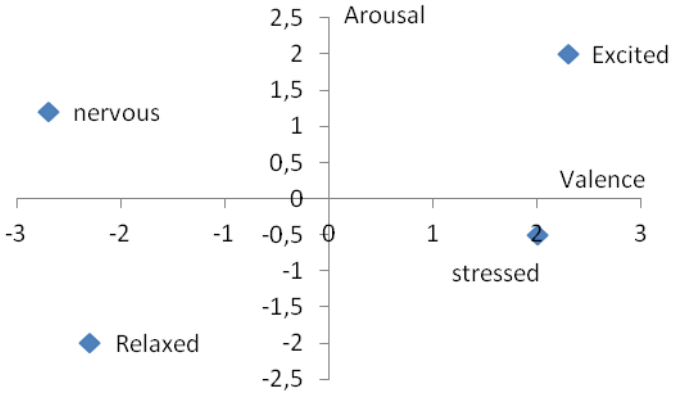

FIGURE 2.5: Mean ratings distribution on the Valence/Arousal scale

2.3.4 Feature extraction

According to the ratings, EEG signals were processed in order to extract the mean power (P_m) and the root mean square (R_{ms}) of five frequency bands ($\delta, \theta, \alpha, \beta, \gamma$), in each second. In this case, each dataset is formed by two eventual configurations; either the Pm per band per sensor per user per second or the Rms per band per sensor per user per second which results in a 5 bands x 14 sensors x 63 seconds x 40 subjects. The extraction step is applied using two methods: Welch method and discrete wavelets transform.

Welch method : Welch's method is an evolution of the standard periodogram and Bartlett [57] methods. Let it be $x_i(n), i = 1, 2, 3, ..., K, K$ uncorrelated realizations of an aleatory process x_n over an interval $0 \leq n \leq L$. It can be directly expressed by:

$$\hat{S}_w(w) = \frac{1}{KLU} \sum_{i=0}^{K-1} |\sum_{n=0}^{L-1} w(n)x(n+iD)exp(-jwn)|^2 \tag{2.1}$$

where : $U = \frac{1}{N}\sum_{i=0}^{N-1} |w(n)^2, N$ is the length of the window $w(n)$, It has been proved that this method reduces the noise in power spectra whilst the resolution R depends on the chosen window and can be given by:

$$R = \frac{1}{LT_s} \tag{2.2}$$

where : T_s the sampling period. Hence the lower L is, the smoother Welch periodogram becomes. The initial signal was filtered between 1 and 64 Hz. In this case, δ (up to 4 Hz), θ (4Hz-8Hz), α (8Hz-13Hz) β (13Hz-30Hz) and γ (30Hz-64Hz) were kept for our study. The power spectral density (PSD) was computed every one second of the whole trial for each user. The Welch periodogram was computed using 512 points FFT and several Hamming windows of length 128, 64, 32 and 16 points with a 50% overlapping. For the bands found in each second, two parameters were computed: the mean Power (P_m) and the Root Mean Square (R_{ms}) calculated as:

$$P_m = \sum_{k=l}^{h} S(k) \tag{2.3}$$

$$R_{ms} = \sqrt{\sum_{k=l}^{h} S(k)} \tag{2.4}$$

where : $S(k)$ are the sampled values of the periodogram $S(f)$ and l and h are the indexes of the higher and lower sampled frequencies for each band.

Discrete wavelets transform : The Discrete Wavelets Transform (DWT) is generated by the function:

$$\psi_{a,b}(t) = 2^{\frac{a}{2}}\psi(2^{\frac{a}{2}}(t \quad b)) \tag{2.5}$$

where : a is called the scales and b the shifts. It is possible to approximate any function by dilating $\psi(t)$ with the coefficient 2^k and shifting the resulting function on interval proportional to $2^{\ k}$. Using Debauches8 wavelet, six levels of DWT are implemented. The first level (between 128Hz and 64Hz) contains noise as the needed waves only occur between 1Hz and 64Hz.In the second level (32Hz and 64Hz), γ waves can be detected as decomposition detail, then β waves (16Hz and 32Hz) and so on until reaching the sixth level (between 1Hz and 4Hz) where δ waves constitute the approximation coefficients of the signal (Figure 2.6).

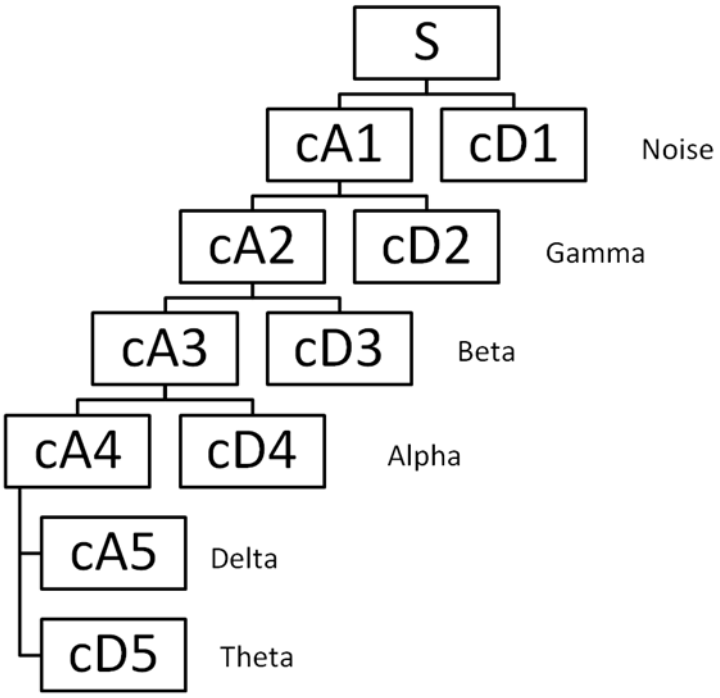

FIGURE 2.6: Multi decomposition algorithm applied on EEG signal

2.3.5 Feature selection

The feature vector contains two configurations with P_m and R_{ms} parameters of 5 band waves in the 14 sensors for the 63 seconds. This means that feature vector suffers from high dimensionality curse [58]. Consequently, features must be selected according to its correlation proportionality with each others. In this section, two selection techniques are used: Principal Component Analysis (PCA) and Genetic Algorithm (GA).

Principal component analysis : Principal Component Analysis (PCA) uses mathematical principals to transform a number of correlated variables into smaller numbers called principal components. For each second, the feature vector X is 200 x 80 length where rows $(x_i^1, \ldots, x_i^80)$ represent the observations and columns $(x_1^j, \ldots, x_{200}^j)$ represent the variables. From the correlation Matrix, the Eigen values and Eigen vectors are calculated to form principal components. The selection of the number of principal components axis to keep is very important in PCA. The criteria used are generally empirical: the elbow method consists of detecting an elbow in the Eigen values plot or Kaiser Criterion. The latter consists on retaining only the Eigen values greater than the mean value.

Genetic algorithm : Genetic Algorithm (GA), a form of learning strategy, is an adaptive search technique which proved its efficiency over a set of search methods [59]. Let it be X, the feature vector of length s. the inclusion or elimination of the corresponding feature is described as follow: if $X_i = 0$, then it represents elimination of the feature otherwise, 1 indicates its inclusion. Evaluation function choice is very important to obtain a successful application of GA. In the current problem, our purpose is to estimate the number of optimal features to keep. The idea is to apply a fitness function on the correlation matrix M. The latter can be presented as follows:

$$M = \begin{pmatrix} 1 & \dots & C_{1,n} \\ \vdots & C_{i,j} & \vdots \\ C_{n,1} & \dots & 1 \end{pmatrix} \tag{2.6}$$

where : $C_{i,j}$ represents the correlation coefficient between feature i and feature j. The proposed fitness function F could be defined:

$$F = min_{i,j}|C_{i,j}| \tag{2.7}$$

For each iteration, the crossing chromosomes with the least correlation coefficient are kept for the next generations while the others are eliminated.

Classification : After selection of features, the classification of the four classes of emotions was investigated using different classifiers; the Linear Discriminate Analysis (LDA), the Multi Layer Perceptron (MLP) and Support Vector Machine (SVM). In a supervised learning, given the feature vector as input, the output could be one of the four studied emotions (stressed, excited, nervous, and relaxed).

Linear Discriminant Analysis (LDA) : The LDA is a linear combination of variables. They are presented in the form of:

$$y_{km} = u_0 + u_1 X_{1km} + u_2 X_{2km} + \ldots + u_p X_{pkm} \tag{2.8}$$

where : y_{km} is the value of the discriminant function for the case m on the group k as well as for X_{ikm} which is the discriminate variable X_i for the case m on the group k, and u_i are the required coefficients. This implies that the number of discriminant functions is determined by the number of considered groups.

Multi layer perceptron (MLP) : The used MLP is composed by an input layer with a size, the selected features of the input vector, a hidden layer with 20 neurons and an output layer with 4 neurons which correspond to the number of emotions. The transfer function used is sigmoid and the cross-validation technique adopted is the testset validation technique; the database is divided into 3 sets: 70% for training, 15% for testing and 15% for validation (and thus avoiding overfitting).

Support vector machine (SVM) : SVM maps input vectors into higher dimensional space to ease classification. Then it finds a linear separation with the maximal margin in the new space. It requires the solution of the following problem:

$$min_{w,b,\epsilon}\frac{1}{2}w^T w + C\sum_{i=1}^{l}\epsilon_i \tag{2.9}$$

$$subject\,to\, y_i(w^T\Phi(x_i)+b) \geq 1 \quad \epsilon_i \tag{2.10}$$

$$\epsilon_i \geq 0 \tag{2.11}$$

where : C is the penalty parameter of the errorϵ_i. The kernel used in this project is the Gaussian radial basis function. This could be expressed as follows:

$$K(x_i, x_j) = e^{\ \gamma\|x_i\ \ xj\|^2} \tag{2.12}$$

A cross-validation technique is used to determine C and γ.

2.3.6 Results

The results found in this work are associated to many combinations made from extraction process (Welch and wavelets), feature selection (Genetic Algorithm and Principal Component Analysis), and classification techniques (Multi Layer Perceptron, Linear Discriminant Analysis and Support Vector Machine). In order to reliably report results, we report the combined F-score (in percentage), based on the precision and recall measures. This measure takes into consideration the class balance and is commonly employed in information retrieval [60]. For the Welch technique, R_{ms} and P_m were compared in different window lengths (128 points, 64 points, 32 points and 16 points) using PCA and GA as features selectors. The results can be summarized in figures 2.7 and 2.8. The figures show that classification accuracy, based on Welch periodogram, depends on the window length chosen for extraction. The plots slopes increase from 128 to 64 and start

dropping to reach the worst classification rate for 16 points. There is no noticeable difference between Pm and Rms but a slight superiority is recorded for R_{ms} with the best classification rate for $R_{ms}MLP64$ at 90%. MLP showed the best classification rates over LDA and SVM. While the latter showed also good performance. Also, the difference between PCA and GA is not significant although GA is the best overall classification as it is recorded for $R_{ms}MLP64$ with GA as feature selector.

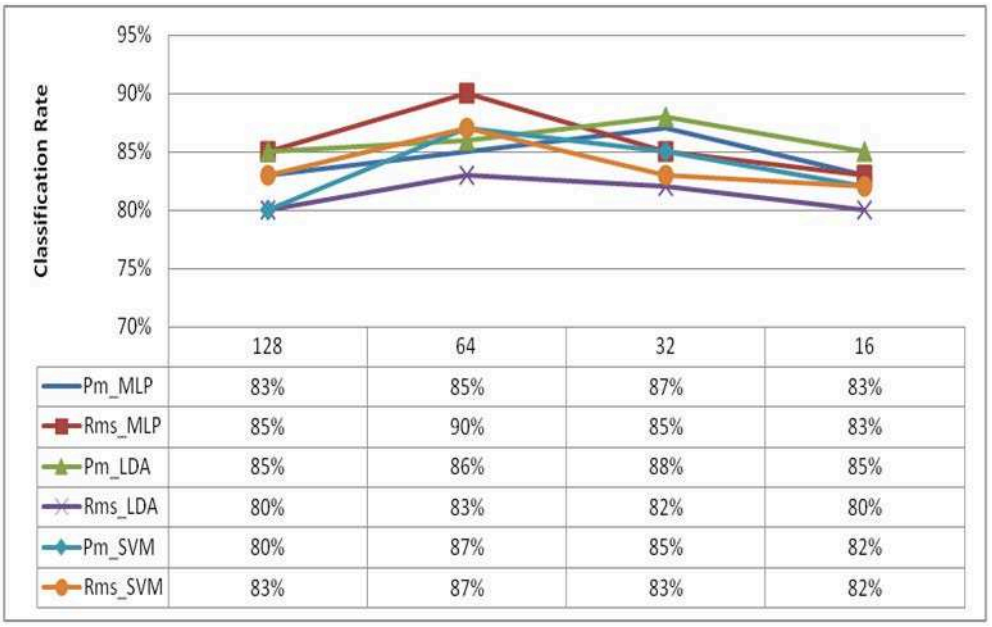

	128	64	32	16
Pm_MLP	83%	85%	87%	83%
Rms_MLP	85%	90%	85%	83%
Pm_LDA	85%	86%	88%	85%
Rms_LDA	80%	83%	82%	80%
Pm_SVM	80%	87%	85%	82%
Rms_SVM	83%	87%	83%	82%

FIGURE 2.7: Classification performance using PCA and Welch periodogram, for different window lengths

This can be justified by the subjective criteria of PCA; in fact, despite the fact that there are a lot of techniques to pick the number of eigen values to keep, these can remain insufficient to select the right number of significant features while for GA, the iterations take a lot of calculation time to achieve the best selection even if the selected features seem to be more suitable than PCA. The results found using wavelets extraction, are summarized in Figures 2.9 and 2.10. The same already-mentioned notes are also noticed for the wavelets case. R_{ms} achieved the best classification rate over P_m. As well as, GA is more efficient than PCA. The best classification rate recorded is 93% assigned to $MLPRms$ which is considered as the best performance for all extraction, selection and classification techniques. The possible explanation for the 7% error rate could be the fact that extraction process was applied for each second of the 63 seconds of the whole experiment which is not necessarily correct; while visualizing a video sequence, we don't ensure that the same feeling is expressed during the whole experiment, it can happen only for a few seconds but not the 63 seconds while in our case, we assumed that each second of the experiment is associated with the expressed rating at the end of the experiment.

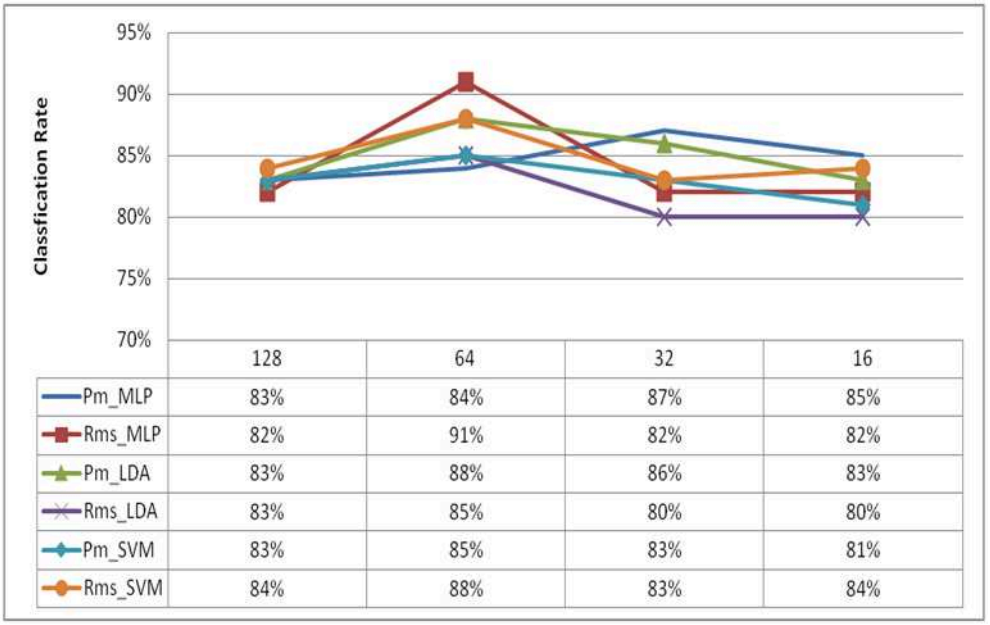

	128	64	32	16
Pm_MLP	83%	84%	87%	85%
Rms_MLP	82%	91%	82%	82%
Pm_LDA	83%	88%	86%	83%
Rms_LDA	83%	85%	80%	80%
Pm_SVM	83%	85%	83%	81%
Rms_SVM	84%	88%	83%	84%

FIGURE 2.8: Classification performance using GA and Welch periodogram, for different window lengths

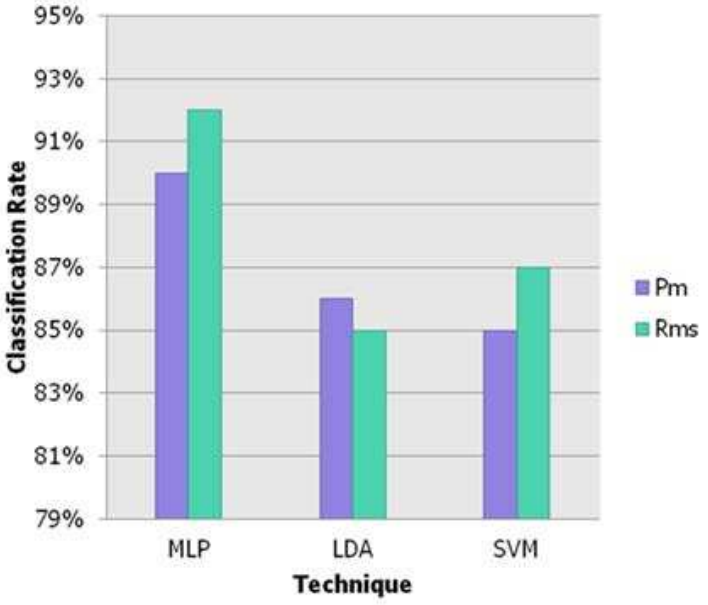

FIGURE 2.9: Classification performance using Wavelets-PCA

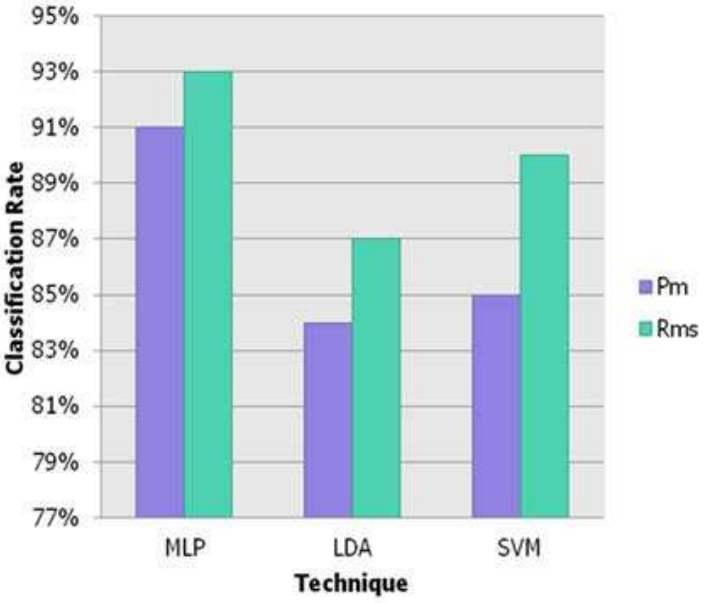

FIGURE 2.10: Classification performance using Wavelets-GA

This is one of the most challenging issues for emotion detection context. In motor imagery, by asking the subject to imagine making a muscular activity, the next seconds correspond more probably to the execution of the asked action, while in emotion detection this is not guaranteed as it depends on many parameters such as the influence of the video sequence on user, the time needed to switch between emotions and the fact that EEG fluctuations don't necessarily mean an emotion trigger. But the classification rate obtained is sufficient to validate the presented approach of this project. This will be treated in the next section.

2.4 Implementation

In the previous section, emotion has been detected using Wavelets as extractor, GA as feature selector and MLP as classification technique. The goal of this section is to assess the influence of the introduction of emotions on navigation safety as braking system; an experiment was set up to compare two navigation scenarios. The first one consists in controlling a wheelchair in a virtual environment going from point A to point G without taking user emotions into consideration while in the second scenario, if one of the four emotions is detected, a braking command is sent to the wheelchair so it decreases its velocity. If the detected emotion has not changed for a certain period of time, the wheelchair stops and a message instructing the user to concentrate and to relax is displayed. While the final goal of the project is to control the wheelchair using gaze and

brain rather than joystick, in this chapter the first step taken was to generate left/right commands using gaze and forward/backward with joystick. The studied parameters for assessment are: obstacles hit, navigation path and outbound points of gaze which will be explained in details later.

2.4.1 Experimental setup

The experimental environment consists of many components. Those can be divided into hardware and software.

Hardware framework : As the experiment targets wheelchair navigation, the use of a wheelchair is crucial and for this purpose, an Invacare Storm 3G Ranger X branded wheelchair is used. Equipped with joystick, encoders were added to its wheels so the wheelchair velocity can be digitized and treated. Those can be useful to control a virtual world projected on a 180 degrees panoramic screen to help the immersion of the user in the world. As to calculate his points of gaze (POG), an ASL EyeTrac 6 branded eye tracker was placed in front of the user. A specific algorithm was used for system calibration and for dividing the screen into command zones. Alternatively, the Emotiv Epoc headgear is added to estimate emotions.

FIGURE 2.11: Virtual world wheelchair navigation

Virtual world : The virtual world was developed using Reality Factory engine [54]. It consists of a virtual maze formed by many rooms labeled from A to G, with a hallway (Figure 2.12). Each room has some special features needed to induce frustration emotion on the user. The room A is the starting point for the navigation. Room B, contains some obstacles but not so many. With more obstacles, room C leads to two rooms D and E. The first is filled with coronas that generate a high illumination effect that can

disturb the user to find the door to navigate to the hallway. The second is a very dark room filled with obstacles and only illuminated with light coming from a torch. Room F is the most difficult because; it contains nine moving obstacles spread all over the room. Finally room G is the goal to reach.

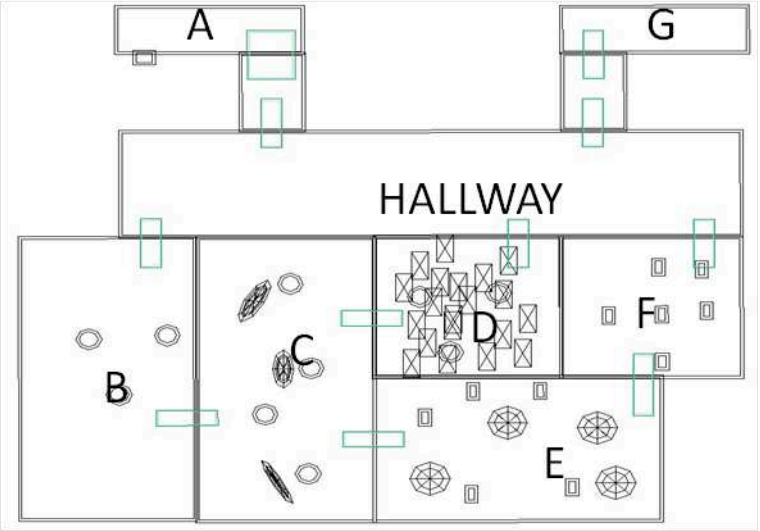

FIGURE 2.12: The plan of the navigation maze with rooms labeled from A to G

Gaze calibration was ensured using nine-point calibration algorithm. For each iteration, a special point is projected on the screen and the user has to look on it. Meanwhile, the system estimates the corresponding points of gaze based on the feature vector defined as the distance between the central point of the corneal reflection and the central point of the pupil reflection. After success of the operation, the screen is divided into command zones. Those are respectively, left, right and idle. A min-right/max-left algorithm was implemented for this purpose. The idea is to ask the user to look straight ahead on the screen, from the points of gaze concentration; the maximum point position and the minimum are recorded. Then, when looking to the right the minimum point is recorded while the same operation is processed but using the maximum point position for left look. The zone separations are calculated from given points as follows:

$$X_{Zone\_left} = \frac{X_{point\_center} \quad X_{point\_max\_left}}{2} \tag{2.13}$$

$$X_{Zone\_right} = \frac{X_{point\_max\_right} \quad X_{point\_center}}{2} \tag{2.14}$$

where : X_{point_center} is the X coordinate of the center point of the points of gaze when the user looks straight. $X_{point\_max\_left}$ is the X coordinate of the maximum point of the gaze concentration when the user looks left and $X_{point\_min\_right}$ is the X coordinate of

the minimum point of the gaze concentration when the user looks right. An example is presented in the Figure 2.13

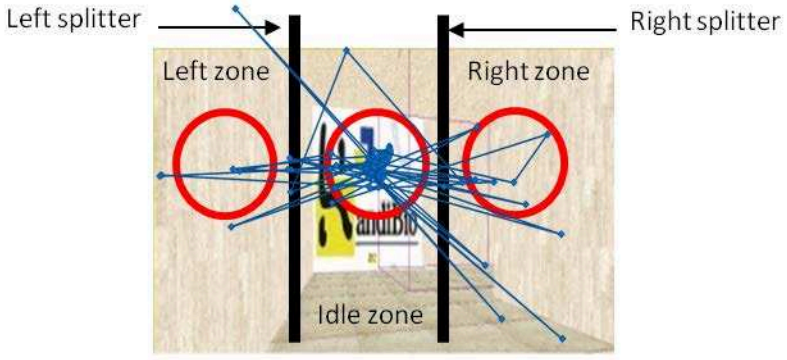

FIGURE 2.13: Example of implementation of the min-right/max-left algorithm

It's undeniable that a wheelchair is considered as wheeled robot, but this introduces some important differences. In fact, because a robot is provided with a communication protocol, it's easy to send it each time the required speed setpoint. This is not necessarily the case for a wheelchair which is considered as an analogical device; for example, in order to decrease velocity, a set of braking commands must be sent until reaching the speed setpoint. In a real wheelchair, the user has to move the joystick forward to accelerate, and backward to decelerate. In the virtual world, as it's basically a video game, to move forward or backward or to turn left or right the user has to push keyboard keys. The idea is to link both systems by simulating keyboard keys in the virtual world each time the user moves the joystick forward or backward. The same idea is applied for turning left and right based on the user's points of gaze and command zone detection.

2.4.2 Procedure

After sitting comfortably in the wheelchair, the calibration process starts by asking the user to look at the nine points of the screen to estimate his points of gaze. After detecting the command zones, the scene is projected on the panoramic screen. The way to command the wheelchair in the environment is explained and the map of the maze is displayed. The user is asked to navigate from the room A to the room G following three different paths or scenarios: the first path, which is the simplest one, consists of going directly from A to G through the hallway. Second path, the user has to go through B, C, D, hallway and G. while the most difficult path consists of going through B, C, E, F, hallway and G. This concludes the first trial. In the second one, which occurs after a week in order to inhibit the learning effect, the user has to perform the same tasks but

with the introduction of emotion detection through the EEG headgear. In this case, if the wheelchair velocity depends not only on joystick and gaze as inputs but becomes moderated through emotions.

2.4.3 Results

10 subjects (8 healthy and 2 palsy) took part in the experiment. The results were studied depending on three essential parameters: number of obstacles hit, navigation path deviation, and outbound points of gaze. The first one is calculated based on the obstacles that the user hit when he was navigating from A to G. For the navigation path deviation, an optimal path for the three scenarios was calculated using a path finder algorithm. Then, the distance between points of the followed path in each scenario and the optimal path are calculated. Finally, the standard deviation is calculated to choose the best path. At the end, the unbound points of gaze are calculated. In fact during the experiment, the user's POG are recorded. Due to some artifacts like searching in the environment, lack of concentration and emotional disturbance, the user can look outside the bounds delimited by the command zones already calculated. This parameter can help us to study the user's psychological aspect while navigating in the environment [61], if the number of outbound points is important, this means that the user was, in the major part of the navigation, uncomfortable. The combination of those parameters can help us to decide if the introduction of emotion is viable or not. To be noted, the discussed results assess healthy users and palsy ones separately. It is assumed that, the duration of one week separation between the emotion-based and non-emotion-based navigations is enough to exclude the learning effect.

Obstacles hit : The mean number of obstacles hit for all subjects, in the two trials (with and without emotion), for the three scenarios (easy, medium, and hard) is reported in the figures 2.14 and 2.15

For healthy subjects, the number of obstacles hit increases in accordance to the difficulty of the scenario. It reaches its maximum in the third scenario where the moving obstacles established in the room F are very difficult to avoid. This can be deduced from the variance that increases considerably in the third scenario. While in the first scenario even if the path to follow is very easy, the user finds it difficult to master the wheelchair navigation especially with the introduction of the gaze to turn left and right. But the difference resides in the way the trials slopes increase. In the first trial, the slope increases considerably especially between the second and the third scenario. While in the second trial, the slope is logarithmic and the number of obstacles hit in the second and the third scenarios are very close. Besides the overall obstacles hit dropped from the first

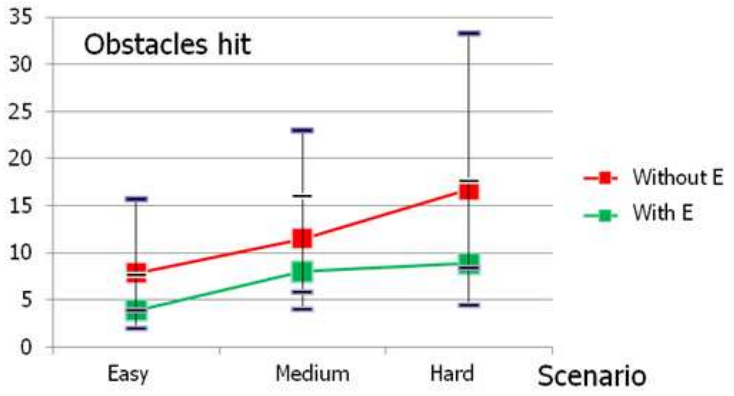

FIGURE 2.14: Number of obstacles hit in during the two trials for healthy subjects

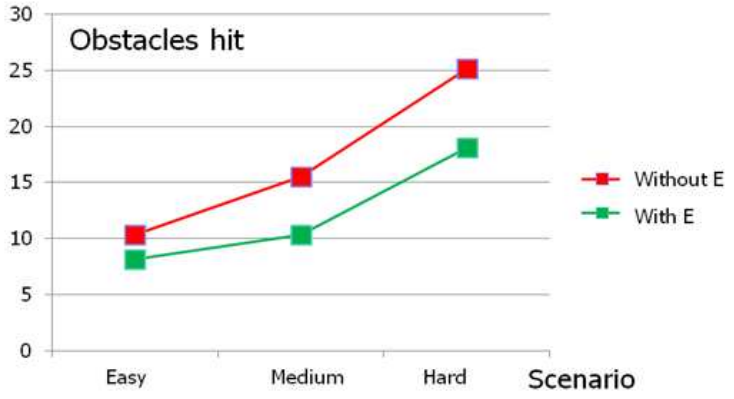

FIGURE 2.15: Number of obstacles hit in during the two trials for palsy subjects

trial to the second by half. Those results are not remarkable for the palsy users; in fact, the two curves have the same shape especially in the third scenario where the number of obstacles hit is very high in the two cases. Even though, in case of emotion-based navigation, the number of obstacles hit is lower than in non-emotion-based navigation.

Navigation path : During the experiment sessions, the wheelchair navigation path is recorded and then compared to an optimal path calculated using a pathfinder algorithm. One should notice, that the comparison is based only on path shape and no navigation time is taken into consideration. An example of navigation trajectory for the two trials in the three scenarios is shown on the figure 2.16.

Notice that the harder the scenario is, the greater the deviation from the optimal path becomes. This could be explained by the fact that the subject could be confused by the obstacles he faces during navigation and looses the control of his wheelchair or even lost the path he had the intention to follow. The distance between each point of the followed path and the optimal one is calculated for the two trials. Then, the standard deviation

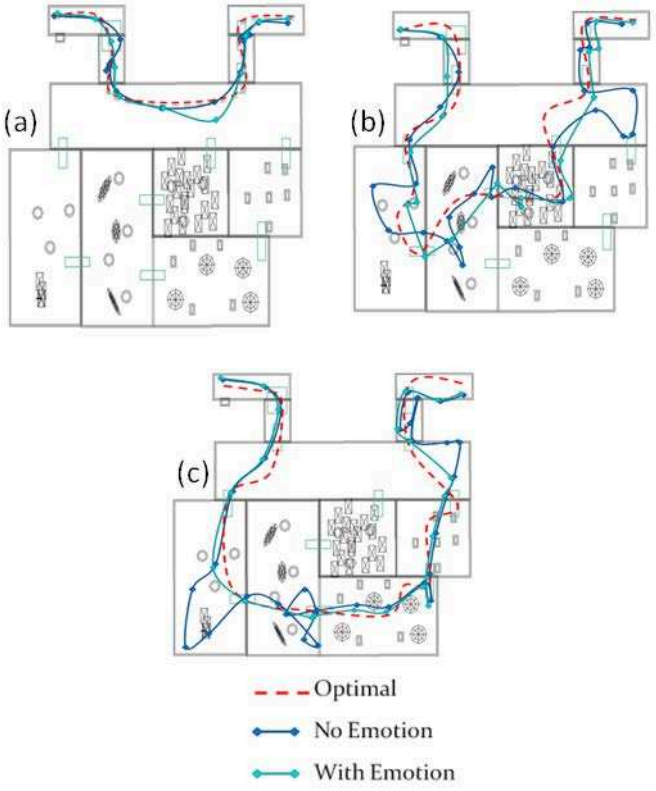

FIGURE 2.16: Navigation path for the three scenarios: easy (a), medium (b) and hard (c)

is calculated for each user, and finally the mean of all standard deviations are reported in the figures 2.17 and 2.18:

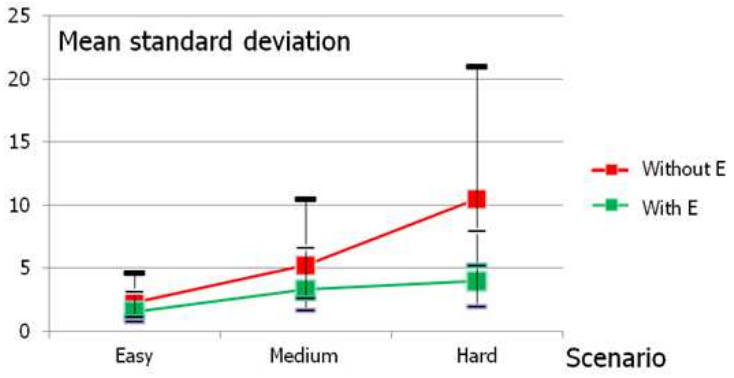

FIGURE 2.17: Mean standard deviations in the two trials for the three scenarios for healthy users

The deviation from the optimal path increases considerably going from the easiest scenario to the hardest one. And it reaches its maximum in the third scenario. Again, the moving obstacles cause a lot of problems in order to maintain a straight trajectory.

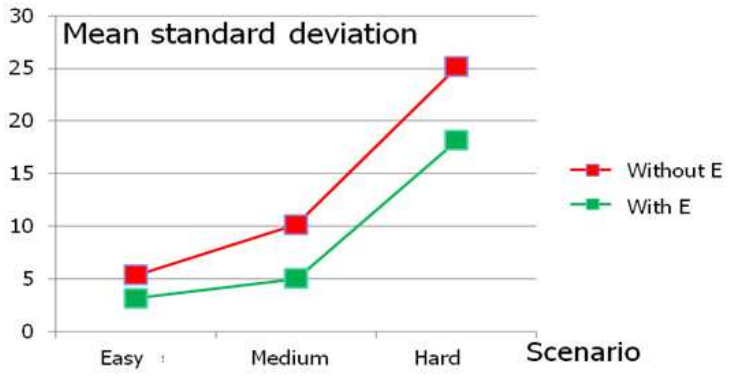

FIGURE 2.18: Mean standard deviations in the two trials for the three scenarios for palsy users

It deviates, in many times, the wheelchair from its initial path. But the same conclusion could be established when comparing both trials: the deviation rate dropped by half and the trials slopes are very different. Notice also that in the second trial, the deviation rate between the second and the third scenarios is very close. This means that the subject can control his wheelchair easily even if the scenario is harder. Again, the variance of the mean standard deviation increases considerably according to the scenario difficulty and can inform about the moving obstacles influence on the navigation performance. For palsy users, the performance is also worse than for healthy users and it can be reported that the deviation distance increases drastically especially in the hardest scenario. But can also confirm that the standard deviation is better in case of emotion-based navigation.

Points of gaze This parameter is very important as it can reflect the satisfaction of the subject during navigation. Even if the user controls the turn left/right by his gaze, it is revealed that he can perform some sporadic fixations that can reflect one of the following scenarios: either he's searching on the screen, confused by the obstacles or lacks concentration. This can be seen by the appearance of some points of gaze outside the command zones (Figure 2.19). The task in this situation is to calculate the number of those points.

The number of outbound points of gaze is calculated for each subject and the mean is presented in the Figure 2.20.

For healthy users, the results found in this study are different from the previous ones. The number of points of gaze increases considerably in both trials. It can be noticed also that in the second trial, the increase was even higher than in the first trial despite the overall number in the second trial is less than the first one. A justification for this fact is

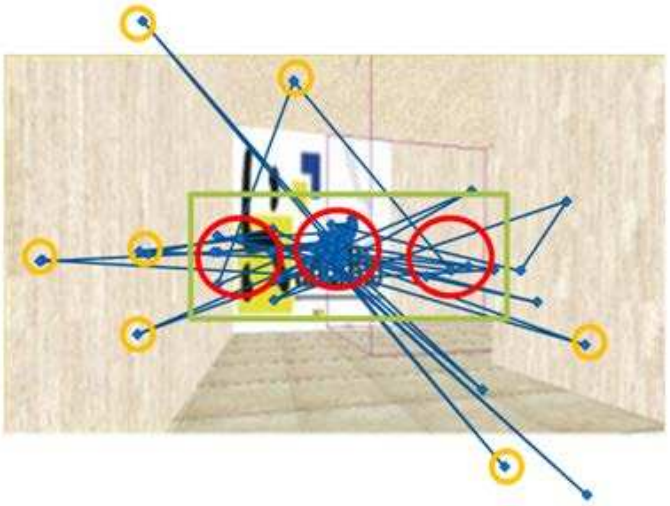

FIGURE 2.19: Outbound points of gaze (in orange)

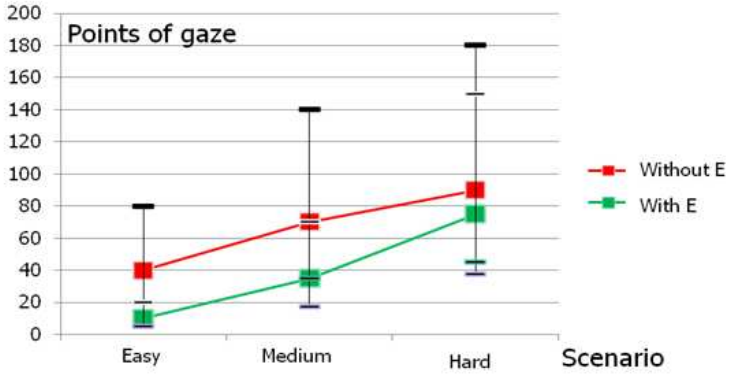

FIGURE 2.20: Outbound points of gaze for the two trials and three scenarios for healthy users

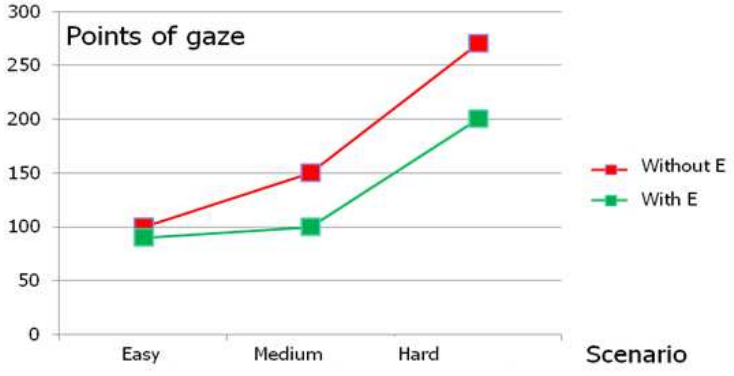

FIGURE 2.21: Outbound points of gaze for the two trials and three scenarios for palsy users

again the moving obstacles that play an important role in the navigation artifacts; even if the user is concentrated on commanding his wheelchair, he performs some unintentional fixations in the moving obstacles that can disturb his normal state. As a matter of fact, the moving obstacles had a lot of influence on the results found on the three parameters. This can imply that during wheelchair navigation, one has to give a lot of importance to the moving entities, such as humans, animals or even objects which can affect the choice of the suitable techniques and results. But for palsy users, the results are again very bad; in both trials and for the three scenarios, the points of gaze detected increase proportionally to the scenario difficulty. It is well reported that for those subjects, the integration of emotions was very embarrassing for them, especially that they are not initiated with such an approach.

2.4.4 Discussion

Emotion detection techniques were applied on a database set up from 40 healthy users but was tested afterward on both healthy and palsy ones. This could explain the bad results found on the latter. In fact, due to the lack of sufficient disabled samples, the collected data were based only on normal EEG activity. Besides, the total number of severely disabled samples (only two) is not enough to apply intelligent techniques and also to bring comparative studies about navigation enhancement using emotion or not. It can be seen from the previous figures that only affordable conclusions were observable on healthy subjects but not palsy. In this case, it was reported in some parameters (obstacles hit and path deviation) that integrating emotions can give better results especially by assuming that a separation of one week between the two trials is sufficient to omit learning effect. Which can imply that maybe by adding some training sessions; the subject performance can be better improved. But in a psychological perspective, and by assessing the points of gaze measures, it was reported that users feel uncomfortable with the integration of an extra component that can interfere with the wheelchair control which also can be enhanced by some training sessions. It was also reported that the moving obstacles have a consistent impact on the navigation performance as the variance of each parameter increases considerably when introducing this artifact. Moving obstacles can refer to real situations such as walking persons in streets, driving cars in roads... and must be deeply studied to enhance more emotion-based navigation. In the case of palsy users, and despite that the number of subjects is very low and that the comparative study couldn't be sufficiently done, it is though observable that emotion-based navigation gives some encouraging results that can be proved later by enlarging the severely disabled subjects database and adapting adequate techniques for this purpose. As for the chosen emotions that correspond to the real problems faced by

severely disabled people, the use of only four emotions from each quadrant needs to be enlarged too; in fact, in the same valence/arousal quadrant, relaxation and sleepiness can be found and if relaxation is considered as positive emotion, sleepiness reveals to be very dangerous in the navigation scenario and consequently, adding other emotions is very crucial.

2.5 Conclusions

In this Chapter, an enhancement to the standard wheelchair navigation was added using emotion detection as a braking system. Different techniques for extraction (Welch and Wavelets), selection (PCA and GA) and classification (MLP, LDA and SVM) were tried to keep finally the best combination consisting of: Wavelets, GA and MLP. The system was tested on a virtual environment and assessed on three parameters: obstacles hit, navigation path deviation and outbound points of gaze. For the first and second parameters, it was clear that the introduction of emotions is very efficient as it decreases the number of obstacles hit and the deviation rate from the optimal trajectory. However, it was not the case for the third parameter which is the outbound points of gaze: although the overall number decreases between the first and second trials, it still shows dependency on the scenario. When the latter gets harder, the number of outbound gaze becomes very high which can reflect dissatisfaction among subjects. The concept of dissatisfaction towards autonomous or semi autonomous systems was already reported in many studies [62]. Another point that can be discussed is the relationship between wheelchair navigation and familiarity with video games; in fact from the subjects who took part in the experiments many of them were familiar with video games and their tendency when turning left or right when moving forward is to perform the two commands in parallel while the others prefer stopping the wheelchair, turning left or right and then moving forward. The investigation is not finished yet but if it is proven that following the first approach is better for navigation safety, it is recommended for the next steps to perform commands one by one and not in parallel. But if it is revealed that the second approach is better, then we would recommend wheelchair users to play video games (car type games) in order to guarantee a safer navigation. As it was mentioned in the introduction, field experts suggest that mental fatigue is also very consistent in navigation enhancement and must be accounted for. For this purpose, fatigue correlations with EEG patterns as well as navigation enhancement based on fatigue scenarios will be conducted in the next chapter. At last, a system based on the fusion of mental fatigue and emotions can be proposed in order setup a wheelchair system with different navigation modes: manual, semi-autonomous and autonomous depending on the subject ability to drive his wheelchair.

Chapter 3

Influence of fatigue on wheelchair navigation

3.1 Introduction

As far as mental fatigue has some influence on cerebral activities, the latter shows specific perturbation on its EEG patterns, which can influence its role as a source of control. We investigate in this chapter two common sources of control namely: P300 and SSVEP. Dempster's work set the origins of the theory of belief functions [63]. It's a popular method to deal with uncertainty and imprecision. Dempster-Shafer theory introduces the notion of beliefs and plausibility assigned to possible measurements hypothesis. Formally, the evidence theory concerns the following notations:

• Frame of discernment: let θ be a finite set of elements; an element can be a hypothesis, an object, or in our case a level of fatigue. A subset of θ can be denoted by $\omega(\theta)$. Suppose that the subject can be one of the three levels of fatigue $LF, MF, andHF$ where LF is Low Fatigue, MF is Medium Fatigue and HF is High Fatigue. In this case, our frame of discernment can be set as :

$$\theta = LF, MF, HF\ and$$
$$\omega(\theta) = \{\emptyset, \{LF\}, \{MF\}, \{HF\}, \{LF, MF\}, \{LF, HF\}, \{MF, HF\}, \{LF, MF, HF\}\}$$

where : $\emptyset$ signifies "no fatigue" condition. If$F = \{LF, MF\}$ is a subset of θ, this implies that fatigue is either LF or MF.

• Mass functions: the mass function m is the mapping of the power set $\omega(\theta)$ to the number $t \in [0,1]$. The mass function can be expressed as follows :

$$\begin{aligned} m : \omega(\theta) \rightarrow [0,1] \\ m(\emptyset) = 0, \sum_{F \in \omega(\theta)} m(F) = 1 \end{aligned} \tag{3.1}$$

The mass function m is a basic probability assignment. $m(F)$ expresses the proportion of relevant evidence which supports the assumption that an element of θ belongs to the set F but to no subset of F. In our case, $m(F)$ can be considered as the belief degree regarding a certain level of fatigue. In general, any subset F of θ that verifies $m(F) > 0$ is called a focal element. In the same way, $C = \bigcup_{m(F) \neq 0}$, F is the kernel element of mass m in θ.

• Belief and plausibility functions: the belief function Bel is defined as follows:

$$Bel : \omega(\theta) \rightarrow [0,1] \; and \tag{3.2}$$

$$Bel(F) = \sum_{A \in F} m(A) \tag{3.3}$$

While the plausibility function is defined as:

$$\begin{aligned} Pls : \omega(\theta) \rightarrow [0,1] \; and \\ Pls(F) = 1 \quad Bel(\bar{F}) = \sum_{A \cap F \neq \emptyset} m(A) \end{aligned} \tag{3.4}$$

The belief function $Bel(F)$ defines the total amount of probability that must be distributed among elements of F and is a lower limit function on the probability of F. Plausibility function $Pls(F)$ measures the maximum amount of probability that can be distributed among the elements in F.

• Belief interval $[Bel(F), Pls(F)]$ is the belief interval that reflects uncertainty. Consequently, the interval span $[Pls(F) \quad Bel(F)]$ describes the unkown with respect to F.

• Properties of the belief function and plausibility are formulated as follows :

$$Bel(\emptyset) = Pls(\emptyset) = 0, Pls(F) \geq Bel(F)$$

$$Bel(F) + Bel(\bar{F}) \leq 1, Pls(F) + Pls(\bar{F}) \geq 1$$

$$if A < F, Bel(A) < Bel(F) \; and \; Pls(A) < Pls(F)$$

• Rules of evidence combination: if we suppose that m_1 and m_2 are two mass functions from two different sources, we have :

$$\begin{aligned} m(\emptyset) = 0, m(F) = \frac{1}{1 \quad K} \sum_{A \cap B = F} m_1(A) m_2(B) \\ where K = \sum_{A \cap B = \emptyset} m_1(A) m_2(B) > 0 \end{aligned} \tag{3.5}$$

K is interpreted as the measure of the conflict between sources. The larger K is, the more the conflicting sources are. The combination of m_1 and m_2 results in a mass function m which carries the joint information of the two sources:

$$m = m_1 \oplus m_2 = m_2 \oplus m_1$$

In general, for n mass functions $m_1, m_2, \ldots, m_n$ in θ, the measure of the conflict K is given by:

$$K = \sum_{\bigcap_{i=1}^{n} E_i = F} m_1(E_1) m_2(E_2) \ldots m_n(E_n) > 0 \tag{3.6}$$

Although there are other fusion theories such as possibilistic and probabilistic theory, but in order to apply a suited fusion technique, one has to formulate the data anomalies in a concise manner. In our case, the problem consists of detecting fatigue level using P300 and SSVEP. More precisely, after correlation study, only parameters (per sensor) the most correlated with fatigue level will be used later for individual classification i.e. each modality (P300 and SSVEP) will have its own classification block. Then, fusion technique will be adapted in order to enhance final decision in the case that the two blocks don't output the same decision. This being said, if we process by elimination, we can state that:

• Data issued from sensors are not perfect; this means that the use of probabilistic theory is not suitable. The latter is not capable to deal with this kind of imperfection

• Data are complete as well as the environment is not poorly informed; this means that the use possibilitic theory is applicable but not efficient. What's more, the fact that possibilistic theory is not very well known by fusion community could make a disadvantage for us as our purpose is not to develop a new theory but to use it as a tool

• The use of evidential and fuzzy sets theories could be the best choices for our context especially that two fusions cases are considered: the fusion of SSVEP and P300 blocks

for fatigue detection, and the fusion of fatigue level with emotion detection block, in order to decide if the system should switch to manual, semi-autonomous or autonomous mode.

In the following, in section 1, we will expose experimental environments setup for the two experiments. In section 2, a statistical study will investigate the correlation between P300 and SSVEP parameters per sensor and the fatigue level rated by subjects in each trial. In section 3, a comparison of different classification techniques will be used in order to suggest the best technique for that purpose. In section 4, Dempster-Shafer fusion technique will be proposed to assess its efficiency in comparison with individual classification. Finally, in section 5, emotion and fatigue blocks will be fused in a fuzzy logics-based decision module in order to help the system triggering into one of the three navigation modes : manual, semi-autonomous and autonomous mode which reflects the subject physical autonomy.

3.2 experimental setup for P300 and SSVEP

In this section, we will present the experimental environments in order to induce fatigue, P300 and SSVEP responses. As far as explaining the different steps taken in order to study correlation between ratings, P300 and SSVEP. At the end we report the techniques used to for classification.

3.2.1 Experimental setup

For the P300 virtual world, it consists of a hallway in which, the user has to navigate from point A to point B placed respectively at the start and at the end of the room. This being said, Three parameters were modified in each navigation scenario: luminosity (low, medium, high), number of obstacles (low, medium, high) and obstacles velocity (no velocity, low, medium, high) The combination of all cases results in 36 scenarios. the subject has to fill two missions; the first one is to be able to navigate from the starting point A to the goal point B by avoiding obstacles (etiher static or moving). In the second part, and in order to induce P300, each time the subject reaches the point B, a set of flickering pictures is displayed (fruits, vegetables and objects). This constitutes the time zero of the P300 waveform tracking recording. in each scenario, the subject is told about the stimulus that he must reach to go to the next level. For example, if the goal is to look for an apple, when the user is presented by the set of stimulus, he must hit that specific stimulus to be able to go for the next scenatio. the onset of the target stimulus marks the beginning of the P300 latency parameter measuring. The scenarios

are chosen randomly in a way, the learning process is inhibited as the subject don't have any idea about the modified parameter.

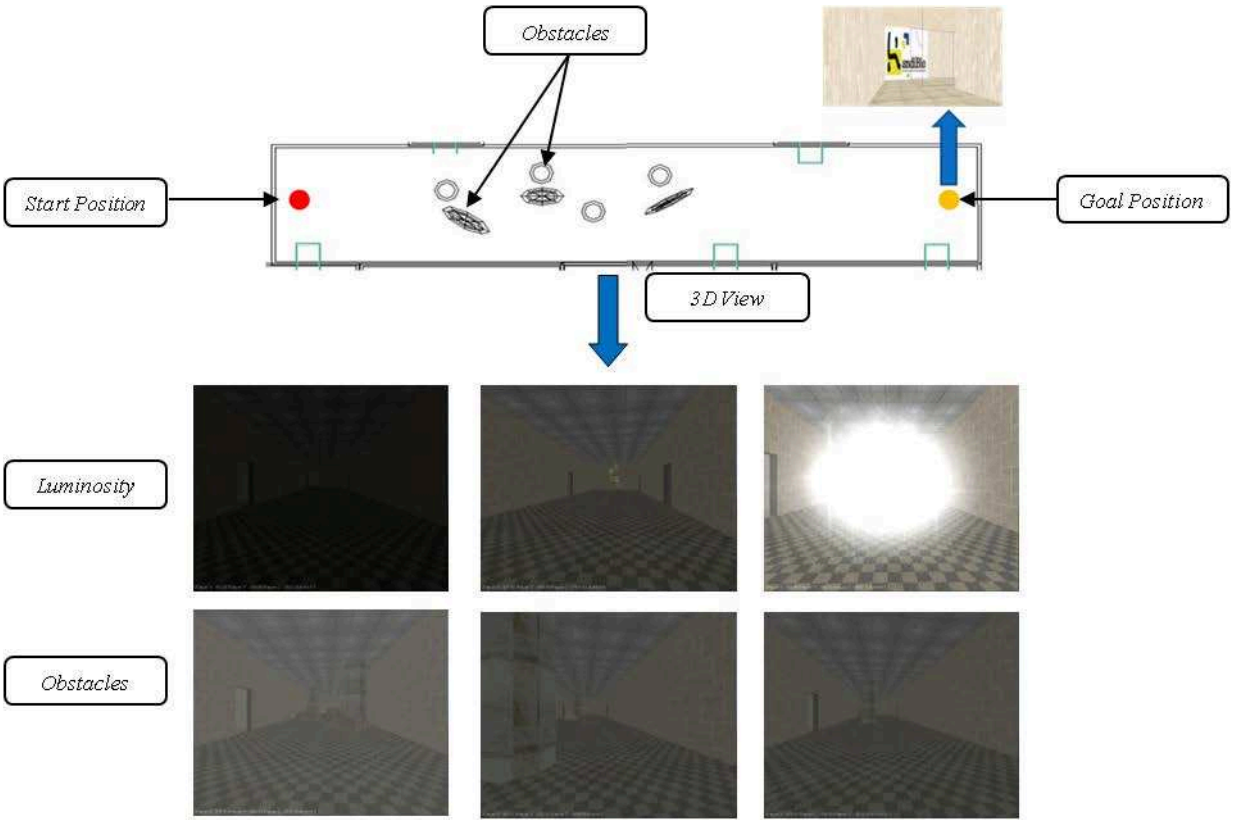

FIGURE 3.1: The plan of the navigation scenarios with the different level of luminosity and obstacles (Low, Medium, High))

In the other hand, for SSVEP experiment, the same hallway was used as far as the user is told navigate from point A to point B placed respectively at the start and at the end of the room. two parameters were modified in each navigation scenario: number of obstacles (low, medium, high) and obstacles velocity (no velocity, low, medium, high). The combination of all cases results in 12 scenarios. To induce SSVEP, flashing lights were placed on the hallway with a flashing frequency of 10 Hz.

3.2.2 procedure

Ten subjects (with two suffering from cerebral palsy) took part in the experiment. they signed a consent form that explains the experiment goals and steps. After sitting comfortably in the wheelchair, they were given a set of instructions informing them of the experiment protocol and the meaning of the different scales used for self-assessment. An experimenter was also present there to answer any questions. After the sensors were

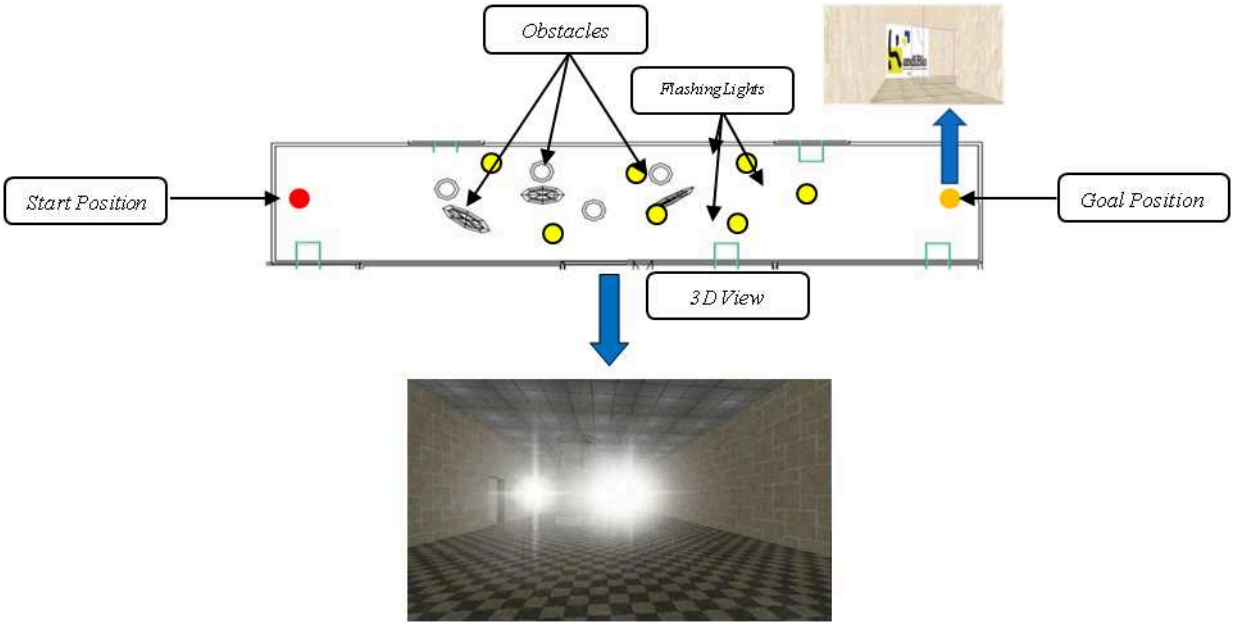

FIGURE 3.2: The navigation scenario with flashing lights integrated)

placed and their signals checked, the participants performed a practice trial to familiarize themselves with the system. Next, the experimenter started the physiological signals recording. The calibration process starts by asking the user to look at the nine points of the screen to estimate his points of gaze. After detecting the command zones, the scene is projected on the panoramic screen. The way to command the wheelchair in the environment is explained and the plan of the maze is displayed. The user is asked to navigate from the starting point A to the ending point B where a specific visual stimulus is displayed. In each scenario, one of the three parameters (luminosity, obstacles and velocity) is modified. After the projection of the scene, the subject can start navigation using gaze to turn left and right and the wheelchair joystick to move backward and forward. At the end of each trial, the subject has to give his assessment on a fatigue scale (ranging from 0 to 10). For the investigation of the correlates of the subjective ratings with the EEG signals, the EEG data was common average referenced, down-sampled to 128 Hz. Eyes artifacts were removed with Blind Source Separation technique (BSS). The signal recorded from the first five seconds of each trial was extracted as baseline. From which amplitudes (maximum and minimum) were averaged yielding to minimum and maximum reference amplitudes. Those were then subtracted from the trial amplitudes, conceding the change of amplitudes. For latency and period, those are compared to the reference mentioned by literature (300ms and 600ms). For each subject, the input measures matrix M and fatigue matrix F are initialized as follows:

$$M = \begin{pmatrix} m_{1,1} & \dots & m_{1,56} \\ \vdots & \ddots & \vdots \\ m_{36,1} & \dots & m_{36,56} \end{pmatrix} \tag{3.7}$$

$$F = \begin{pmatrix} f_1 \\ \vdots \\ f_{36} \end{pmatrix} \tag{3.8}$$

where : $m_{i,j}$ is the measure associated to the trial i and variable j defined by the combination of the parameter $par \in \{min, max, lat, per\}$ per sensor $s \in \{AF_3, AF_4, O_1, O_2, P_7, P_8$ $,F_3, F_4, T_7, T_8, FC_5, FC_6, F_7, F_8\}$ resulting in 56 possible crossings. f_i is the fatigue rating given by the subject in the i^th trial. We computed the Spearman correlated coefficients between the power changes and the subjective ratings, and computed the p-values, (p). The spearman coefficient is calculated as follows:

$$p = 1 \quad \frac{6 \sum d_i^2}{n(n^2 \quad 1)} \tag{3.9}$$

where : d_i is defined as $d_i = x_i \quad y_i$ in each observation, x_i and y_i are the ranks of the raw scores $X_i = m_{i,j}$ and $Y_i = f_i$ and n is the number of samples. This was done for each subject individually and, assuming independence, the 10 resulting p-values per sensor and power were then combined to one p-value via Fisher's method:

$$\chi^2 = \quad 2 \sum_{i=1}^{k} log_e(p_i) \tag{3.10}$$

where : p_i is the p-value associated to the subject i. While $k = 10$ is the total number of subjects in this experiment. For SSVEP experiment, The user is asked to navigate from the starting point A to the ending point B where a specific visual stimulus is displayed. In each scenario, one of the two parameters (obstacles and velocity) is modified while keeping the flashing lights in each scenario. After the projection of the scene, the subject can start navigation using gaze to turn left and right and the wheelchair joystick to move backward and forward. At the end of each trial, the subject has to give his assessment on a fatigue scale (ranging from 0 to 10). For the investigation of the correlates of the subjective ratings with the EEG signals, The frequency power of trials and baselines between 3 Hz and 64 Hz were then extracted using Welch's method with window of 64 samples. The baseline power was then subtracted from the trial one, yielding the change. The latter are averaged over the frequency bands of δ (1Hz and 3Hz), θ (4Hz

and 7Hz), α (8Hz and 13Hz), β (14Hz and 29Hz) and γ (30Hz and 60Hz). For each subject, the input measures matrix M and fatigue matrix F are initialized as follows:

$$M = \begin{pmatrix} m_{1,1} & \dots & m_{1,70} \\ \vdots & \ddots & \vdots \\ m_{12,1} & \dots & m_{12,70} \end{pmatrix} \tag{3.11}$$

$$F = \begin{pmatrix} f_1 \\ \vdots \\ f_{12} \end{pmatrix} \tag{3.12}$$

where : $m_{i,j}$ is the measure associated to the trial i and variable j defined by the combination of band wave signals $w \in \{\delta, \theta, \alpha, \beta, \gamma\}$ per sensor $s \in \{AF_3, AF_4, O_1, O_2, P_7, P_8$ $,F_3, F_4, T_7, T_8, FC_5, FC_6, F_7, F_8\}$ resulting in 70 possible crossings. then the same techniques in 3.9 and 3.10 are used to calculate p-values per sensor and power.

3.2.3 Classification

The best correlated sensors/parameters were kept for classification. And for this purpose, three classification algorithms were used namely: Support Vector Machine (SVM), Linear Discriminant Analysis (LDA) and Multi Layer Perceptron (MLP). In a supervised learning, given the feature vector as input, the output could be one of the three studied fatigue levels (Low Fatigue, Medium Fatigue, and High Fatigue). Those algorithms were explained in the previous chapter (see for example equations 2.8 and 2.9). but for SVM technique, w is the normal vector to the hyperplane containing the training set of the instances label pairs $(x_i, y_i)i \in \{1 \dots 36\}, x_i \in \mathbb{R}^8, ((x_i, y_i)i \in \{1 \dots 12\}, x_i \in \mathbb{R}^6$ in case of SSVEP) parameters of the i^th trial and $y_i \in \{\ \ 1, 1\}$ indicating the class to which x_i belongs, and b the offset of the hyperplane.

3.3 Results

3.3.1 Correlation between fatigue and environmental parameters

In order to quantify the term of mental fatigue, we referred to a correlation study between mental fatigue ratings and environment parameters mainly: number of obstacles hit and duration of the trial. In fact many studies suggested the influence of fatigue on the navigation performance [64]. In the present experiment, the following figure presents

the variation of the average of obstacles hit and durations over all participants for each trial session and explains the relationship between those parameters and fatigue scale ratings. Notice that the trial number presented in the figure 3.3 is just for identification as in reality, the subjects performed the trials in a randmized sequence.

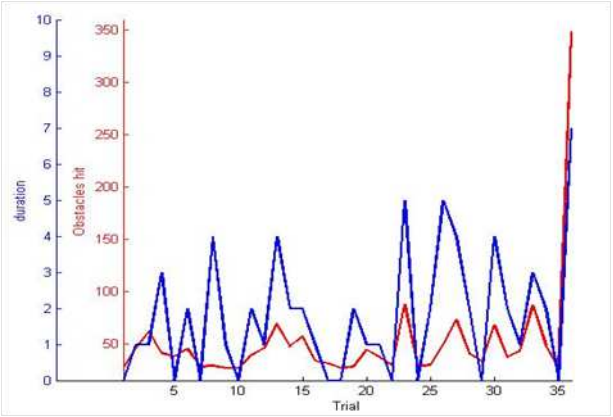

FIGURE 3.3: (average) obstacles hit and navigation duration variation for the chosen trials

It could be noticed that number of obstacles hit and the duration of the navigation are proportional. This could be explained by the fact that if one becomes tired, he could easily hit obstacles as it affects the duration of the navigation. But other important factors could explain such a result; in some trials, obstacles are moving toward many directions with variant velocities which can make it difficult for the user to navigate with no damage. Especially in the trial 36, where the navigation time reached almost 6 minutes as well as the number of hit obstacles are 8. The same correlation study was brought to investigate the relationship between mental fatigue and environmental parameters. Let the matrix E be the environment matrix that is formulated as follows:

$$E = \begin{pmatrix} e_{1,1} & e_{1,2} \\ \vdots & \vdots \\ e_{36,1} & e_{36,2} \end{pmatrix} \tag{3.13}$$

where : $e_{i,j}$ is the measure of the j^{th} parameter ($j \in \{1,2\}, 1 =$ "*duration*" *and* $2 =$ "*obstacles*") in the i^th *trial*($i \in \{1,\ldots,36\}$). Applying the same methodology as to calculate p-values for each parameter and subject, yields to the inter-correlations of different parameters over participants which are summarized in the following table :

It could be observed from this table the Obstacle and duration highly correlated (p=0.0134) which is explained by the fact that an increase of the number of obstacles hit will influence the navigation time. Notice also that fatigue has a highly positive correlation

TABLE 3.1: subject inter-correlations between parameters and correlation between each environmental parameter and fatigue

Parameter	Duration	Obstacle	Fatigue
Duration	-	0.0134	0.024
Obstacle	-	-	0.019
Fatigue	-	-	-

with both parameters with a stronger one regarding obstacles hit (0.019). It seems that people, even when they are tired, could manage to reach the navigation goal even if the number of obstacles hit is high. This is due to the fact that in virtual navigation, in some cases, when obstacles are hit, the wheelchair gets through the wall or the pillar and doesn't stop. The results reflect that the experiment was successful to induce mental fatigue even that some bugs on the virtual reality program biased some of the results. In some other cases, the trial on itself was repeated as the subject wasn't able to avoid obstacles they hit.

3.3.2 Correlation between ERP parameters and subjective ratings

Before proceeding to the results presentation, the subjects were gathered in two samples: the healthy sample which involves all healthy subjects, the pathological sample which contains our two palsy ones. from now on, the reported results of the applied techniques will present the average of each sample individually and the overall classfication rate for the combined samples as we report the combined F-score (in percentage), based on the precision and recall measures. For P300, the results are summarized in Table 3.2 and Figure 3.4 show the (average) correlations with significantly ($p < .05$) correlating electrodes highlighted.

TABLE 3.2: The electrodes for which the correlations with the scale were significant ($p < .05$) for each considered parameter

Parameters			
Maximum	Minimum	Latency	Period
O_1 0,01596** O_2 0,04556* T_8 0,01214**	-	-	F_3 0,03811* F_4 0,01922** FC_6 0,03136* O_1 0,01717** O_2 0,021558*

For minimum and latency, no correlation was found between them and the subjective ratings ($p > .05$). This is due to the fact that the minimum is considered as response phenomena so that the signal could reach its normal state and it's not related to fatigue as well as for latency, this could be justified by the fact that latency depends on the presented stimulus which was the same in all experiments. This was also reported in

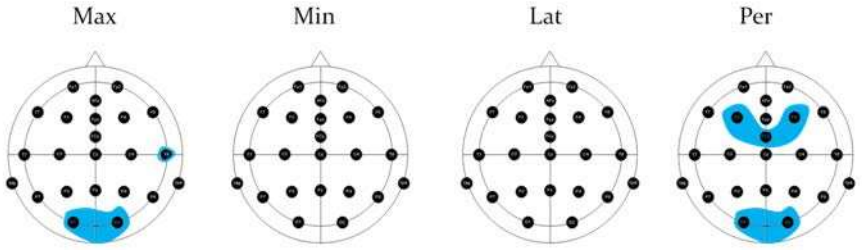

FIGURE 3.4: Mean correlations over subjects between fatigue ratings and P300 components

many studies (see for example [65]). While other studies [64] have stated that the latency depends on the complexity of the visual stimulus presentation, this is not the case for our experiment where the same picture was used.. For maximum, it can be noticed that the latter occurs especially in the occipital region, thus over visual cortices. The latter showed the strongest correlations ($p = .01$). This is due to the fact that the presented stimuli are of visual nature. Fatigue influenced maximum amplitude in three steps: first an increase in the Positive amplitude was noticed due to the engagement of the subject with the experiments (this takes roughly between fifteen and twenty minutes). In the second part, these amplitudes become more stable as the user reaches his maximum concentration in this period (until forty minutes). Finally, these amplitudes started to decrease as mental fatigue starts to increase considerably and with special effects injected in the environment especially the moving obstacles and the changing lights (Figure 3.5). Notice also that maximum amplitude of temporal sensor T_8 correlates with subjective ratings which can be explained by the fact that temporal lobe interprets the meaning of visual stimuli and establish object recognition. In fact, the ventral part of the temporal cortices appears to be involved in high-level visual processing of complex stimuli such as faces and scenes. Anterior parts of this ventral stream for visual processing are involved in object perception and recognition [66].

For the duration of the P300, the latter also passes through many states: the period starts to shorten as the subject becomes more concentrated, after that it becomes longer when he feels mentally tired. This can be explained by the fact that the user's reaction attitude becomes too slow as far as fatigue increases. The results of the classification are summarized in the table 3.3:

The results show that MLP has the best classification rate with 80%. LDA (79%) presents, generally, good results as well as MLP. SVM obtained lower than MLP and LDA but the difference is neglected. In this case, two observations can be given; The number of palsy subjects is relatively low (only 2), thus there is no noticeable differences in classification rates as they are relatively low. The overall number of subjects is ten,

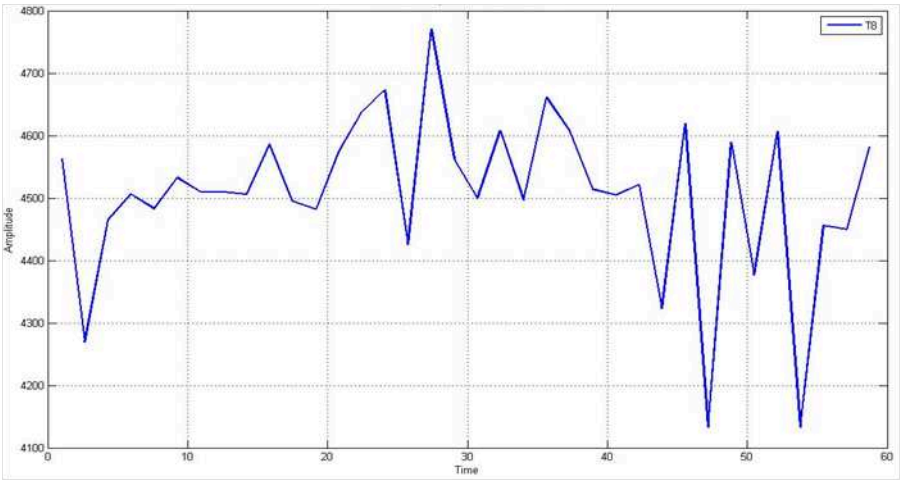

FIGURE 3.5: Maximum amplitude changes in the sensor T_8

TABLE 3.3: Classification rate for P300 modality

Technique	Classification rate		
	Healthy	Pathological	All
SVM	80%	74%	77%
LDA	82%	76%	79%
MLP	83%	77%	80%

the classification rate can be acceptable as it could be more enhanced by adding more subjects, thus enlarging the database, and providing more learning time. One of the subjects was excluded from this study due to his familiarity with video games; in fact, he was able to finish all the scenarios without being affected with fatigue which led to a very low rating scale over all experiments while for the others, the average ratings were relatively balanced. In the other hand, for SSVEP, The results are reported in table 3.4 and Figure 3.6 show the (average) correlations with significantly ($p < .05$) with correlating electrodes highlighted.

TABLE 3.4: The electrodes for which the correlations with the scale were significant ($p < .05$) for each considered parameter

Parameters				
δ	θ	α	β	γ
-	-	O_1 0,01755** O_2 0,01832** P_7 0,0354* P_8 0,032*	O_1 0,0335* O_2 0,045*	-

For the band waves δ, θ and γ, no correlation was found between them and the subjective ratings ($p > .05$). This can be explained by the fact that the frequency of the flashing lights is 10Hz; as a result, response frequency is more prominent in the bands close to the stimulus frequency of presentation or to its harmonics which is not the case for the

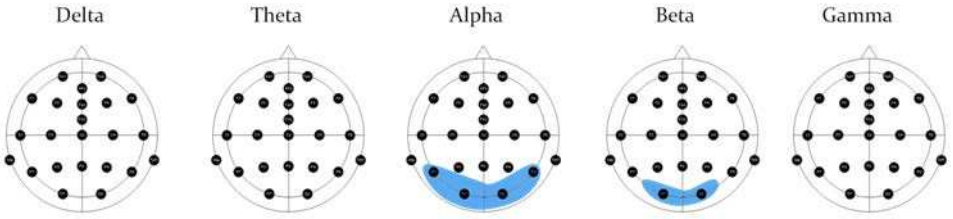

FIGURE 3.6: Mean correlations over subjects between fatigue ratings and SSVEP components

mentioned band waves. For α and β, it can be noticed that the latter occur especially in the occipital region, thus over visual cortices. The latter showed the strongest correlations ($p = .01$). This could be explained by the fact that the presented stimuli are of visual nature. Also, as the presentation frequency was fixed to 10Hz, the principal response frequency and its second harmonic are localized in the frequency bands ranging from 8Hz to 29Hz which encloses the α and β waves. This also explains the fact that α waves show the strongest correlations especially for O_1 and O_2. It could be noticed also that parietal lobe of the brain (P_7 and P_8) show a good correlation with fatigue; The parietal lobe plays important roles in integrating sensory information from various parts of the body, knowledge of numbers and their relations, [35] and in the manipulation of objects. Its function also includes visuospatial processing.

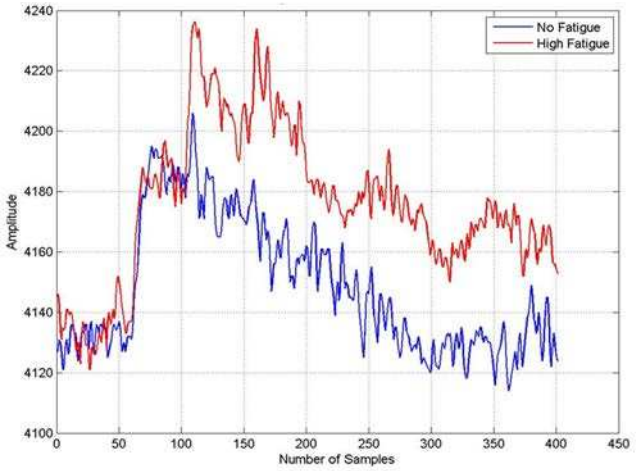

FIGURE 3.7: Amplitude changes of SSVEP in the sensor O2

The SSVEP maximum amplitude is influenced by the subject state and evolutes following many steps: in the first part, the maximum amplitude increases as the user becomes more concentrated, this amplitude starts slightly to decrease as the subject becomes more and more tired. At the end, this amplitude attends its minimum as the subject is exhausted. The results of the classification are summarized in the following table:

TABLE 3.5: Classification rate for SSVEP modality

Technique	Classification rate		
	Healthy	Pathological	All
SVM	85%	65%	75%
LDA	88%	68%	76%
MLP	86%	64%	75%

The results show that LDA has the best classification rate with 76%. MLP presents, generally, good results as well as SVM (75%). SVM and MLP were lower than LDA but the difference is not very big. The classification rate is not good enough due to many explanations; the number of subjects isn't many as it could form a good database which is also the case for the number of trials. Despite that, the classification rate could be acceptable for such conditions and may give better results if the experiment involved many subjects and many trials. There is a big difference in classification rate between healthy anf pathological samples ; the latter present a very bad performance as only two subjects are not sufficent to train the used techniques as well as the number of trials per subject in case of SSVEP (12 trials) is lower than those of P300 (36 trials).

3.3.3 Fusion of data using evidential theory

In this section, a fusion technique is proposed in order to merge features and sensors that showed the best correlations in the previous section with fatigue levels. We consider four states: "No Fatigue" (NF), "Low Fatigue" (LF), "Medium Fatigue" (MF) and "High Fatigue" (HF). In total, 8 sensors are used: O_1, O_2, T_8, F_3, F_4, FC_6, P_7, and P_8. From the first two, maximum amplitude, period (extracted from time domain), α and β waves (extracted from the frequency domain). From T_8 maximum amplitude is extracted. From F_3, F_4 and FC_6 periods are extracted. Finally from P_7, and P_8 are extracted α waves. The total number of features is 14. One of the most important steps in evidential reasoning is the calculation of the mass function based on information provided by sensors. let :

$$f = [x_1, x_2, \ldots, x_{14}] \tag{3.14}$$

f represents the fatigue level. x_i is the i^{th} feature given according to the corresponding fatigue level. For all fatigue levels F, the matrix could expressed as follows:

$$F = \begin{pmatrix} f_1 \\ \vdots \\ f_4 \end{pmatrix} = \begin{pmatrix} x_{1,1} & x_{1,2} & \ldots & x_{1,14} \\ \vdots & & \ddots & \vdots \\ x_{4,1} & x_{4,2} & \ldots & x_{4,14} \end{pmatrix} \tag{3.15}$$

f_i is the feature vector describing the i^{th} fatigue level. $x_{i,j}$ is the j^{th} feature of the i^{th} fatigue level. Let S_k represent the measurement vector obtained from k_{th} sensor:

$$S_k = [S_{k1}, S_{k2}, \ldots, S_{ke_k}] \; with \; k = 1, 2, \ldots, 8 \tag{3.16}$$

S_{ki} is i^{th} element of sensor S_k. $i = 1, 2, \ldots, e_k$ where e_k is the number of elements provided by the k^{th} sensor. As for example for the sensor O_1, $e_k = 4$ as 4 parameters are extracted from this sensor : maximum amplitude, period, α and β. The next step consists on calculating the distance between the measured features and the feature that describes each fatigue level. One of the best known distance measure is Minkowski one [67]. This could be defined as:

$$d_{ki} = \begin{cases} \left[\sum_{j=1}^{e_k} (S_{kj} \quad x_{ij})^{\alpha}\right]^{\frac{1}{\alpha}} & \text{if } k = 1 \\ & \text{i=1,2,3,4; k=1,2,...,8} \\ \left[\sum_{j=1}^{e_k} (S_{kj} \quad x_{i(j+e_k \;\; 1)})^{\alpha}\right]^{\frac{1}{\alpha}} & \text{if } k > 1 \end{cases} \tag{3.17}$$

d_{ki} is the distance between S_k and f_i.α is the parameter that defines the type of the distance. If the latter is equal to 2, than the distance converges to an Euclidian one. In the other hand, if $\alpha = 1$ this means that the distance converges to a corner distance. Consequently, a distance matrix could be established in the following form:

$$D = \begin{pmatrix} d_{1,1} & d_{1,2} & \ldots & d_{1,4} \\ \vdots & & \ddots & \vdots \\ d_{8,1} & d_{8,2} & \ldots & d_{8,4} \end{pmatrix} \tag{3.18}$$

where each row in the matrix D, is the distance between the measurements issued from one sensor and all fatigue levels. While each column is the distance of one fatigue level to all sensors measurements. d_{ki} is inversely proportional to the i^{th} fatigue level. In order to normalize data, we define $p_{ki} = \frac{1}{d_{ki}}$ .This results in the following matrix:

$$P = \begin{pmatrix} p_{1,1} & p_{1,2} & \ldots & p_{1,4} \\ \vdots & & \ddots & \vdots \\ p_{8,1} & p_{8,2} & \ldots & p_{8,4} \end{pmatrix} = \begin{pmatrix} p_1 \\ \vdots \\ p_8 \end{pmatrix} \tag{3.19}$$

$p_k = [p_{k1}, p_{k2}, \ldots, p_{k4}]$ with $k = 1, 2, \ldots, 8$ is termed as the mass function assigned by the kth sensor to the 4 levels of fatigue. Once the basic probability or the mass function is obtained, the final mass function can be formed as follows:

$$m = p_1 \oplus p_2 \oplus \ldots \oplus p_8 = (m_1 m_2 \ldots m_4)$$

where : m_i is calculated as follows:

$$m_i = \frac{\prod_{k=1}^{8} p_{ki}}{1 \quad \sum_{i=1}^{4} \prod_{k=1}^{8} p_{ki}} \tag{3.20}$$

In this method, two conditions are to be considered carefully:

• Mutual exclusion: fatigue levels should be independent from one to another. As well as, only one fatigue level could be expected to occur at a given instance. This means that for example $m(\{LF, MF\})$ or $m(\{LF, HF\})$ or $m(\{MF, HF\})$ is zero.

• Sensor weighting: the information detected from each sensor could vary depending on the sensitivity of the latter due to its placement for example. For example sensitivity of T_8 and P_8 differs in a way that the first is more sensitive in the case of P300 detection while the second is more sensitive in SSVEP one. This aspect could be accounted for by adding a weight factor should be added to the p_{ki} . though, it comes that

$$p'_{ki} = w_{ki}\ p_{ki} \tag{3.21}$$

where : w_{ki} is the weight associated to each sensor capability. Finally the rules for decision making are very important as it can inform about the decision we have to carry. In this context, many rules were presented. But we give here the most commonly used:

• Maximum support rule; hypothesis with maximum belief function is chosen

• Maximum plausibility rule; hypothesis with maximum plausibility function is chosen

• Absolute supporting rule; hypothesis with maximum belief function is chosen; it will not give a decision if the width of evidence interval is larger than the difference between the two largest supports.

• Maximum support and plausibility rule; hypothesis with maximum belief and plausibility functions is chosen.

Each used sensor for classification can be considered as a piece of the whole information. Thus, each sensor can represent a belief structure. In the tables 3.6 - 3.9, the features extracted from sensors $O_1, O_2, T_8, F_3, F_4, FC_6, P_7, and\ P_8$ are presented for each fatigue level NF (No Fatigue), LF (Low Fatigue), MF (Medium Fatigue), HF (High Fatigue). The features are collected using the following algorithm:

Data: Features from all sensors
Result: Features extracted for a specific fatigue level
initialization;
for *each fatigue level* **do**
  while *not finalizing all features* **do**
    read current feature;
    if *Feature corresponds to the current level of fatigue* **then**
      Save it;
    else
      Search for another one;
    end
  end
  average all saved features
end

Algorithm 1: How to collect features that correspond to the same level of fatigue

The matrix F (3.22) depicts fatigue levels according to the calculated features.

$$F = \begin{pmatrix} f_1 \\ f_2 \\ f_3 \\ f_4 \end{pmatrix} = \begin{pmatrix} 4655.4 & 495.1 & 19.2 & 11.1 & 164.7 & 305.7 & 8.9 & 5 & 119.7 & 392.7 & 505.8 & 562.6 & 6 & 5.6 \\ 4709.5 & 239.7 & 20.3 & 14 & 166.2 & 233.6 & 12 & 8.6 & 79.7 & 549.8 & 350 & 323.1 & 6.9 & 7.5 \\ 4623.8 & 321.7 & 15.1 & 8.85 & 164.8 & 198.5 & 9.1 & 5 & 45.2 & 313.8 & 194.5 & 174.3 & 8.6 & 8.1 \\ 4572.7 & 133.3 & 11.6 & 8.94 & 169.5 & 157.9 & 8 & 5 & 40 & 192.2 & 161.3 & 166.9 & 8.5 & 4.5 \end{pmatrix} \tag{3.22}$$

Applying equations 3.17 and 3.18 results in the distances matrix denoted by D and expressed using Minkowski distance with ($\alpha = 2$). The next steps are already known as they were explained earlier. Once F is determined, the evidence theory could be carried out. To be noticed, the weights used for each sensor is 1/3 as they are considered sensitive with the same capacity to the fatigue level. Performance and decision classification are made using distance measures, combination of all mentioned information of all sensors and applying the rationality rules. Table 3.10 presents a comparison between the best techniques applied earlier (MLP for P300, SVM for SSVEP) and the use of Demspter-Shafer (D-S) evidential theory.

TABLE 3.6: Features extracted from sensors $O_1, O_2, T_8, F_3, F_4, FC_6, P_7$, *and* P_8 under NF level

O_1				O_2				T_8	F_3	F_4	FC_6	P_7	P_8
Max	Per	α	β	Max	Per	α	β	Max	Per	Per	Per	α	α
4661	590.36	13.5	10.5	162.4	304.14	5.5	3.4	182.9	399.71	520	781	6.3	5.9
4664	596.59	20.7	11.3	160.63	308.06	7.6	4	188	399.61	597	500	5.2	4.8
4632	599.57	14.5	11.5	163.8	306.59	10.1	5.3	107.55	395.43	700	600	5.3	5.7
4654	595.31	18.6	10.7	169.6	302.13	11.6	5.1	107.55	400.12	750	750	5.7	6.7
4683	595.31	20.2	12.1	172.68	305.55	11.3	4.5	87.547	393.37	594.24	592.65	6	6.2
4662	397.31	13.4	11.5	165.76	308.19	10.8	4.2	126.53	353.79	592.73	783.76	7.5	5.4
4671	394.62	18.6	10.8	160.05	305.35	8.7	5.4	95.758	394.65	201.87	590.27	4.9	4.7
4684	390.76	23.6	10.6	165.5	305.75	9.3	7.6	90.6	396.04	394.88	394.63	5.2	3.8
4624	398.61	28.5	10.1	162.68	303.49	8	7.4	100.13	394.65	391.17	396.96	7.4	6.7
4619	392.57	20.6	12	163.45	307.33	6.5	2.8	110.15	400	316.16	237.11	6.8	5.8
4655.4	495.1	19.2	11.1	164.7	305.7	8.9	5.0	119.7	392.7	505.8	562.6	6	5.6

TABLE 3.7: Features extracted from sensors $O_1, O_2, T_8, F_3, F_4, FC_6, P_7$, *and* P_8 under LF level

O_1				O_2				T_8	F_3	F_4	FC_6	P_7	P_8
Max	Per	α	β	Max	Per	α	β	Max	Per	Per	Per	α	α
4737	358.17	15.6	15.2	193.19	202.78	7.5	6.3	74.85	703	592.73	300.58	9.3	7
4632	201.87	23.5	18.2	145.49	236.44	9	7.8	59.49	702	397.83	306.52	3.3	5.3
4712	277.35	10.3	13.5	155.76	278.24	13	6.3	31.274	747	201.88	305.54	6.7	13.2
4876	201.87	19.6	9.4	180.88	302.13	12.7	15.3	163.075	784.25	750	302.66	8.2	8.4
4683	237.26	22.4	14.1	193.19	198.95	11.5	11.5	99.08	600	244.15	307.03	7.5	6
4721	243.7	20.8	12.7	143.45	120.97	12.1	12.2	47.695	490	240.13	394.63	9	7.2
4669	201.29	15.7	17	142.42	158.75	18.5	8.3	165.122	399.71	234.52	396.96	3.5	5.9
4711	202.32	24.7	12.2	165.5	238.66	19.1	8.8	73.337	594.25	283.31	308.34	7.1	6.2
4666	236.84	29	13.1	171.65	201.67	10.2	5.3	49.23	238.63	354.16	306.35	6.8	7.8
4688	236.84	21.2	15	170.12	397.31	11.8	4.8	33.842	239.36	201.87	302.36	7.5	8.1
4709.5	239.751	20.3	14	166.2	233.59	12	8.66	79.6995	549.82	350.058	323.097	6.89	7.51

TABLE 3.8: Features extracted from sensors $O_1, O_2, T_8, F_3, F_4, FC_6, P_7$, *and* P_8 under MF level

O_1				O_2				T_8	F_3	F_4	FC_6	P_7	P_8
Max	Per	α	β	Max	Per	α	β	Max	Per	Per	Per	α	α
4692	202.32	5.5	7.3	113.71	278.24	3	3.4	37.811	593.89	202.01	87.429	5.4	4
4615	236.84	19.1	8.5	172.68	158.36	5.8	4	34.526	238.36	398.86	278.91	10.1	5
4605	390.76	12	5.7	147.07	236.44	9.7	5.3	38.316	395.44	87.723	157.67	7.8	3.6
4561	392.25	20.3	12.3	157.29	158.77	10.3	5.1	41.905	398.72	279.36	237.99	4.4	10
4688	163.35	10.5	10.1	142.42	120.97	9.4	4.5	47.092	197.25	158.97	162.54	5.2	4.3
4602	398.61	13.2	6.6	131.14	198.95	15.9	4.2	49.895	785.61	241.32	124.76	6.4	8.2
4640	398.61	10.5	12.7	215.76	158.31	6	5.4	96.779	84.116	161.97	203.24	3	9.1
4618	243.33	22.1	11.2	193.19	235.06	12.4	7.6	42.189	162.96	124.74	84.693	7.2	2.3
4615	398.61	25.5	5.1	182.6	201.67	5.5	7.4	34.526	80.358	203.01	165.31	5.4	6.6
4602	392.57	12.6	9	192.45	238.66	13.2	2.8	29.368	200.88	86.618	240.09	8	5
4623.8	321.725	15.1	8.85	164.83	198.54	9.1	4.97	45.2407	313.76	194.4581	174.2632	8.65	8.11

TABLE 3.9: Features extracted from sensors $O_1, O_2, T_8, F_3, F_4, FC_6, P_7$, *and* P_8 under HF level

O_1				O_2				T_8	F_3	F_4	FC_6	P_7	P_8
Max	Per	α	β	Max	Per	α	β	Max	Per	Per	Per	α	α
4587	201.87	3.5	5.5	171.65	121.4	3.2	3	12.453	400.51	157.97	195.61	5	4.6
4568	196.28	2.6	10	151.65	244.08	5.5	4.5	59.632	87.594	84.409	166.03	5	4
4645	120.5	4.8	8.6	133.71	243.75	9.1	2.7	44.737	277.51	161.64	83.265	4.3	5.2
4426	156.83	9	11.3	170.12	123.83	10	3.2	26.295	164.69	84.49	162.99	4.2	7.3
4579	79.116	12.2	10.2	133.71	196.08	12.5	6.3	33.989	243.76	197.19	82.937	7.4	8.1
4561	163.6	15.1	8.5	116.78	157.62	9.9	3.8	58.095	166.18	244.36	164.62	5.3	5
4537	44.912	11.3	4.7	270.63	83.473	8	4.7	95.758	125.38	274.85	88.804	3.6	3.9
4654	165.94	20	8.3	82.421	163.13	10.2	10.2	31.653	205.02	84.322	199.22	4.6	3.2
4596	80.544	20.1	9.1	177.29	87.721	7.5	8	12.958	86.154	202.1	243.07	7	5.7
4574	124.03	18.3	13.2	287.04	157.79	4.3	3.6	24.242	164.62	121.84	282.53	8.9	5.6
4572.7	133 .36	11.6	8.94	169.5	157.88	8	5	39.9812	192.15	161.3171	166.9076	8.5	4.5

TABLE 3.10: Comparison of the different techniques used for classification

Technique	Features used	Classification rate		
		Healthy	Pathological	all
MLP	$O_{1max}O_{2max}O_{1per}O_{2per}T_{8max}F_{3per}F_{4per}FC_{6per}$	83%	76%	80%
LDA	$O_{1\alpha}$ $O_{2\alpha}$ $O_{1\beta}$ $O_{2\beta}$ $P_{7\alpha}$ $P_{8\alpha}$	88%	68%	76%
D-S	$O_{1max}O_{2max}O_{1per}O_{2per}T_{8max}F_{3per}F_{4per}FC_{6per}$ $O_{1\alpha}$ $O_{2\alpha}$ $O_{1\beta}$ $O_{2\beta}$ $P_{7\alpha}$ $P_{8\alpha}$	86%	80%	84%

It could be noticed that the fusion of data using D-S theory is very efficient in a way that it could improve the classification rate among the use of techniques separately.Although the classification rate for pathological sample is not good, the superiority of D-S theory over LDA and MLP is evident. It is very well understood that the fusion of data could be very important; in fact, information issued from different sensors are highly conflicting as for the same sensor we can extract different features. Example: for sensor O_1 or O_2, features extracted are: O_{1max}, O_{2max}, O_{1per} and O_{2per} when assessing P300 and at the same time $O_{1\alpha}$, $O_{2\alpha}$, $O_{1\beta}$, and $O_{2\beta}$ are extracted as to assess SSVEP. This could lead to a critical problem if this aspect is not very well assessed and defined. The use of fusion technique could handle this issue. Defining belief intervals for each sensor and feature is very benefic in a way that it could improve the classification of fatigue data.

3.4 Navigation mode switching decision

In this part of the study, a combination between fatigue and emotion is proposed. The latter is based on the use of fuzzy sets to describe the different levels of emotions and fatigue. Those should be combined neatly in order for the system to decide if it should switch to the manual, semi-autonomous or autonomous mode. In the first one, it suggests that the user is totally able to command his wheelchair by his own. In the second case,

it suggests that the user can still command his wheelchair; however the system should assist him (the form of assistance could be vocal or visual feedback such as traffic lights, voice noticing the presence of obstacles...) and finally in the last case, the system supposes that the user is totally unable to use his wheelchair and by doing so, it could present a danger for him; think of the situation that the user is highly tired (High Fatigue level detected) it could be mapped as the system should take the control autonomously to transport him to the desired place. The use of threshold value to determine emotions is conservative: those values are static and no flexibility is offered to counter variations in input patterns. This limitation could be overcome this problem, a fuzzy decision inference module is proposed for all classifiers as well as final decision. In our context, the general architecture is proposed as follows:

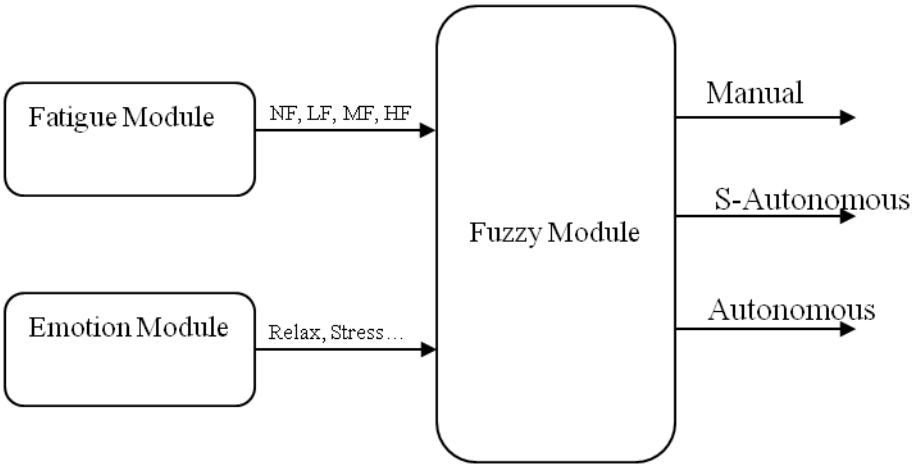

FIGURE 3.8: Final decision fusion architecture

The fuzzy logic decision module is used in the verification stage. As it is mentioned, fatigue module uses evidence theory in order to detect in the first part the belief interval for each fatigue level and at the end decides which level to keep based on the rules already mentioned. This being said, the middle point of each interval is then calculated and considered as input to the fuzzy block which maps it into membership function. In the other hand emotion level is also mapped into membership function: the score attributed to the most probable emotion is kept as input to the fuzzy system and though mapped into membership function. After combining different rules, the defuzzification centroid strategy is used. Input membership functions are presented in Figures 3.9 and 3.10. The mapping of emotion level to membership functions has to follow many steps: First the distance between the tested parameter and the different classes is calculated. The minimum distance is chosen based on KNN (K-Nearest Neighbor). The latter is mapped into the considered level to be later projected and membership function is calculated. For the fatigue level, the mean of the confidence interval is kept as input to the membership function in order to be combined with fuzzy rules. Once membership

functions calculated, fuzzy rules are set following the different combinations that could be done and the according to the desired scenarios (see Algorithm 2).

At the final stage, defuzzification is done and the output membership function could be calculated. This concerns three states of the system which are: Manual (M), Semi-Autonomous (SA) and Autonomous (A). Those are presented in the Figure 3.11.

In order to test the efficiency of the system, a set of measures were injected into the latter to assess the switching mode. Input measures are collected from the sensors for both blocks according to the studies done in chapter 3 and 4 in order to detect emotion and fatigue levels. For the output, an exhaustive list of results was made according to the estimation of the expert as to combine between maximum of cases that could be presented. Performance was then assessed according to the comparison between results of the system and the estimated one. In conclusion, performance rate reached 78%. This could be justified by the fact that the two blocks are not synchronized together. As far as the treatment time needed for emotion block is much more than fatigue one due to the huge number of data that must be filtered. Consequently, this rate must increase in order to ensure better security for users. To be noted also, the membership functions could be fine tuned more by addressing more experiments to detect the thresholds of the mapping.

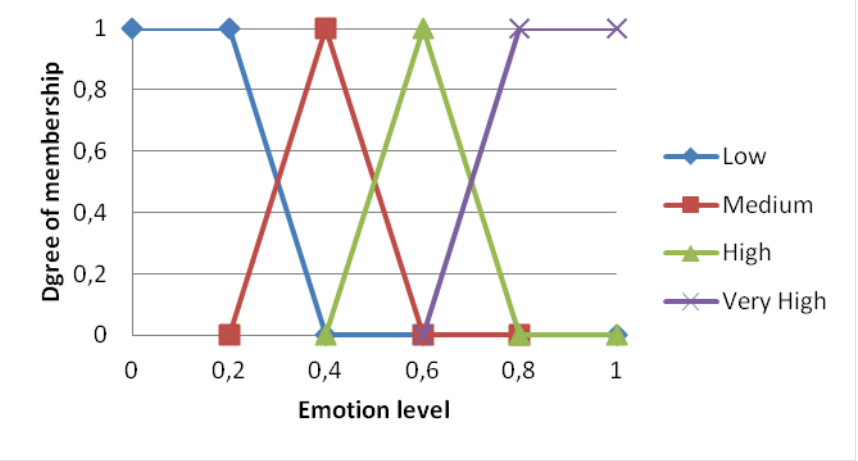

FIGURE 3.9: Membership function for Emotion level with (Low=relaxed), (Medium=sad), (High= excited) and (Very High= nervous)

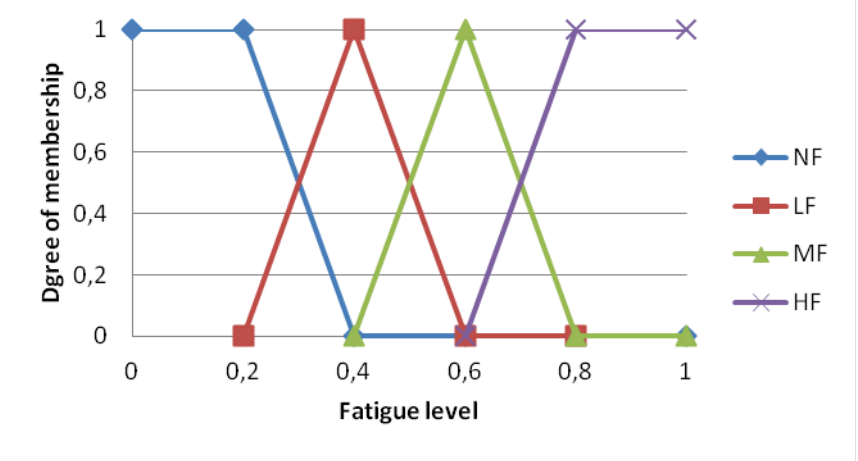

FIGURE 3.10: Membership function for fatigue levels

Data: Fatigue and Emotions membership degrees
Result: Decision of the inference system
if *fatigue level is HF AND emotion level is LOW* **then**
  system is Autonomous;
end
if *fatigue level is MF AND emotion level is MEDIUM* **then**
  system is Semi-Autonomous;
end
if *fatigue level is LF AND emotion level is HIGH* **then**
  system is Semi-Autonomous;
end
if *fatigue level is LF AND emotion level is LOW* **then**
  system is Manual;
end
⋮

Algorithm 2: Example of fuzzy rules with different combinations

3.5 conclusion

In this chapter, an investigation about mental fatigue influence on cerebral activity was put in place. This one is based on two sources of control namely: P300 and SSVEP. The former contains five parameters that could be correlated with mental fatigue which are maximum amplitude, minimum amplitude, latency and period per sensor. While for the latter, five frequency bands (delta, theta, alpha, beta and gamma) were investigated in order to be kept as classifier inputs. For this purpose a special experiment was

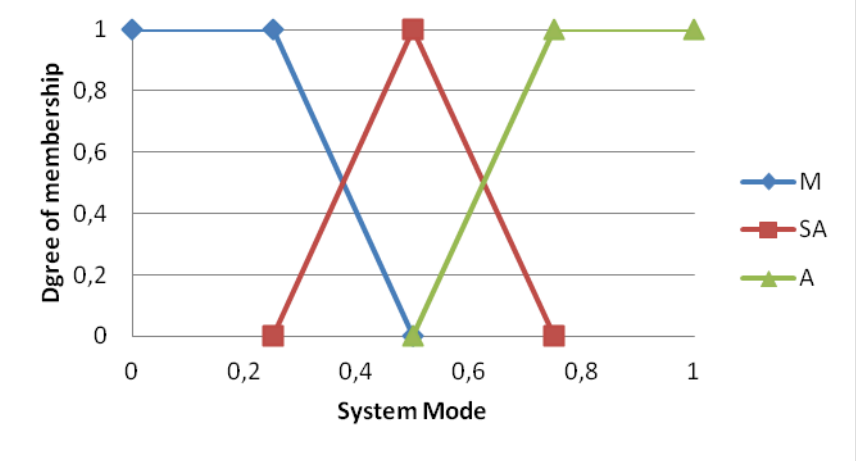

FIGURE 3.11: Output membership function of the fuzzy module

put in place in which the user is told to navigate through a hallway to reach the goal target where a picture is placed to induce P300. Several environmental parameters were modified and combined in different scenarios. Those are luminosity level, obstacles number and obstacles velocity. For SSVEP, flashing lights were placed with flashing lights at 10 Hz. Through investigation study eight parameters were kept for P300 and five for SSVEP. In the next step, these parameters were classified separately in an MLP and LDA classifiers. Then a combination technique based on Dempster and Shafer evidential theory was used to combine between them and it showed that classification performance was better than individual one. In the final stage, a fuzzy block was proposed to combine the outputs issued from fatigue block and emotion block. The idea was to map the output values into membership functions through fuzzification process, inference system and defuzzification to output final decisions: Manual, Semi-Autonomous or Autonomous. This approach was original in a way that it explores the impact of mental fatigue in the context of wheelchair navigation through P300 and SSVEP as it can assist the user during his wheelchair navigation. Nonetheless, those approaches were applied only on a simulated environment but not in real world. This could make the biggest shortage as challenges imposed by real wheelchair navigation differ to challenges faced in a simulated one. For example, in a simulated environment, all objects coordinates are already known as they are communicated by the software but this is not the case in real world. Another problem is that vibrations, wheelchair real velocity and synchronization issue biases much more the results.

Conclusion

In order to enhance navigation, emotion was integrated as a velocity modulator. For this purpose, emotion induction protocol was used and four emotions were extracted. This was done in order to conceive a classifier that can detect emotion level during navigation. After that, the classifier block was injected to control wheelchair velocity in a simulated environment. Two trials were proposed; the first one without emotion inference and the second with emotion. Three scenarios were developed: easy, medium and hard paths in which obstacles were injected as well as luminosity varied from brilliant to dark. The results were compared based on three parameters: obstacles hit, navigation path deviation and outbound gaze. At the end, mental fatigue was also assessed. For this purpose, we studied its influence on P300 and SSVEP sources. A new experimental setup was made. The user has to navigation a long a hallway from point A to a point B where a special picture is used in order to induce P300. The navigation circumstances changed from a trial to another; either by changing luminosity, or by increasing obstacles number or by variation of obstacles velocities. This was made to induce fatigue after all those trials. For SSVEP, flashing lights were added to the environment with a flashing frequency of 10 Hz. A correlation study was made to assess the best parameters that can be kept for a later classification. In total, fourteen parameters were just used (eight for P300 and six for SSVEP). In the first part, each input was classified separately, and after that a combination, using Dempster-Shafer theory, was used. The results show that combination gave better results than individual ones. This concludes the fatigue block Finally, as the project consists on assessing the best parameters for safer navigation, those blocks (emotion and fatigue) were also combined in order to decide if the user is able to control his wheelchair manually, or does he need some assistance in a semi-autonomous context, or is he totally unable to do that and in this case, the wheelchair takes a full control. For this purpose, a fuzzy block was put in place that takes as inputs; fatigue and emotions levels, but makes a certain mapping between original and fuzzfied ones. The latter will be used for fuzzy process: fuzzification, applying fuzzy rules, inference system and defuzzificiation. The system performance was assessed and reached 78%. As for any project, it has its advantages but also it

presents some drawbacks. This is very important in a way it can help us building the next project to setup. For example, all experiments made were only in simulated environments: controlling robot or controlling a wheelchair in simulation is almost the same despites that the second is closer to reality. But this being said, in real wheelchair navigation, many other problems could occur such as system response time, vibration, human interference in the experiment (such as speaking with others while navigating). What's more, emotion study wasn't precise enough to account many other emotion cases; this is done intentionally because the chosen emotions were representative for each quadrant in order to not complicate the study. But in reality for each quadrant, many emotions could be situated in the same region which can create some confusion during classification. Another point, the comparison between emotion-based and non-emotion-based navigation, specifically in path deviation, didn't account for time being. As it was mentioned before, the deviation using emotion is better but regarding time, it took a lot of time due to some synchronization problems between data issued from gaze and brain and time for classification to be processed. This work can be the basis of many perspectives, emotion classification, can account for more than four emotions and in this case, navigation could be more enhanced and fine tuned. The implementation of real wheelchair navigation is also affordable; by shortening the joystick and implementing a direct command from distant computer to wheelchair inputs, one can conduct more experiences on a real wheelchair. Especially when speaking about semi or autonomous navigation, many sensors have to be mounted: We propose two parts of avoidance. If we take an example of a wheelchair in hospital and user wants to go to the rest room. The problems could be modulated as follows: i. How can the wheelchair detect the place to go and by auto localization, how can he calculate the distance that separates the wheelchair to the rest room ii. How can it find the path to reach that place iii. How can it avoid in place obstacles which can be static or dynamic. For all those questions we propose a complementary solution: i. A global navigation based on GPS or other sensors ii. A local navigation that ensures the avoidance of the wheelchair relative to obstacles. iii. Combining those two modalities can result on an advanced wheelchair that can reach the target goal and avoid obstacles. In the context of ubiquitous society, severely disabled people assistance could be done using only intelligent machines such as robots, wheelchairs... Thus a communication between them is highly needed. A multi robot assistance could be an ambitious project and very trendy. Presenting some societal service to a human being is very important; people suffering from autism can benefit a lot from such a favor. And though for an autistic disabled person, being accompanied with a robot could have better curing impacts. But this should be proved by scientific community. At the end, as humans evolution is spectacular and very fast especially with the introduction of internet, mobile phones, tablets... new needs emerge and

disable people are part of humanity. This is why, their needs won't stop and scientific community will be forever ready to come for help.

Appendix A

A proof of concept: Comparison between gaze based and gaze-brain based navigations

A.1 Introduction

Regarding navigation problems, the current project proposes the combination between gaze and brain to offer a new modality for LIS or palsy users to control easily their wheelchairs. This should be justified in a way that based only on gaze or brain individually, can't offer the best solution. This is why, in this chapter, many definitions must be presented such as encephalography and occulography systems that have as role to map user's points of gaze into screen coordinates for the former, and brainwave activities for the latter.

BEWHEELI project, offers the possibility to combine between these two modalities to command a wheelchair. To justify the concept, the system was implemented on a Khepera robot with different scenarios; the first scenario used standard gaze based navigation and the second one used a combined one. The results issued from those experiments, show that gaze based system is faster while the combined one is more efficient and caused less errors. The choice is made based on the context of the project which is wheelchair navigation. In this context, safety of navigation is critical and this point will favorite combined navigation among the other.

A.2 BEWHEELI interface description

The BEWHEELI Beta interface into many modules (Figure A.1) :

• Five areas which correspond to commands: Forward, Backward, Turn left / right and stop. Each zone appears as a rectangle which is compared with the gaze coordinates in order to send the appropriate command.

• User profile: the user, before starting the experiment, has to provide data relating to his profile: name, age, sex.

• The robot parameters: it consists of the communication port and communication speed, manual control interface and the speed of the robot (by default it is set to 10)

• The brain parameters: the same connection parameters, the raw values from the EEG headset are detected and the attention and meditation values extracted.

• The gaze parameters: it is used to extract the gaze sequence as horizontal and vertical coordinates and an overview of the visual coordinates.

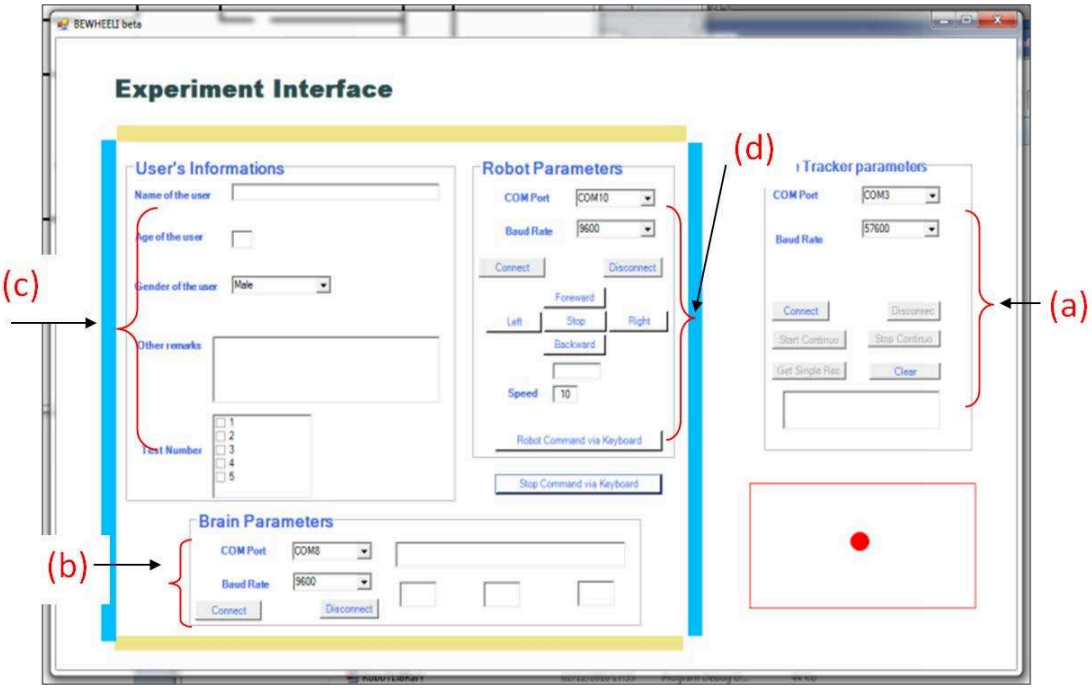

FIGURE A.1: BEWHEELI Interface (a): EyeTracker parameters, (b): Brain parameters, (c): user profile, (d): robot parameters

During the experimental tests, the coordinates of gaze are recorded and compared with control areas, using an ASL Eyetrac 6. When gaze is located in a control area its color changes to red indicating that the command is selected and pending activation. For EEG recordings, a Neurosky mindset headgear was used. It can estimate attention and

meditation levels through e-sense meter algorithm with a frequency of measurements of 1Hz.

A.3 Experiment description

Each user is required to sit in front of the screen proceeding to the different calibrations (visual and brain): the first is provided by the method of "nine points" where the user has set nine points that appear successively in different positions of the screen.

For brain calibration, based on the algorithm of e-sense Neurosky [68]], it is possible to detect the values of the attention and meditation. Once the calibration is completed, the user can visualize a maze in real time through the camera of the robot (Figure A.2 and A.3). By default, the robot is set to region A of the maze and must reach the region H along a predefined circuit (Figure A.4).

Initially, the user has to navigate according to a standard control system based on gaze; as soon as the system detects gaze concentrations in a control zone, it sends directly the preset speed to the robot to move forward, backward or to turn right or left.

In the second step, the users are asked to navigate using BEWHEELI interface, this means that gaze is combined with brain activity: when the visual command is detected, user must focus enough (i.e. above the threshold of 50) for the order to be validated.

In this experiment we assume that all users may exceed the predetermined threshold concentration and they are all in their neutral state (they are not upset or stressed ...). Also they do not suffer from dyspraxia or visual abnormalities that may influence their choice (this means that if the user looks to the right, he wants effectively to send a turn right command).

To navigate in the predefined circuit, the user must perform successive commands namely forward (A1), right (D1) forward (A2), right (D2) forward (A3), left (G1) forward (A4), left (G2) forward (A5). These commands are spelled out by the experimenter who scores each time if the system has executed the command properly or not, the time for each test and if the robot is able to reach the end of the course. Users must undergo two sessions, each of which contains two tests: the first session concerns the system based on gaze. And so, it contains the first test in which the user has no prior knowledge of the course while in the second one, he starts to become familiar with. We separated the two experiments with a period of one week to ensure that the user forgets the sent commands and the followed course to put him on the same conditions for any technique he wants to use. Our study concerns the comparison of these two systems in case the

user does not know the environment in which he navigates (even if assisted) and in the other case.

FIGURE A.2: Experimental maze

FIGURE A.3: Experimental environment visualized by the robot camera

A.4 Results and discussion

The interface has been tested with five subjects of different ages (between 23 and 35 years) who have tried to control the robot using the two methods from starting point

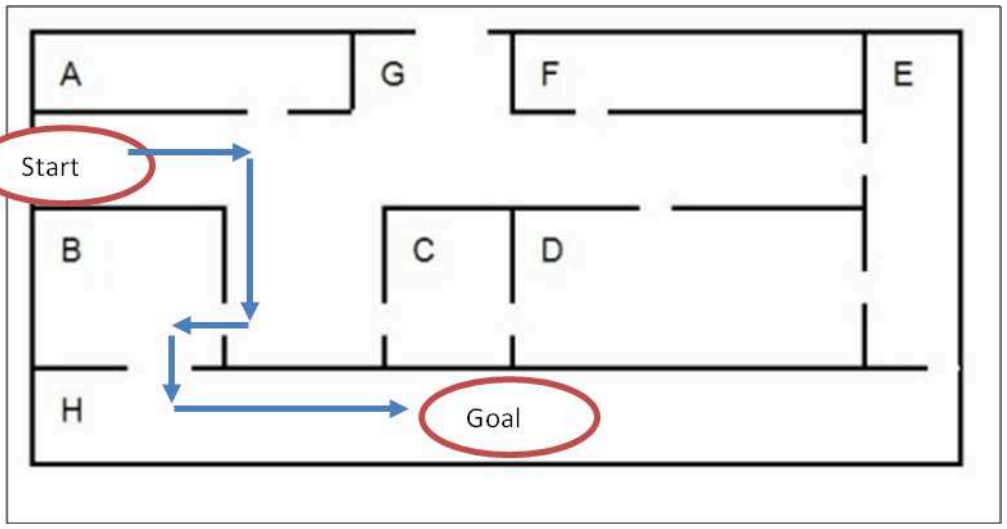

FIGURE A.4: and Goal positions and predefined path

TABLE A.1: Experiment results for the gaze based system

Subject	Criteria	Session	Values
1	System error	1	70%
		2	57%
	Navigation time	1	15s
		2	9s
2	System error	1	80%
		2	58%
	Navigation time	1	20s
		2	14s
3	System error	1	65%
		2	40%
	Navigation time	1	12s
		2	10s
4	System error	1	50%
		2	56%
	Navigation time	1	13s
		2	16s
5	System error	1	40%
		2	45%
	Navigation time	1	11s
		2	14s

(zone A) to the arrival point (zone H). In this study, two parameters were evaluated: the error "system" for each command and the total navigation time and this is done for each session. The error is defined as the sent command is different from the spelled one (e.g. the system runs "forward" while the command is spelled "right"). The results are summarized in the following table:

These experiments show that the system leads to errors in excess of 50In conclusion, such

TABLE A.2: Experience results for the gaze/brain based system

Subject	Criteria	Session	Values
1	System error	1	40%
		2	30%
	Navigation time	1	30s
		2	20s
2	System error	1	20%
		2	12%
	Navigation time	1	23s
		2	18s
3	System error	1	35%
		2	25%
	Navigation time	1	27s
		2	23s
4	System error	1	50%
		2	35%
	Navigation time	1	38s
		2	30s
5	System error	1	25%
		2	10%
	Navigation time	1	26s
		2	17s

a system is fast in the point of view of navigation but many orders are misinterpreted. This is reflected by the fact that the system does not give the user the needed time to move from one control to another especially that eye movements are very fast, in a second, could generate several commands at once. For the system based on gaze and brain, Table A.2:

The same applies to this table; the system errors are also present. This is because the visual system and brain are not synchronous: indeed for a second, and a single measurement system on the brain, the Eyetracking system makes 60 measures for points of gaze which may impose an error in processing the command. We can also notice that the error rate, unlike the first system follows a considerable decrease of no more than 50The same notes are applied for the navigation time which decreases in concordance with the error rate. These comparisons lead us to say that the second system is more stable compared to the first but it is slower. We notice also that the efficiency of the BEWHEELI system is much better than the gaze-based one (over than 60The choice could be done by evaluating the project context; for example, if we want to use such a system for internet navigation purposes, the speed assessment would be very important and in this case, a gaze based system would be the best placed. For a LIS, security is very crucial and the use of a fast system is not the most important criteria to consider and this leads us to opt for the BEWHEELI system.

Appendix B

Feature extraction and selection techniques : an overview

B.1 Introduction

This appendix, goes deeper into mathematical and physical explanations in order to extract and select the needed features from EEG signal. Since our purpose is to extract brainwave signals : $\delta, \theta, \alpha, \beta, \gamma$ which appear in the Power/frequency presentation, Power Spectral Density (PSD) should be treated. This section will introduce some techniques used such as Bartlett, Welch and Wavelets with the associated matehmatical explanations. Moreover, selection techniques such as Principal Component Analysis (PCA) and Genetic Algorithm (GA) are presented.

B.2 Spectral estimation methods

We will consider the problem of estimating power spectral density (or spectrum) of an aleatory second-order stationary process. There are two main approaches for estimating spectral. The first one contains traditional or non-parametric based on periodogram. The second class contains non-traditional or parametric methods using a model for the process. Consider a discrete aleatory stationary process $x(n)(n = 0, \pm 1, \pm 2, \ldots, \pm N)$ of the second order with a null mean where autocorrelation function is expressed as follows:

$$r_x(k) = Ex(n+k)x^*(n) \tag{B.1}$$

The Fourier transform of $r_x(k)$ is the spectrum x(n) where:

$$S_x(w) = \sum_{k=+\infty}^{\infty} r_x(k) e^{\ jwk} \tag{B.2}$$

Where w is the angular frequency. In fact the power spectral density (PSD) represents the distribution of the power of the signal x(n) on the frequency axis. And so those properties are provided:

$S_x(w)$is real $S_x(w) \geq 0$

$$E|x(n)|^2 = r_x(0) = \frac{1}{2n} \int_{\pi}^{\pi} S_x(w) dw \tag{B.3}$$

As the spectrum of a signal is its Fourier transform of its autocorrelation function, estimating the spectrum is equivalent to the autocorrelation estimate. For an ergodic process, we have:

$$\lim_{N \to \infty} \frac{1}{2N+1} \sum_{n=\ N}^{N} x(n+k) x^*(n) \tag{B.4}$$

So, if x(n) is known for any n, estimating the spectrum is a simple task in theory, as we have simply to calculate $r_k(x)$ using (3) and calculate its Fourier transform. However, in practice, there are two major issues: The number of data is always very limited The noise Thus, estimating a spectrum consists on estimating $S_x(w)$ from a finite number of noised data.

B.2.1 The periodogram

Periodogram method was introduced by Schuster in 1898. For an ergodic process, the autocorrelation sequence can be determined with a temporal mean (see equation B.4). Nonetheless, if x(n) is measured only over a finite interval ($n = 0, 1, \ldots, N$), autocorrelation function should be estimated with a finite sum:

$$\breve{r}_x(k) = \frac{1}{N} \sum_{n=0}^{N\ 1} x(n+k) x^*(n) \tag{B.5}$$

To be sure that the values of x(n) which are out of the interval [0,N-1] are excluded from the sum, B.5 will be expressed as follows:

$$\breve{r}_x(k) = \frac{1}{N} \sum_{n=0}^{N \quad 1 \quad k} x(n+k)x^*(n), k = 0, 1, \ldots, N \quad 1 \tag{B.6}$$

For k¡0, we use the property $\breve{r}_x(\quad k) = \breve{r}_x * (k)$, and $\breve{r}_x(k)$ equals zero for $|k| \geq N$. By applying Fourier transform, we obtain an estimated spectrum: the periodogram.

$$S_{per}(w) = \sum_{k= \quad N+1}^{N \quad 1} \breve{r}_x(k) e^{\quad jwk} \tag{B.7}$$

It's more practical to express periodogram as a function of process x(n). Let

$$x_N(n) = \begin{cases} x(n), & \text{if } 0 \leq n \leq N \quad 1 \\ 0, & \text{else} \end{cases} \tag{B.8}$$

This means that $x_N(n)$ is the product of x(n) by a rectangular window $w_R(n)$ where:

$$x_N(n) = w_R(n)x(n) \tag{B.9}$$

And so we have:

$$\breve{r}_x(k) = \frac{1}{N} \sum_{n= \quad \infty}^{\infty} x_N(n+k)x_N^*(n) \tag{B.10}$$

$$= \frac{1}{N} x_N(k) * x_N^*(\quad k) \tag{B.11}$$

By taking the Fourier transform the expression of the periodogram becomes:

$$S_{per}(w) = \frac{1}{N} X_N(w) * X_N^*(w) = \frac{1}{N} |X_N(w)|^2 \tag{B.12}$$

Where

$$X_N(w) = \sum_{n= \quad \infty}^{\infty} X_N(n) e^{\quad jwn} = \sum_{n=0}^{N \quad 1} x(n) e^{\quad jwn} \tag{B.13}$$

By increasing the data number, the periodogram will be close to the spectrum value $S_x(w)$. We are interested in, if yes or no:

$$\lim_{N\to\infty} E[S_{per}(w) \quad S_x(w)]^2 = 0 \tag{B.14}$$

For quadratic convergence, this must be asymptotically non biased:

$$\lim_{N\to\infty} E\{S_{per}(w)\} = S_x(w) \tag{B.15}$$

And so its variance converges to zero when N tends to infinity:

$$\lim_{N\to\infty} varS_{per}(w) = 0 \tag{B.16}$$

In other terms, $S_{per}(w)$ must estimate consistently the spectrum.

B.2.2 The modified periodogram

In a modified periodogram, the window $W_R(n)$ is replaced by a general window w(n) to obtain:

$$S_{per.m}(w) = \frac{1}{NU}|\sum_{n=\ \infty}^{\infty} x(n)w(n)e^{\ jwn}|^2 \tag{B.17}$$

Where N is the length of the window and

$$U = \frac{1}{N}|\sum_{n=0}^{N\ 1} w(n)|^2 \tag{B.18}$$

Is a constant introduced so that $S_{per.m}(w)$ be asymptotically non biased. Tha variance of the modified periodogram is almost the same as for the standard periodogram. In fact, the window introduces a compromise between spectral resolution (principal lobe width) and spectral leak (adjacent lobe amplitude).

B.2.3 Bartlett Method

The Bartlett method consists on averaging the periodogram. It produces a consistent estimator of the spectrum. Let it be $x_i(n), i = 1, 2, \ldots, K$, K uncorrelated realizations of an aleatory process x(n) over an interval $0 \leq n \leq L$. If

$$S_{per}^{(i)}(w) = \frac{1}{L}|\sum_{n=0}^{L\ 1} x_i(n)w(n)e^{\ jwn}|^2,\ i = 1, 2, \ldots, K \tag{B.19}$$

Is the periodogram of $x_i(n)$. The averaging of these periodograms is:

$$S_x(w) = \frac{1}{K}|\sum_{i=1}^{K} S_{per}^{(i)}(w) \tag{B.20}$$

The evaluation of the average of the sets of $S_x(w)$, gives:

$$E\{S_x(w)\} = E\{S_{per}^{(i)}(w)\} = \frac{1}{2\pi}S_x(w) * W_B(w) \tag{B.21}$$

Where $W_B(w)$ is the Fourier transform of the Bartlett window, $w_B(k)$, that goes from -L to L. So, as for periodogram, $S_x(w)$ is asymptotically unbiased. Besides, with the hypothesis of uncorrelated data, it follows that:

$$var\{S_x(w)\} = \frac{1}{K}var\{S_{per}^{(i)}(w)\} = \frac{1}{K}S_x^2(w) \tag{B.22}$$

That tends to zero when K tends to infinity. Consequently, $S_x(w)$ is a consistent estimator of the spectrum when K and L tend to infinity. The problem with this approach is that uncorrelated realizations of a process are not generally available. Typically, one realization of length N is in our disposition. To avoid this problem, Bartlett proposed that x(n) will be partitioned in K sequences, of length L, that don't cover each other, where N=KL. We have:

$$x_i(n) = x(n + iL), n = 0, 1, \ldots, L \quad 1,\ i = 0, 1, \ldots, K \quad 1 \tag{B.23}$$

Finally Bartlett estimator is defined as follows:

$$S_B(w) = \frac{1}{N}\sum_{i=0}^{K\ 1}|\sum_{n=0}^{L\ 1} x_(n + iL)e^{\ jwn}|^2 \tag{B.24}$$

Because periodograms in $S_B(w)$ are calculated using sequences of length L, the resolution is:

$$res[S_B(w)] = 0.89\frac{2\pi}{L} = 0.89K\frac{2\pi}{L} \tag{B.25}$$

Which is K times larger than periodogram.

B.2.4 Welch method

In 1967, Welch proposed an approach to estimate spectral density at different frequencies. It's based on the concept of the periodogram spectrum estimates [69]. The latter is the result of converting signal from time to frequency domain. Welch's method is an evolution of the standard periodogram and Bartlett methods. consider $x_i(n), i = 1, 2, \ldots, K$, K uncorrelated measurements of a randomized process x(n), over an interval of $0 \leq n < L$. Suppose that successive sequences are decaled by $D(\leq L)$ samples and that each of them is of length L, the i-th sequence is given by:

$$x_i(n) = x(n + iD), n = 0, 1, \ldots, L \quad 1 \tag{B.26}$$

Though, the overlapping quantity between $x_i(n)$ and $x_{(i+1)}(n)$ is L-D points, and if K sequences cover N data of the signal, then

$$N = L + D(K \quad 1) \tag{B.27}$$

This means, if we consider that sequences are overlapped by 50% ($D = \frac{L}{2}$), then we can form $K = 2NL \quad 1$ sections of length L. The Welch method can be directly expressed by:

$$\hat{S}_w(w) = \frac{1}{KLU} \sum_{i=0}^{K \quad 1} | \sum_{n=0}^{L \quad 1} w(n)x(n + iD)exp(\quad jwn)|^2 \tag{B.28}$$

where $U = \frac{1}{N} \sum_{i=0}^{N \quad 1} |w(n)^2, N$ is the length of the window $w(n)$, It has been proved that this method reduces the noise in power spectra whilst the resolution R depends on the chosen window and can be given by:

$$R = \frac{1}{LT_s} \tag{B.29}$$

where T_s the sampling period. Hence the lower L is, the smoother Welch periodogram becomes. This can be shown in Figure B.1, with different Hamming window lengths (16, 32, 64, and 128).

The initial signal was filtered between 1 and 64 Hz. In this case, δ (up to 4 Hz), θ (4Hz-8Hz), α (8Hz-13Hz) β (13Hz-30Hz) and γ (30Hz-64Hz) were kept for our study.

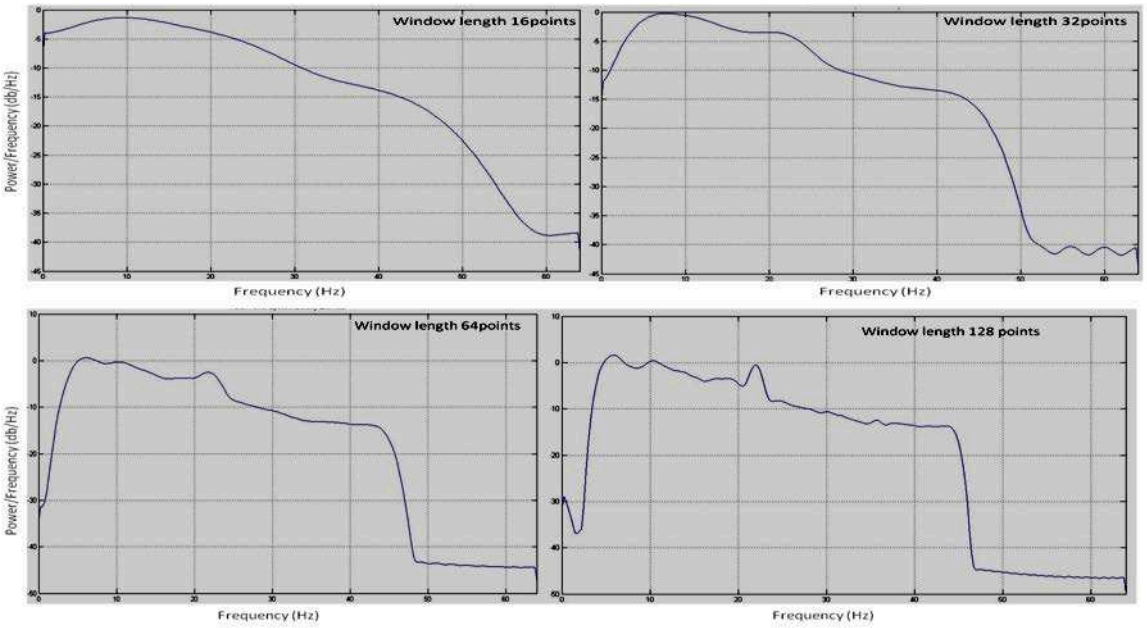

FIGURE B.1: Welch method with 128 FFT points and different window lengths during experimental session, extracted from sensor FP1

The power spectral density (PSD) was computed every one second of the whole trial for each user. The Welch periodogram was computed using 512 points FFT and several Hamming windows of length 128, 64, 32 and 16 points with a 50% overlapping. For the bands found in each second, two parameters were computed: the mean Power (P_m) and the Root Mean Square (R_{ms}) calculated as:

$$P_m = \sum_{k=l}^{h} S(k) \tag{B.30}$$

$$R_{ms} = \sqrt{\sum_{k=l}^{h} S(k)} \tag{B.31}$$

Where $S(k)$ are the sampled values of the periodogram $S(f)$ and l and h are the indexes of the higher and lower sampled frequencies for each band. The decomposition results are shown on the figure below:

B.2.5 Discrete wavelets transform

The Discrete Wavelets Transform (DWT) is generated by the function:

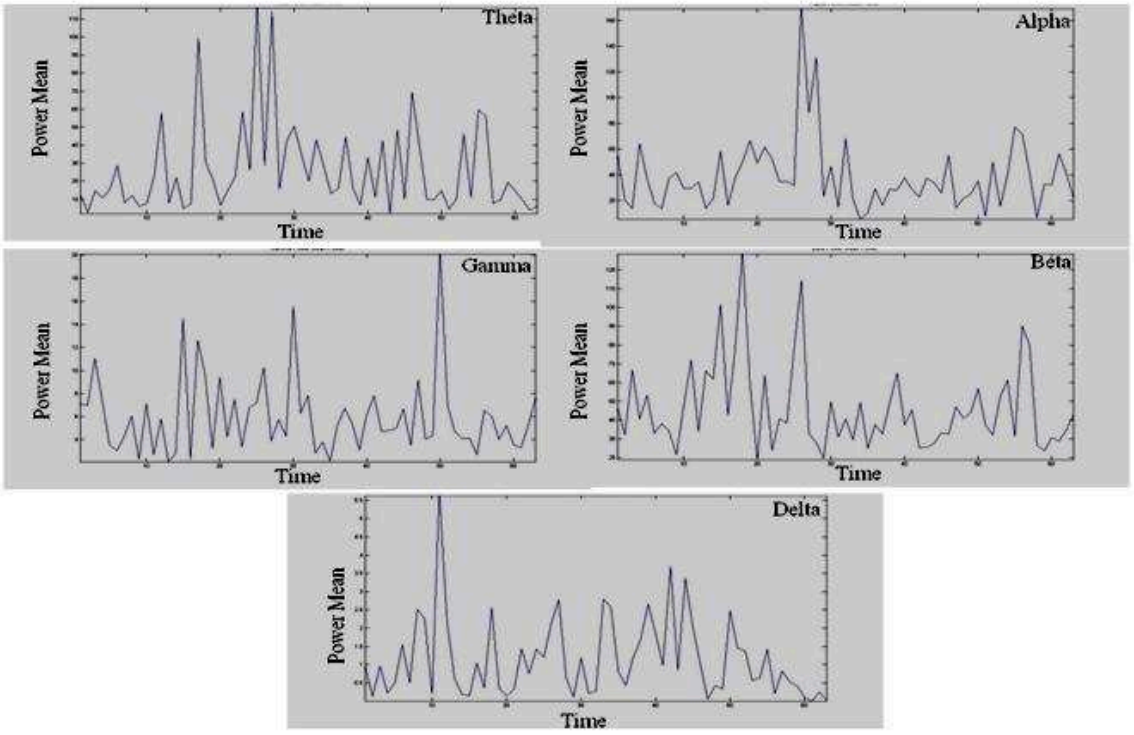

FIGURE B.2: Power mean values over the 63 seconds using Welch method

$$\psi_{a,b}(t) = 2^{\frac{a}{2}}\psi(2^{\frac{a}{2}}(t \quad b)) \tag{B.32}$$

Where a is called the scales and b the shifts. It is possible to approximate any function by dilating $\psi(t)$ with the coefficient 2^k and shifting the resulting function on interval proportional to $2^{\ k}$. To obtain a compressed version of a wavelet function, a high-frequency component must be applied while a low frequency one is needed for dilated version. By correlating the original signal with wavelet functions of different sizes, the signal details can be obtained for many scales. Because these correlations can be arranged in a hierarchical scheme, the so called multi resolution decomposition algorithm can proceed by separating the signal into "details" at different scales from coarser representation named "approximation". This algorithm can be represented as follows:

• Given a discrete signal "S" with length of N. the first step, is to apply the algorithm by producing two sets of coefficients: approximations (cA1) and details (cD1). These can be obtained by a convolving S with a low-pass filter Lo_D for approximation, and with high-pass filter Hi_D for detail.

• Approximation coefficients cA1 are split into two parts using the above step but instead of using the signal S, it will be replaced by cA1 and in this case, producing cA2 and cD2

and so on, until at the need level i, the signal S has the following structure: [cAi, cDi. . . cD1].

• The process can be inverted by using the inverse discrete wavelet transform (IDWT) and, starting from cAi and cDi, cAi-1 can be reconstructed at the level i-1 and so on until reconstructing the initial signal S.

These steps are recapitulated in the Figure B.3.

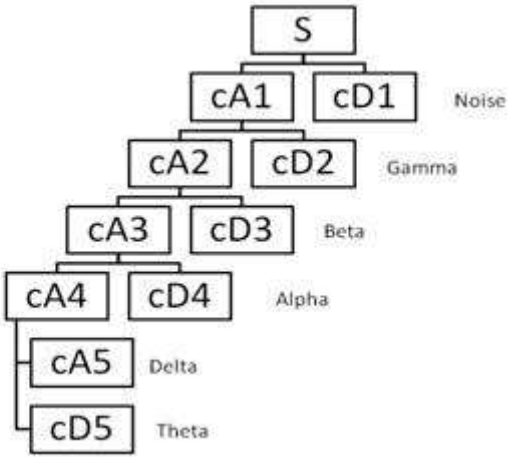

FIGURE B.3: Multi decomposition algorithm applied on EEG signal

DWT works as filters where the initial signal S is divided into two bands at each level called approximation and details which are respectively high-scale (low frequency) and low-scale (high frequency) of the signal. Then the samples of the signal are divided by two creating sub samples. At each level, the sub-sampling will divide the number of samples by half. In our case, raw data contain EEG waves. Those can be extracted by decomposition of the data using multilevel discrete wavelet transform algorithm (DWT).

B.3 Selection features methods

As it was mentioned before, extracted features need to be selected to avoid high dimensionality curse. For this purpose, two selection techniques are introduced.

B.3.1 Principal Component Analysis (PCA)

Principal Component Analysis (PCA) uses mathematical principals to transform a number of correlated variables into smaller numbers called principal components. Some of the common applications include data compression, blind source separation and de-noising

signals. PCA uses a vector space transformed to reduce the dimensionality of large data sets. Using mathematical projection, the original data set, with its high dimension, can be interpreted in fewer variables (principal components). This is important as it can reduce the processing time during classification and let the user interpret outliers, patterns and trends in the data. The aim of this section is to explain how to apply PCA on the feature vector in each second. For each second, the feature vector X is 200 x 80 length where rows $(x_i^1, \ldots, x_i^{80})$ represent the observations and columns $(x_1^j, \ldots, x_{200}^j)$ represent the variables. The first step is to rescale data to obtain a new vector Z:

$$z_j^i = \frac{x_j^i \quad \bar{x}^j}{s^j} \tag{B.33}$$

Where $\bar{x}^j = \frac{1}{n}\sum_{i=1}^{n} x_i^j$ is the mean of the j^{th} variable,s^j is the corresponding standard deviation. The correlation matrix R contains correlation coefficients between each pair of variables. It's symmetric and composed by ones in its diagonal. It's defined as follows

$$R = D_{\frac{1}{s}} V D_{\frac{1}{s}} \tag{B.34}$$

Where V is the variance matrix of X and $D_{\frac{1}{s}}$ is a diagonal matrix containing$(\frac{1}{s1}, \frac{1}{s2}, \ldots, \frac{1}{sp})$. The next step is to calculate the Eigen values of the correlation matrix. In fact, the Eigen values contain the projection inertia of the original space on the sub space formed by the Eigen vectors associated to each of them. Eigen vectors constitute the loadings of the Principal Component; that's the strength of the relation between the variable and principal component. The following Figure gives an example about Eigen values, the associated principal component and the projection inertia (in percent) for each of them.

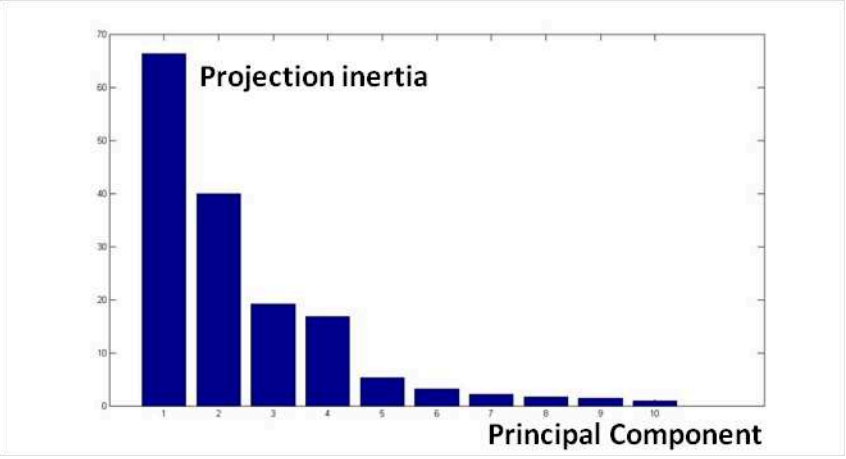

FIGURE B.4: The projection inertia of the Eigen values associated with the principal component

The selection of the number of principal components axis to keep is very important in PCA. The criteria used are generally empirical: the elbow method consists of detecting an elbow in the Eigen values plot or Kaiser Criterion. The latter consists on retaining only the Eigen values greater than the mean value. The next step consists on recalculating the new scores of the data on each retained principal component, by multiplying the loadings of the axis by the scaled data. Figure B.5 shows an example of representation on a plot composed by the first, second and third components

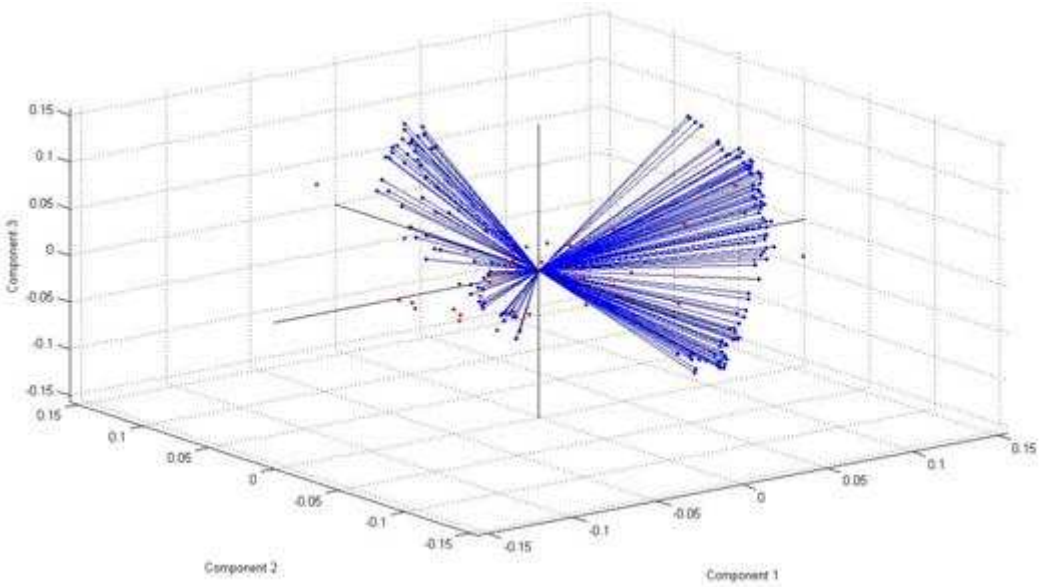

FIGURE B.5: Data projection on the first, second and third principal component axis

The variables (vectors) and the scores (points) are represented in the factorial plan formed by the three components axis. The cosine of the angle between vectors expresses the correlation between them. If the angle difference tends to 0, then cosine tends to 1 which indicates highly correlated variables and respectively if the angle difference tends to 180 then the cosine tends to -1 which also indicates an inverse high correlation. On the other side if the angle difference tends to 90 or -90, then the cosine tends to 0 which means that variables are uncorrelated.

B.3.2 Genetic Algorithm (GA)

Genetic Algorithm (GA), a form of learning strategy, is an adaptive search technique which proved its efficiency over a set of search methods [59]. The power of such a method is its ability to fine tune an initially unknown search space into more convenient subspaces. The main issue for a GA problem is the selection of a suited representation and evaluation function. This is very well suited to solve a feature selection problem. In this case, each feature is considered as a binary gene and each individual a binary string

representing the subset of the given feature set. Let it be X, the feature vector of length s. the inclusion or elimination of the corresponding feature is described as follow: if $X_i = 0$, then it represents elimination of the feature otherwise, 1 indicates its inclusion. Evaluation function choice is very important to obtain a successful application of GA. In the current problem, our purpose is to estimate the number of optimal features to keep. The idea is to apply a fitness function on the correlation matrix M. The latter can be presented as follows:

$$M = \begin{pmatrix} 1 & \dots & C_{1,n} \\ \vdots & C_{i,j} & \vdots \\ C_{n,1} & \dots & 1 \end{pmatrix} \tag{B.35}$$

Where $C_{i,j}$ represents the correlation coefficient between feature i and feature j. this value varies between -1 and 1. If $C_{i,j}$ tends to 1 or -1, then the features are highly correlated otherwise, if it tends to 0 then there is no correlation. Starting from the initial population which is constituted by the correlation of the pairs of features, the proposed fitness function F could be defined:

$$F = min_{i,j}|C_{i,j}| \tag{B.36}$$

Where $M(i,j) = C_{i,j}$. For each iteration, the crossing chromosomes with the least correlation coefficient are kept for the next generations while the others are eliminated. An example of a feature selection process using GA for a one second period is presented on the Figure B.6

FIGURE B.6: Number of features selected over trials

B.4 Conclusion

In this section, an overview of different techniques used for features extraction and selection were exposed. The performance of the combined techniques could be assessed through the classification rates. Those are summarized in chapter 2. Depending on the context, the best combination found was associated to wavelets as extraction technique and genetic algorithm as for features selection.

Appendix C

Information fusion theories: State of the art

C.1 Introduction

Data fusion is a technology to enable combining information from several sources in order to form a unified decision. Those systems are widely used in many fields such as robotics, sensor networks, image processing... its research community have achieved spectacular advancements yet the emulation of the human brain data fusion capacity is still far from reach. In literature the definition of the term "data fusion" refers to many terms such as multi-level, multifaceted process, data combination from several sources.

The definition is also generalized to state that data can be provided from either a single source or multiple ones [70]. Performing data fusion has many advantages [71] that mainly involve data authenticity and availability enhancement, confidence and detection improved and reduction in data ambiguity.

One of the most common and famous concept of fusion system, is the Joint Direct Laboratory model (JDL) [72]. Its classification is based on the input data and produced outputs. It considers the fusion process in four levels: object, situation, impact, and process refinement.

Despite its efficiency, this model suffers from many shortages such as being too restrictive and limited to military area. Also it focused only on data as input/output but not as processing. Another proposal [73], presents data fusion from a software engineering perspective; a data flow characterized by input/output and functionalities (processes). Another approach presented by [74], is based on the notion of random sets.

This framework has many distinctive aspects of this framework, are the ability to combine decision uncertainty with the decision itself. On the other hand, [75] proposed a framework based on category theory which is sufficient to capture all kinds of fusion such as data fusion, feature fusion, decision fusion... its major advantage it can express all aspects of multi-source information processing such as data and processing.

C.2 Data fusion challenges

This being said, many issues rise from data fusion. The majority originate from the data to be fused. Those can be presented as follows:

• Imperfection in data: data fusion algorithms should be able to express imperfections provided by sensors such as impreciseness and uncertainty in the measurements.

• Outliers and spurious data: in addition to what was mentioned before, environment can present inconsistencies that could be difficult to distinguish between them. This is why, redundancy should be eliminated.

• Conflicting data: this one poses a lot of problems especially when fusion is based on evidential belief reasoning [76]. Conflicting data must be treated with special care.

• Data modality: data collected could be homogenous or heterogeneous such as auditory, visual and tactile measurements.

• Data correlation: in some cases, sensors are exposed to the same external artifact that biases its measurements. These should be accounted for.

• Data alignment/registration: each sensor's local frame should be transformed into a common one before fusion. This is known as data registration.

• Data association: this generally occurs when multi-targets are tracked. It introduces more complexity if compared to the single-target tracking. This problem is identified as from which target each measurement is originated.

• Processing framework: processing can be done in a centralized or decentralized way. Each sensor processes data locally and all measurements have to be sent to a central processing node for fusion.

• Operational timing: operation frequencies may differ from a sensor to another. A multiple time scale framework must be put in place to ensure synchronization between sensors measurements.

• Static and dynamic phenomena: the phenomenon in each experiment may be variant with time or invariant. A track of the recent history measurements must be incorporated into fusion process [77].

• Data dimensionality: when the treated data suffer from high dimensionality, those should be compressed into lower dimensions. This preprocessing is very important it can be time and power saving.

The forehead mentioned issues can be summarized in the following figure:

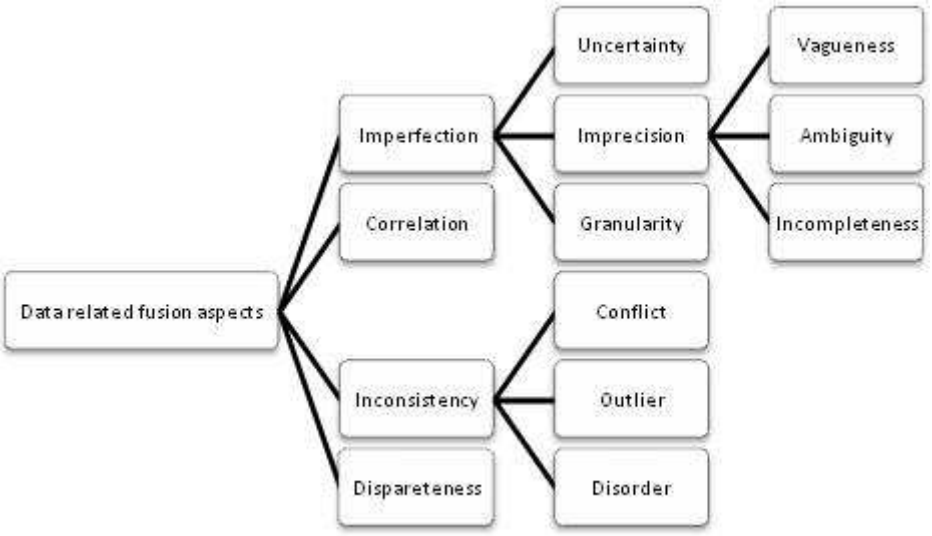

FIGURE C.1: Data fusion challenging problems

C.3 Data fusion algorithms

Real-world fusion applications have to deal with many challenges. In this paragraph, fusion algorithms will be proposed based on data related challenge. Historically, the probability theory was used to deal with all kinds of imperfections. New techniques have emerged since then, such as fuzzy set theory and evidential reasoning [78]. Our aim is to discuss each of these families along with hybridization such as fuzzy rough set theory [79]...

C.3.1 Probabilistic fusion

Those methods rely on the probability distribution/density functions for data uncertainty. Those rely mainly on the Bayes estimator that fuses many pieces of data; this

is named "Bayesian fusion". The Bayes estimator provides a method to compute conditional probability distribution/density of the state x_k at time k given measurements $Z^k = \{z_1 \dots z_k\}$ and the prior distribution as following:

$$p(x_k|Z^k) = \frac{p(z_k|x_k)p(x_k|Z^{k\ 1})}{p(Z^k|Z^{k\ 1})} \tag{C.1}$$

Where$p(z_k|x_k)$ is the likelihood function and is based on the sensor measurement model, $p(x_k|Z^{k\ 1})$ is the prior distribution that incorporates the transition model of the system. The denominator is a normalizing term. The Bayes estimator can be applied and updated in real time in a way it fuses and updated new coming piece of data recursively with the probability distribution density. The kalman filter, which is an exceptional case of the Bayes filter, is one of the most popular fusion methods due to its simplicity and ease of implementation. Yet, it is very sensitive to corrupted data with outliers. What's more, it's not suitable for applications whose error characteristics are not very well parameterized. If the systems dynamics are non-linear, one usually uses approximation techniques. From best known ones we can cite: Sequential Monte Carlo (SMC) [80] or Markov Chain Monte Carlo (MCMC) [81]. They don't make assumptions regarding the probability densities to be approximated. The idea is to deploy a weighted set of random particles as an approximation of the probability density of interest. Applied within a Bayesian framework, particle filters approximate the posterior probability of the system as a weighted sum of random samples. Those are predicted from the prior density with the updated weights according to the likelihood of the given measurements. Similar to Kalman filter, particle filters are sensitive to outliers in data. Also, they are computationally expensive as they use a large number of random samples for probability density estimation. What's more is that such a technique is not suitable for high dimensional state space problems because the number of particles required estimating such a problem increases potentially. In order to solve this issue, a Markov chain was used to evolve the samples instead of simply drawing them randomly at each step. This technique is proved to be very efficient and can converge to a unique stationary density of interest which occurs after a sufficient number of iterations called: burn-in period. It was deployed by Metropolis and Ulam [82] and extended by Hastings [83] resulting in Metropolis-Hastings algorithm. It works by successively sampling a candidate point from the conditional probability of a potential sample given a current sample. This algorithm is sensitive to the initialization sample and the jumping distribution. Research on optimal starting point and jumping distribution is the subject of many works.

C.3.2 Evidential belief reasoning

Demster's work set the origins of the theory of belief functions. It's a popular method to deal with uncertainty and imprecision. Dempster-Shafer theory introduces the notion of beliefs and plausibility assigned to possible measurements hypothesis. Formally, the evidence theory concerns the following notations:

• Frame of discernment: let θ be a finite set of elements; an element can be a hypothesis, an object, or in our case a level of fatigue. A subset of θ can be denoted by $\omega(\theta)$. Suppose that the subject can be one of the three levels of fatigue $LF, MF, andHF$ where LF is Low Fatigue, MF is Medium Fatigue and HF is High Fatigue. In this case, our frame of discernment can be set as :

$$\theta = LF, MF, HF \; and$$
$$\omega(\theta) = \{\emptyset, \{LF\}, \{MF\}, \{HF\}, \{LF, MF\}, \{LF, HF\}, \{MF, HF\}, \{LF, MF, HF\}\}$$

Where $\emptyset$ signifies "no fatigue" condition. If$F = \{LF, MF\}$ is a subset of θ, this implies that fatigue is either LF or MF.

• Mass functions: the mass function m is the mapping of the power set $\omega(\theta)$ to the number $t \in [0, 1]$. The mass function can be expressed as follows :

$$\begin{gathered} m : \omega(\theta) \to [0, 1] \\ m(\emptyset) = 0, \sum_{F \in \omega(\theta)} m(F) = 1 \end{gathered} \tag{C.2}$$

The mass function m is a basic probability assignment. $m(F)$ expresses the proportion of relevant evidence which supports the assumption that an element of θ belongs to the set F but to no subset of F. In our case, $m(F)$ can be considered as the belief degree regarding a certain level of fatigue. In general, any subset F of θ that verifies $m(F) > 0$ is called a focal element. In the same way, $C = \bigcup_{m(F) \neq 0}$, F is the kernel element of mass m in θ.

• Belief and plausibility functions: the belief function Bel is defined as follows:

$$Bel : \omega(\theta) \to [0, 1] \; and \tag{C.3}$$
$$Bel(F) = \sum_{A \in F} m(A) \tag{C.4}$$

While the plausibility function is defined as:

$$\begin{array}{cc} & Pls : \omega(\theta) \rightarrow [0,1] \; and \\ Pls(F) = 1 & Bel(\bar{F}) = \sum_{A \cap F \neq \emptyset} m(A) \end{array} \tag{C.5}$$

The belief function $Bel(F)$ defines the total amount of probability that must be distributed among elements of F and is a lower limit function on the probability of F. Plausibility function $Pls(F)$ measures the maximum amount of probability that can be distributed among the elements in F.

• Belief interval $[Bel(F), Pls(F)]$ is the belief interval that reflects uncertainty. Consequently, the interval span $[Pls(F) \quad Bel(F)]$ describes the unkown with respect to F.

• Properties of the belief function and plausibility are formulated as follows :

$$\begin{array}{c} Bel(\emptyset) = Pls(\emptyset) = 0, Pls(F) \geq Bel(F) \\ Bel(F) + Bel(\bar{F}) \leq 1, Pls(F) + Pls(\bar{F}) \geq 1 \\ if A < F, Bel(A) < Bel(F) \; and \; Pls(A) < Pls(F) \end{array}$$

• Rules of evidence combination: if we suppose that m_1 and m_2 are two mass functions from two different sources, we have :

$$\begin{array}{c} m(\emptyset) = 0, m(F) = \frac{1}{1 \quad K} \sum_{A \cap B = F} m_1(A) m_2(B) \\ where K = \sum_{A \cap B = \emptyset} m_1(A) m_2(B) > 0 \end{array} \tag{C.6}$$

K is interpreted as the measure of the conflict between sources. The larger K is, the more the conflicting sources are. The combination of m_1 and m_2 results in a mass function m which carries the joint information of the two sources:

$$m = m_1 \oplus m_2 = m_2 \oplus m_1$$

In general, for n mass functions $m_1, m_2, \ldots, m_n$ in θ, the measure of the conflict K is given by:

$$K = \sum_{\bigcap_{i=1}^{n} E_i = F} m_1(E_1) m_2(E_2) \dots m_n(E_n) > 0 \tag{C.7}$$

C.3.3 Fusion and fuzzy reasoning

For the well understanding of fuzzy logic to fusion context in order to realize fuzzy logic multimodal data fusion, many issues need to be very well addressed. In order to conceive efficient system architecture, the methodology to use is very important to take off. Other concern is how to combine modalities (Fatigue and Emotion) as well as the practical side of application of fuzzy logic concept.

Overview of fuzzy logic concept Originated by Zadeh [84], the idea of fuzzy sets wasn't very well accepted by scientific community. However, in the last decade, it has attached so much attention. It was implemented in almost all fields such as commercial devices, transportation, economic systems... The motivation of the use of fuzzy logics is that many problems in the real world are not exact and almost imprecise. Take for example the Human Brain, its efficiency is not only originated from its precise part but also from using fuzzy reasoning in order to solve problems. It is almost the same concept for classification which provides soft decision which describes the degree of belonging of a pattern to a class rather than a crisp membership that matches or not a certain class. Another advantage in the use of fuzzy logics is the fact that it can overcome the shortages of nonlinear functions. Besides, it is based on formulation of expert knowledge. In our project, the use of fuzzy logic is motivated by the fact that EEG signals are often affected by external conditions and variables as far as fuzzy logics are used as a complementary tool to neural networks or other classifiers...

Fuzzy set Fuzzy set can be considered as the core of fuzzy logic. The difference between a fuzzy set and a standard one, is the introduction of degrees of membership of an element to the set expressed by a number in [0 1] interval. Let X be the input space variable and its elements are denotes by x, a fuzzy set A included in X is defined as a pair $(x, \mu_A(x))$ such that

$$A = \{x, \mu_A(x) | x \in X, 0 \leq \mu_A(x) \leq 1\} \tag{C.8}$$

Where $\mu_A(x)$ is the membership function (MF) of x in A. In crisp logic, the membership function is of $\mu_A(x)$ is formulated as follows:

$$\begin{cases} \mu_A(x) = 1, & \text{if } x \in A \\ \mu_A(x) = 0, & \text{if } x \notin A \end{cases} \tag{C.9}$$

In fuzzy theory we speak about truth value. Fuzzy logic was extended to many other interpretations such as:

• Applicability: $\mu_A(x)$ measures the degree of applicability of the description A to the individual x. This interpretation takes the definition of fuzzy logics as ontologically crisp and puts vagueness to decision

• Possibility: $\mu_A(x)$ measures the possibility that individual x has the property A. In this way, $\mu_A(x)$ is seen as the degree of possibility that state x satisfies the predicate A.

• Similarity: $\mu_A(x)$ measures the degree of similarity between individual x and concept A.

• Utility: $\mu_A(x)$ measures the utility of x having the property A.

Fuzzy variable Fuzzy variable or linguistic variable, X_f, is a variable whose values or not numbers but words, terms or labels. X_f is the fuzzy representation of X. If we have n linguistic terms L_i over a fuzzy variable, the fuzzy set associated to each variable can be formulated as follows:

$$X_f = L_i | 1 \leq i \leq n \tag{C.10}$$

$$L_i = \{x, \mu_{L_i}(x) | 0 \leq \mu_{L_i}(x) \leq 1\} | 1 \leq i \leq n \tag{C.11}$$

Those labels can be even inaccurate human terms for interpretation. It can be for instance: Low, Medium, and High ...

Fuzzy operators Like classic logic, it is needed to redefine operations such as NOT, AND, OR. Generally the following operators are defined:

• Not: if $A = \{x, \mu_A(x) | x \in X, 0 \leq \mu_A(x) \leq 1\}$ then Not A=$A' = \{x, \mu_{A'}(x) | x \in X, \mu_{A'}(x) = 1 \quad \mu_A(x)\}$

• AND (fuzzy Conjunction $\cap$):T-Norm operators

• OR (fuzzy Disjunction $\cup$):T-conform

T-norm and T-conform should comply with conditions which also verify them for the traditional crisp logic.

T-norm is a binary relation that satisfies:

- Boundary: $T_{norm}(0,0) = 0, T_{norm}(\mu,1) = T_{norm}(1,\mu) = 1$
- Monotonicity:if$\mu_A \leq \mu_C$ and$\mu_B \leq \mu_D$ then $T_{norm}(\mu_A,\mu_B) \leq T_norm(\mu_C,\mu_D)$
- Commutativity: $T_{norm}(\mu_A,\mu_B) = T_{norm}(\mu_B,\mu_A)$
- Associativity: $T_{norm}(T_{norm}(\mu_A,\mu_B),\mu_C) = T_{norm}(\mu_A,T_{norm}(\mu_B,\mu_C))$

T-conform satisfies almost the same conditions:

- Boundary: $T_{conform}(1,1) = 1, T_{conform}(\mu,0) = T_{conform}(0,\mu) = \mu$
- Monotonicity:if $\mu_A \leq \mu_C$ and $\mu_B \leq \mu_D$ then $T_{conform}(\mu_A,\mu_B) \leq T_{conform}(\mu_C,\mu_D)$
- Commutativity: $T_{conform}(\mu_A,\mu_B) = T_{conform}(\mu_B,\mu_A)$
- Associativity: $T_{conform}(T_{conform}(\mu_A,\mu_B),\mu_C) = T_{conform}(\mu_A,T_{conform}(\mu_B,\mu_C))$

Membership Degree and Probability Membership degree and probability expose the imprecision by a number between 0 and 1. Membership degrees are special characteristics of the considered object. However probability is associated with the notion of occurrence. Chances to obtain the realization of the event depend on the value assigned to its probability.

Fuzzy logic process As it was exposed before, fuzzy logic uses the concept of partial membership which investigates the belonging of an element to a fuzzy set.

For this purpose, a fuzzy logic inference system has to be put in place, based on four components (see Figure C.2): Fuzzification, Rule inference Engine, Fuzzy rules, Defuzzification.

Fuzzification The first step in fuzzification process is to convert measured data into a set of fuzzy variables. This is done by assigning value to each membership function. To get the membership function, a projection operation is made from the input value on the membership function axis. Many membership functions exist such as triangular, trapezoidal, Gaussian or Bell function. Those are formulated as follows:

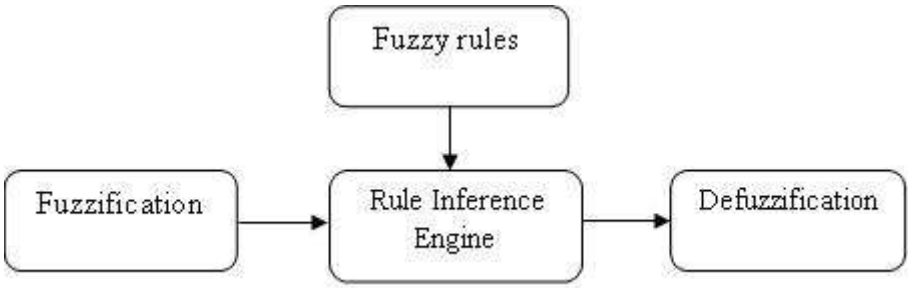

FIGURE C.2: Fuzzy inference system

$$Triangular(x,a,b,c) = \begin{cases} 0, & \text{if } x \leq a \\ \frac{x \quad a}{b \quad a}, & \text{if } a \leq x \leq b \\ \frac{c \quad x}{c \quad b}, & \text{if } b \leq x \leq c \\ 0, & \text{if } x \geq c \end{cases} \tag{C.12}$$

$$Trapezoidal(x,a,b,c) = \begin{cases} 0, & \text{if } x \leq a \\ \frac{x \quad a}{b \quad a}, & \text{if } a \leq x \leq b \\ 1, & \text{if } b \leq x \leq c \\ \frac{d \quad x}{d \quad c}, & \text{if } c \leq x \leq d \\ 0, & \text{if } x \geq d \end{cases} \tag{C.13}$$

$$Gaussian(x,m,\sigma) = e^{\frac{(x \quad m)^2}{2\sigma^2}} \tag{C.14}$$

$$Bell(x,a,b,c) = \frac{1}{1 + \| \frac{x \quad c}{a} \|^{2b}} \tag{C.15}$$

Other membership functions such as sigmoid and single functions are good candidates. Experimental results and type of data should indicate the best function to use.

Fuzzy rules After fuzzification, fuzzy inputs and outputs should be connected together through fuzzy rules. In human fuzzy reasoning, rules are expressed in the form of:

if x is A then y is B

Where x and y are fuzzy variables and A and B are fuzzy values defined by the fuzzy sets. The first part with x is A is called antecedent or premise while y is B is called the consequent or the conclusion. In fuzzy reasoning, there are many types of fuzzy reasoning but the most commonly used are:

• Mamdani: if x_1 is A_1 and... and x_p is A_p then y_1 is B_1 and... and y_p is B_p . Mamdani rule uses algebraic product and maximum as T-norm and S-norm respectively

• Takagi/Sugeno: if x_1 is A_1 and... and x_p is A_p then $y = b_0 + b_1x_1 + \ldots + b_px_p$. The rules aggregation is in fact the weighted sum of rules outputs.

Rules Inference Engine It's the process of formulating the correspondence between a given input and an output using fuzzy logic. This process involves membership functions, operators and rules. Many models are used but the commonly known are:

• Mamdani model: it consists of linguistic description in antecedent and conclusion. To describe the mapping from inputs $U_1 \times U_2 \times \ldots \times U_n$ to output W as follows: if x_1 is A_{i1} and... and x_n is A_{in} then y is $C_i,\ i = 1, \ldots, L$, where L is the number of fuzzy rules, x_i input variables and y is the output and C_i are linguistic variables or fuzzy sets.

• Takagi-Sugeno Model: this model is based on rules where antecedent was composed of linguistic variables and though the conclusion was represented by a function of the input variables. A typical rule in Sugeno fuzzy model has the following form: if input1 is x and input2 is y then Output is z=a.x+b.y+c input1 and input2 are the system inputs, a,b,c numerical constant parameters and x,y linguistic labels. It has to be mentioned that, the output level z of each rule is weighted by the firing strength W_i of the method. The relationship can be formulated as follows:

$$W_i = \text{ AndMethod}(F_1(Input1), F_2(Input2))$$

Where F_1 and F_2 are the membership functions for Input1 and Input2. The final output F_O is formulated as follows:

$$F_O = \frac{\sum_{i=1} nW_iz_i}{\sum_{i=1}^{n} W_i}$$

This inference is based on the interpolation of the entire relevant model. To be noted, the degree of relevance is determined by the degree of the input data belong to fuzzy subspace associated with the linear model.

Defuzzification This last step consists on building a fuzzy logic system by turning the fuzzy variables generated by rules into real world again to perform the needed action. Defuzzification methods are also of many varieties. But the most commonly used are:

$$Centroid of Area = \frac{\sum_{i=1}^{n} \mu_A(x_i) x_i}{\sum_{i=1}^{n} \mu_A(x_i)}$$

$$Bisector of Area = x_m; \sum_{i=1}^{M} \mu_A(x_i) = \sum_{j=M+1}^{n} \mu_A(x_j)$$

$$MeanOfMaximum = \frac{\sum_{i=1}^{N} x_i^*}{N}$$

$$SmallestOfMaximum = min(x_i^*)$$

$$LargestOfMaximum = max(x_i^*)$$

Where x_i^* (i=1,2,...,N) reach the maximal values of $\mu_A(x)$.

Fuzzy logic multi-modal data fusion approach Fuzzy fusion theory is a theoretical reasoning that deals with imperfect data. It evokes the notion of partial membership which enables imprecise reasoning [85]. A fuzzy set $F \subseteq X$ is defined by the membership function $\mu_f(x) \in [0,1], \forall x$. This makes fuzzy data fusion very efficient to avoid vagueness in sensory data. Fuzzy rules are divided into two categories: Conjunctive: it represents the standard intersection and product of two fuzzy sets

$$\mu_1^{\cap}(x) = min[\mu_{f_1}(x), \mu_{f_2}(x)] \forall x \in X$$

$$\mu_2^{\cap}(x) = \mu_{f_1}(x).\mu_{f_2}(x) \forall x \in X$$

Disjunctive: it represents the standard union and algebraic sum of two fuzzy sets

$$\mu_1^{\cup}(x) = max[\mu_{f_1}(x), \mu_{f_2}(x)] \forall x \in X$$

$$\mu_2^{\cup}(x) = \mu_{f_1}(x) + \mu_{f_2}(x) \quad \mu_{f_1}(x).\mu_{f_2}(x) \forall x \in X$$

Conjunctive fuzzy are appropriate when fusing data by reliable and homogeneous sources. Disjunctive fuzzy is appropriate when fusing data are highly conflicting. There have been some adaptive fuzzy rules developed as a compromise between those two categories. In contrast to probability and evidence theory, fuzzy sets theory is very well suited in the case that the class is not very well defined. As for probability theory, which requires prior knowledge of the distributions, fuzzy sets require prior knowledge of the membership functions for different fuzzy sets. This technique is very powerful in a way that it fuses data produced in a linguistic fashion.

Methodology Preparing a good methodology is very important. Fuzzy set theory offers a wide variety of operators in order to combine between inputs and outputs. This being said, there is no standard for interpreting fuzzy inference systems. Fuzzy sets offer the possibility to make all possible combinations. One of the most important steps is to build rules that take into consideration maximum combinations between inputs to account all possible situations. Normally, membership functions should be established according to the recommendations of the expert. In the case of the current project membership functions will be based on fatigue level and emotion detected from the fatigue block and emotion block. It must be defined such as parameters are easy to bear. For fuzzy rules construction, the decision should be made a priori again according to the expert recommendation. For example, in our case if fatigue level is the highest, this should mean that the system has to switch to autonomous mode. On important point, is that rules shouldn't be conflicting. Normally speaking, most of fuzzy inference aggregation models use Mamdani or Takagi-Sugeno ones. The output membership functions make the difference between the two approaches. The first model the output membership functions to be fuzzy sets while the second, considers linear or constant outputs.

C.3.4 Possibilistic fusion

Founded by Zadeh and extended by Dubois and Prade [86], it was originally based on fuzzy sets and was oriented to deal with incomplete rather than vague data. A possibility measure $\prod$ defined on a propositional language and valued on [0,1] and satisfies the following assumptions :

$$\prod(\bot) = 0 \text{ and } \prod(\top) = 1$$

$$\forall p, \forall q, \prod(p \vee q) = max(\prod(p), \prod(q))$$

$$if p is equivalent to q then \prod(p) = \prod(q)$$

Where $\perp$ and $\top$ are respectively the ever-false and the ever-true propositions. This means that p $\vee$ q is possible if one of p or q is, including the case when both are so. $\prod(p) = 1$ means that p is unsurprising but not that p is sure since $\prod(\bar{(}p)) = 1$ as well. But not the case when $\prod(p) = 0$ which implies that $\prod(\bar{(}p)) = 1.\prod(p \wedge q) \leq min(\prod(p), \prod(q))$ holds the general truth : while $p \wedge q$ is rather impossible, p and q may remain possible especially when the information is incomplete. A necessity measure is associated by duality with a possibility measure by:

$$\forall p, N(p) = 1 \quad \prod(\bar{(}p))$$

This could be explained as that p is more certain as $\bar{(}p)$ is impossible. It could be translated as follows:

$$\forall p, \forall, \prod(p \wedge q) = min(N(p), N(q))$$

This could mean that if we want to be certain about $p \wedge q$, we have to be so for both p and q. This means also that, by duality with respect to $\prod$, we have:

$$N(p \vee q) \geq max(N(p), N(q))$$

There are some conventions adopted in possibility theory presented in the following figure:

• N(p) = 1 means that, given the available knowledge, p is certainly true; conversely, if p is true, it can be considered as true

• $0 < N(p) < 1$ means that p is certain while $\bar{(}p)$ is not certain. $N(p) > 0$ is a tentative of acceptance of p, to a degree N(p)

• $\prod(p) = \prod(\bar{p}) = 1$ or $\prod(p) = \prod(\bar{p}) = 0$ is the case of total ignorance i.e. the available knowledge can't decide if p is true or false

• $0 < \prod(p) < 1$ or $0 < \prod(\bar{p}) < 1$ means that p is impossible or that $\bar{p}$ is certain

• $\prod(p)$ means that p is certainly false.

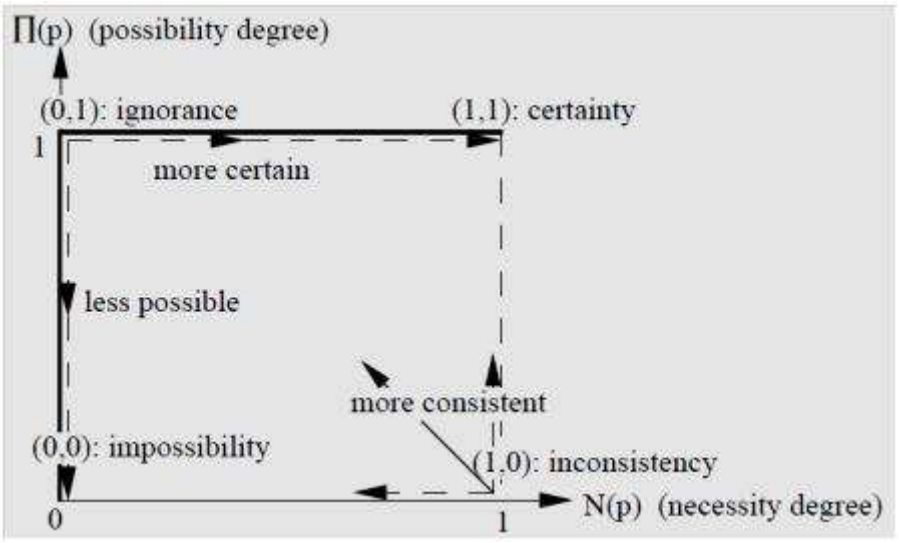

FIGURE C.3: Possibility theory conventions

$\prod$ is associated with a possibility distribution π valued between [0,1] which defines the set of interpretation of the language (if we have two propositions p and q, this means that we have four interpretations : p true and q true, p false and q true...). This is supposed to code the fuzzy set of the plausible interpretations. One can define the possibility measure as:

$$\prod(p) = max_{w \in [p]} \pi(w)$$

Where [p] are the interpretations that defines p as true or the so called the models of p. Possibility theory is a common framework which helps modeling uncertainty and imprecision in systems. In the same way, we can use finite ordered chain of levels of certainty ranging between 0 and 1 such as $\omega_1 = 0 < \omega_2 < \ldots < \omega_n = 1$ instead of using the whole interval [0, 1]. It has to be noted that min $(\omega_i, \omega_k) = \omega_i$ and $max(\omega_i, \omega_k) = \omega_k$ if $i \leq k$ and 1 $\omega_i = \omega_{(n+1\ i)}$.

C.4 Comparison of different theories

The use of many theories in data fusion reflects the importance of the latter in the scientific field. Each of these theories has its own characteristics. Probabilistic theory relies on probability distribution to represent data and fuses them using Bayesian framework. Evidential theory uses the probability mass and characterizes data using belief and plausibility. It fuses those using Dempster rules. For vague data representation,

fuzzy reasoning uses memberships and fuzzy rules. Finally for possibilistic theory, combines between probabilistic and evidential in data representation but uses fuzzy set for fusion. However each of these theories has its capabilities and weaknesses. Those are summarized in the table below:

TABLE C.1: Capacities and limitations of each fusion theory

Theory	Capacity	Weakness
Probabilistic	Very well understood Treats data uncertainty	Incapable of addressing other data imperfections
Evidential	Fuses uncertain and ambiguous data	Not efficient when data is imprecise or highly conflicting
Fuzzy reasoning	Efficient to treat vague data Uses human data labels	Limited only to vague data
Possibilistic	Handling incomplete data Efficient in poorly informed environment	Not very well understood by fusion community

C.5 conclusion

In order to apply a suited fusion technique, one has to formulate the data anomalies in a concise manner. In our case, the problem consists of detecting fatigue level using P300 and SSVEP. More precisely, after correlation study, only parameters (per sensor) the most correlated with fatigue level will be used later for individual classification i.e. each modality (P300 and SSVEP) will have its own classification block. Then, fusion technique will be adapted in order to enhance final decision in the case that the two blocks don't output the same decision. This being said, if we process by elimination, we can state that:

• Data issued from sensors are not perfect; this means that the use of probabilistic theory is not suitable. The latter is not capable to deal with this kind of imperfection,

• Data are complete as well as the environment is not poorly informed; this means that the use possibilitic theory is applicable but not efficient. What's more, the fact that possibilistic theory is not very well known by fusion community could make a disadvantage for us as our purpose is not to develop a new theory but to use it as a tool,

• The use of evidential and fuzzy sets theories could be the best choices for our context especially that two fusions cases are considered: the fusion of SSVEP and P300 blocks for fatigue detection, and the fusion of fatigue level with emotion detection block, in order to decide if the system should switch to manual, semi-autonomous or autonomous mode.

Bibliography

[1] Axel Lankenau and Thomas Röfer. Smart wheelchairs - state of the art in an emerging market. *KI*, 14(4):37–39, 2000. URL http://dblp.uni-trier.de/db/journals/ki/ki14.html#LankenauR00.

[2] E. Demeester, M. Nuttin, D. Vanhooydonck, and H. Van Brussel. A model-based, probabilistic framework for plan recognition in shared wheelchair control: experiments and evaluation. In *Intelligent Robots and Systems, 2003. (IROS 2003). Proceedings. 2003 IEEE/RSJ International Conference on*, volume 2, pages 1456–1461 vol.2, Oct 2003. doi: 10.1109/IROS.2003.1248849.

[3] Hendrik Koesling, Martin Zoellner, Lorenz Sichelschmidt, and Helge Ritter. With a flick of the eye: Assessing gaze-controlled human-computer interaction. In Helge Ritter, Gerhard Sagerer, Rüdiger Dillmann, and Martin Buss, editors, *Human Centered Robot Systems*, volume 6 of *Cognitive Systems Monographs*, pages 83–92. Springer Berlin Heidelberg, 2009. ISBN 978-3-642-10402-2. doi: 10.1007/978-3-642-10403-9_9. URL http://dx.doi.org/10.1007/978-3-642-10403-9_9.

[4] Päivi Majaranta and Kari jouko Räihä. Text entry by gaze: Utilizing eye-tracking, 2007.

[5] Dane Powell and Marcia K. O'Malley. The task-dependent efficacy of shared-control haptic guidance paradigms. *EEE Trans. Haptics*, 5(3):208–219, January 2012. ISSN 1939-1412. doi: 10.1109/TOH.2012.40. URL http://dx.doi.org/10.1109/TOH.2012.40.

[6] Emmanuel B. Vander Poorten, Eric Demeester, Alexander Hüntemann, Eli Reekmans, Johan Philips, and Joris De Schutter. Backwards maneuvering powered wheelchairs with haptic guidance. In *Proceedings of the 2012 International Conference on Haptics: Perception, Devices, Mobility, and Communication - Volume Part I*, EuroHaptics'12, pages 419–431, Berlin, Heidelberg, 2012. Springer-Verlag. ISBN 978-3-642-31400-1. doi: 10.1007/978-3-642-31401-8_38. URL http://dx.doi.org/10.1007/978-3-642-31401-8_38.

[7] C. Urdiales, E.J. Perez, G. Peinado, M. Fdez-Carmona, J.M. Peula, R. Annicchiarico, F. Sandoval, and C. Caltagirone. On the construction of a skill-based wheelchair navigation profile. *Neural Systems and Rehabilitation Engineering, IEEE Transactions on*, 21(6):917–927, Nov 2013. ISSN 1534-4320. doi: 10.1109/TNSRE.2013.2241454.

[8] Ming Ren and HassanA. Karimi. A fuzzy logic map matching for wheelchair navigation. *GPS Solutions*, 16(3):273–282, 2012. ISSN 1080-5370. doi: 10.1007/s10291-011-0229-5. URL http://dx.doi.org/10.1007/s10291-011-0229-5.

[9] Jean-Pierre Chevance. Existence et infirmité motrice cérébrale. *AFP Ecoute Infos*, 21:1–11, December 2007.

[10] Jun-Pyo Hong, Oh-Sang Kwon, Eung-Hyuk Lee, Byung-Soo Kim, and Seung-Hong Hong. Shared-control and force-reflection joystick algorithm for the door passing of mobile robot or powered wheelchair. In *TENCON 99. Proceedings of the IEEE Region 10 Conference*, volume 2, pages 1577–1580 vol.2, December 1999. doi: 10.1109/TENCON.1999.818739.

[11] Mohammed A. Quddus, Washington Y. Ochieng, and Robert B. Noland. Current map-matching algorithms for transport applications: State-of-the art and future research directions. *Transportation Research Part C: Emerging Technologies*, 15(5):312 – 328, 2007. ISSN 0968-090X. doi: http://dx.doi.org/10.1016/j.trc.2007.05.002. URL http://www.sciencedirect.com/science/article/pii/S0968090X07000265.

[12] Fernando Lopes da Silva Ernst Niedermeyer. *Électroencéphalographie: Principes de base, les applications cliniques, et les domaines connexes*. Lippincott Williams and Wilkins, 2004. ISBN 0-7817-5126-8 , 9780781751261.

[13] I. Scott MacKenzie and Kumiko Tanaka-Ishii. *Text Entry Systems: Mobility, Accessibility, Universality*. Morgan Kaufmann Publishers Inc., San Francisco, CA, USA, 2007. ISBN 0123735912, 9780080489797.

[14] Tansheng Li, Yoshitsugu Yasui, Qian Tian, and Noriyoshi Yamauchi. New methods and algorithms for analyzing human biological signals. In *Proceedings of the 1st WSEAS International Conference on Biomedical Electronics and Biomedical Informatics*, BEBI'08, pages 86–90, Stevens Point, Wisconsin, USA, 2008. World Scientific and Engineering Academy and Society (WSEAS). ISBN 978-960-6766-93-0. URL http://dl.acm.org/citation.cfm?id=1980983.1981001.

[15] Katie Crowley, Aidan Sliney, Ian Pitt, and Dave Murphy. Evaluating a brain-computer interface to categorise human emotional response. In *Proceedings of*

the 2010 10th IEEE International Conference on Advanced Learning Technologies, ICALT '10, pages 276–278, Washington, DC, USA, 2010. IEEE Computer Society. ISBN 978-0-7695-4055-9. doi: 10.1109/ICALT.2010.81. URL http://dx.doi.org/10.1109/ICALT.2010.81.

[16] Eija Haapalainen, SeungJun Kim, Jodi F. Forlizzi, and Anind K. Dey. Psychophysiological measures for assessing cognitive load. In *Proceedings of the 12th ACM International Conference on Ubiquitous Computing*, Ubicomp '10, pages 301–310, New York, NY, USA, 2010. ACM. ISBN 978-1-60558-843-8. doi: 10.1145/1864349.1864395. URL http://doi.acm.org/10.1145/1864349.1864395.

[17] Paulo Rogério de Almeida Ribeiro, Fabricio Lima Brasil, Matthias Witkowski, Farid Shiman, Christian Cipriani, Nicola Vitiello, Maria Chiara Carrozza, and Surjo Raphael Soekadar. Controlling assistive machines in paralysis using brain waves and other biosignals. *Adv. in Hum.-Comp. Int.*, 2013:3:3–3:3, January 2013. ISSN 1687-5893. doi: 10.1155/2013/369425. URL http://dx.doi.org/10.1155/2013/369425.

[18] B. Obermaier, C. Guger, C. Neuper, and G. Pfurtscheller. Hidden markov models for online classification of single trial eeg data. *Pattern Recogn. Lett.*, 22(12):1299–1309, October 2001. ISSN 0167-8655. doi: 10.1016/S0167-8655(01)00075-7. URL http://dx.doi.org/10.1016/S0167-8655(01)00075-7.

[19] Anton Nijholt, Brendan Z. Allison, and Rob J.K. Jacob. Brain-computer interaction: Can multimodality help? In *Proceedings of the 13th International Conference on Multimodal Interfaces*, ICMI '11, pages 35–40, New York, NY, USA, 2011. ACM. ISBN 978-1-4503-0641-6. doi: 10.1145/2070481.2070490. URL http://doi.acm.org/10.1145/2070481.2070490.

[20] Lance J. Myers and J. Hunter Downs. Parsimonious identification of physiological indices for monitoring cognitive fatigue. In *Proceedings of the 5th International Conference on Foundations of Augmented Cognition. Neuroergonomics and Operational Neuroscience: Held As Part of HCI International 2009*, FAC '09, pages 495–503, Berlin, Heidelberg, 2009. Springer-Verlag. ISBN 978-3-642-02811-3. doi: 10.1007/978-3-642-02812-0_58. URL http://dx.doi.org/10.1007/978-3-642-02812-0_58.

[21] Ling-Fu Meng, Chiu-Ping Lu, Bo-Wei Chen, and Ching-Horng Chen. Fatigue-induced reversed hemispheric plasticity during motor repetitions: A brain electrophysiological study. In *Proceedings of the 13 International Conference on Neural Information Processing - Volume Part I*, ICONIP'06, pages 65–71, Berlin,

Heidelberg, 2006. Springer-Verlag. ISBN 3-540-46479-4, 978-3-540-46479-2. doi: 10.1007/11893028_8. URL http://dx.doi.org/10.1007/11893028_8.

[22] Chong Zhang, Chongxun Zheng, Xiaomei Pei, and Xiaolin Yu. Estimating mental fatigue based on multichannel linear descriptors analysis. In *Proceedings of the 1st International Conference on Digital Human Modeling*, ICDHM'07, pages 521–529, Berlin, Heidelberg, 2007. Springer-Verlag. ISBN 978-3-540-73318-8. URL http://dl.acm.org/citation.cfm?id=1784074.1784136.

[23] Alessandro Crippa, Natasha M. Maurits, Monicque M. Lorist, and Jos B. T. M. Roerdink. Visual computing in biology and medicine: Graph averaging as a means to compare multichannel eeg coherence networks and its application to the study of mental fatigue and neurodegenerative disease. *Comput. Graph.*, 35(2):265–274, April 2011. ISSN 0097-8493. doi: 10.1016/j.cag.2010.12.008. URL http://dx.doi.org/10.1016/j.cag.2010.12.008.

[24] Matthew Schlesinger, Dima Amso, and Scott P. Johnson. The neural basis for visual selective attention in young infants: A computational account. *Adaptive Behavior - Animals, Animats, Software Agents, Robots, Adaptive Systems*, 15(2): 135–148, June 2007. ISSN 1059-7123. doi: 10.1177/1059712307078661. URL http://dx.doi.org/10.1177/1059712307078661.

[25] Árpád Csathó, Dimitri van der Linden, Gergely Darnai, and Jesper F. Hopstaken. The same-object benefit is influenced by time-on-task. *Journal of Cognitive Psychology*, 25(3):319–327, 2013. doi: 10.1080/20445911.2012.753875. URL http://dx.doi.org/10.1080/20445911.2012.753875.

[26] Manson Cheuk-Man Fong, James William Minett, Thierry Blu, and William Shi-Yuan Wang. Brain–computer interface (bci): Is it strictly necessary to use random sequences in visual spellers? In *Proceedings of the 10th Asia Pacific Conference on Computer Human Interaction*, APCHI '12, pages 109–118, New York, NY, USA, 2012. ACM. ISBN 978-1-4503-1496-1. doi: 10.1145/2350046.2350071. URL http://doi.acm.org/10.1145/2350046.2350071.

[27] Janir Nuno da Cruz, Chi Man Wong, and Feng Wan. An ssvep-based bci with adaptive time-window length. In *Proceedings of the 10th International Conference on Advances in Neural Networks - Volume Part II*, ISNN'13, pages 305–314, Berlin, Heidelberg, 2013. Springer-Verlag. ISBN 978-3-642-39067-8. doi: 10.1007/978-3-642-39068-5_38. URL http://dx.doi.org/10.1007/978-3-642-39068-5_38.

[28] Xiaorong Gao, Dingfeng Xu, Ming Cheng, and Shangkai Gao. A bci-based environmental controller for the motion-disabled. *Neural Systems and Rehabilitation*

Engineering, IEEE Transactions on, 11(2):137–140, June 2003. ISSN 1534-4320. doi: 10.1109/TNSRE.2003.814449.

[29] S.M.T. Muller, T.F. Bastos-Filho, and M. Sarcinelli-Filho. Using a ssvep-bci to command a robotic wheelchair. In *Industrial Electronics (ISIE), 2011 IEEE International Symposium on*, pages 957–962, June 2011. doi: 10.1109/ISIE.2011.5984288.

[30] Eleanor A Curran and Maria J Stokes. Learning to control brain activity: A review of the production and control of {EEG} components for driving brain–computer interface (bci) systems. *Brain and Cognition*, 51(3):326 – 336, 2003. ISSN 0278-2626. doi: http://dx.doi.org/10.1016/S0278-2626(03)00036-8. URL http://www.sciencedirect.com/science/article/pii/S0278262603000368.

[31] P. Badia, B. Myers, M. Boecker, J. Culpepper, and J.R. Harsh. Bright light effects on body temperature, alertness, {EEG} and behavior. *Physiology and Behavior*, 50(3):583 – 588, 1991. ISSN 0031-9384. doi: http://dx.doi.org/10.1016/0031-9384(91)90549-4. URL http://www.sciencedirect.com/science/article/pii/0031938491905494.

[32] Dennis J. McFarland, William A. Sarnacki, Theresa M. Vaughan, and Jonathan R. Wolpaw. Brain-computer interface (bci) operation: signal and noise during early training sessions. *Clinical Neurophysiology*, 116(1):56 – 62, 2005. ISSN 1388-2457. doi: http://dx.doi.org/10.1016/j.clinph.2004.07.004. URL http://www.sciencedirect.com/science/article/pii/S1388245704002664.

[33] A. Nijholt and D. Tan. Brain-computer interfacing for intelligent systems. *Intelligent Systems, IEEE*, 23(3):72–79, May 2008. ISSN 1541-1672. doi: 10.1109/MIS.2008.41.

[34] Léon G. Faber, Natasha M. Maurits, and Monicque M. Lorist. Mental fatigue affects visual selective attention. *PLoS ONE*, 7(10):e48073, 10 2012. doi: 10.1371/journal.pone.0048073. URL http://dx.doi.org/10.1371%2Fjournal.pone.0048073.

[35] Raquel Prado, Mike West, and Andrew Krystal. Multi-channel eeg analyses via dynamic regression models with time-varying lag/lead structure, 1999.

[36] Roman Rosipal and Leonard J. Trejo. Kernel partial least squares regression in reproducing kernel hilbert space. *J. Mach. Learn. Res.*, 2:97–123, March 2002. ISSN 1532-4435. URL http://dl.acm.org/citation.cfm?id=944790.944806.

[37] Cynthia Breazeal. Emotion and sociable humanoid robots. *Int. J. Hum.-Comput. Stud.*, 59(1-2):119–155, July 2003. ISSN 1071-5819. doi: 10.1016/S1071-5819(03)00018-1. URL http://dx.doi.org/10.1016/S1071-5819(03)00018-1.

[38] Eva Hudlicka. Guidelines for designing computational models of emotions. *Int. J. Synth. Emot.*, 2(1):26–79, January 2011. ISSN 1947-9093. doi: 10.4018/jse.2011010103. URL http://dx.doi.org/10.4018/jse.2011010103.

[39] Paul Ekman, Wallace V. Friesen, and Phoebe Ellsworth. *Emotion in the Human Face*. Oxford University Press, 1972. ISBN 0195155327. URL http://www.amazon.com/exec/obidos/redirect?tag=citeulike07-20&path=ASIN/0195155327.

[40] James A. Russell. A circumplex model of affect. *Journal of Personality and Social Psychology*, 39(6):1161–1178, December 1980. ISSN 0022-3514. doi: 10.1037/h0077714. URL http://dx.doi.org/10.1037/h0077714.

[41] A.A. Sozinov, S.J. Laukka, T. Tuominen, A. Siipo, M. Nopanen, and Yu.I. Alexandrov. Transfer of simple task learning is different in approach and withdrawal contexts. *Procedia - Social and Behavioral Sciences*, 69(0):449 – 457, 2012. ISSN 1877-0428. doi: http://dx.doi.org/10.1016/j.sbspro.2012.11.433. URL http://www.sciencedirect.com/science/article/pii/S1877042812054195. International Conference on Education and Educational Psychology (ICEEPSY 2012).

[42] R.W. Picard, E. Vyzas, and J. Healey. Toward machine emotional intelligence: analysis of affective physiological state. *Pattern Analysis and Machine Intelligence, IEEE Transactions on*, 23(10):1175–1191, Oct 2001. ISSN 0162-8828. doi: 10.1109/34.954607.

[43] ImenTayari Meftah, Nhan Thanh, and Chokri Amar. Emotion recognition using knn classification for user modeling and sharing of affect states. In Tingwen Huang, Zhigang Zeng, Chuandong Li, and ChiSing Leung, editors, *Neural Information Processing*, volume 7663 of *Lecture Notes in Computer Science*, pages 234–242. Springer Berlin Heidelberg, 2012. ISBN 978-3-642-34474-9. doi: 10.1007/978-3-642-34475-6_29. URL http://dx.doi.org/10.1007/978-3-642-34475-6_29.

[44] James J. Gross and Robert W. Levenson. Emotion elicitation using films. *Cognition and Emotion*, 9(1).

[45] CarlosA. Estrada, AliceM. Isen, and MarkJ. Young. Positive affect improves creative problem solving and influences reported source of practice satisfaction in physicians. *Motivation and Emotion*, 18(4):285–299, 1994. ISSN 0146-7239. doi: 10.1007/BF02856470. URL http://dx.doi.org/10.1007/BF02856470.

[46] Holly A. Yanco. A robotic wheelchair system: Indoor navigation and user interface. In *Lecture notes in Artificial Intelligence: Assistive Technology and Artificial Intelligence*, pages 256–268. Springer-Verlag, 1998.

[47] Wen-Chen Chen Chuang-Chien Chiu chern-sheng Lin, Chien-Wa HO and Mau-Shiun Yeh. Powered wheelchair controlled by eye-tracking system. *optica applicata*, XXXVI(2-3), 2006.

[48] Achim Wagner Meike Jipp Christian Bartolein and Essameddin Badreddin. Easing wheelchair control by gaze-based estimation of intended motion. July 2008.

[49] D. Puanhvuan and Y. Wongsawat. Semi-automatic p300-based brain-controlled wheelchair. In *Complex Medical Engineering (CME), 2012 ICME International Conference on*, pages 455–460, July 2012. doi: 10.1109/ICCME.2012.6275713.

[50] Maria M. Martins, Cristina P. Santos, Anselmo Frizera-Neto, and Ramón Ceres. Assistive mobility devices focusing on smart walkers: Classification and review. *Robotics and Autonomous Systems*, 60(4):548 – 562, 2012. ISSN 0921-8890. doi: http://dx.doi.org/10.1016/j.robot.2011.11.015. URL http://www.sciencedirect.com/science/article/pii/S0921889011002181.

[51] S.M.T. Muller, T.F. Bastos-Filho, and M. Sarcinelli-Filho. Using a ssvep-bci to command a robotic wheelchair. In *Industrial Electronics (ISIE), 2011 IEEE International Symposium on*, pages 957–962, June 2011. doi: 10.1109/ISIE.2011.5984288.

[52] AlfredL. Yarbus. Eye movements during perception of complex objects. In *Eye Movements and Vision*, pages 171–211. Springer US, 1967. ISBN 978-1-4899-5381-0. doi: 10.1007/978-1-4899-5379-7_8. URL http://dx.doi.org/10.1007/978-1-4899-5379-7_8.

[53] Roman Vilimek and ThorstenO. Zander. Bc(eye): Combining eye-gaze input with brain-computer interaction. In Constantine Stephanidis, editor, *Universal Access in Human-Computer Interaction. Intelligent and Ubiquitous Interaction Environments*, volume 5615 of *Lecture Notes in Computer Science*, pages 593–602. Springer Berlin Heidelberg, 2009. ISBN 978-3-642-02709-3. doi: 10.1007/978-3-642-02710-9_66. URL http://dx.doi.org/10.1007/978-3-642-02710-9_66.

[54] Daniel Queteschiner. Reality factory, 2012. URL http://www.realityfactory.info/cms/tutorials.html.

[55] J. Condry and S. Condry. Sex Differences: A Study of the Eye of the Beholder. *Child Development*, 47:812–819, 1976.

[56] G.G. Molina, T. Tsoneva, and A. Nijholt. Emotional brain-computer interfaces. In *Affective Computing and Intelligent Interaction and Workshops, 2009. ACII 2009. 3rd International Conference on*, pages 1–9, Sept 2009. doi: 10.1109/ACII.2009.5349478.

[57] L. F. Barrett and J. A. Russell. Independence and bipolarity in the structure of current affect. *Journal of Personality & Social Psychology*, 74(4):967–984, 1998. URL http://doi.apa.org/index.cfm?fuseaction=showUIDAbstract&uid=1998-01060-010.

[58] JeromeH. Friedman. On bias, variance, 0/1—loss, and the curse-of-dimensionality. *Data Mining and Knowledge Discovery*, 1(1):55–77, 1997. ISSN 1384-5810. doi: 10.1023/A:1009778005914. URL http://dx.doi.org/10.1023/A%3A1009778005914.

[59] Kenneth Jong. Learning with genetic algorithms: An overview. *Machine Learning*, 3(2-3):121–138, 1988. ISSN 0885-6125. doi: 10.1007/BF00113894. URL http://dx.doi.org/10.1007/BF00113894.

[60] S. Koelstra, C. Muhl, M. Soleymani, Jong-Seok Lee, A. Yazdani, T. Ebrahimi, T. Pun, A. Nijholt, and I. Patras. Deap: A database for emotion analysis ;using physiological signals. *Affective Computing, IEEE Transactions on*, 3(1):18–31, Jan 2012. ISSN 1949-3045. doi: 10.1109/T-AFFC.2011.15.

[61] Ronny Mardiyanto Kohei Arai. Method for Psychological Status Estimation by Gaze Location Monitoring Using Eye-Based Human- Computer Interaction. *International Journal of Advanced Computer Science and Applications(IJACSA)*, 4(3), 2013. URL http://ijacsa.thesai.org/.

[62] Vinod Sharma, Richard Simpson, Edmund Lopresti, and Mark Schmeler.

[63] ArthurP. Dempster. A generalization of bayesian inference. In RolandR. Yager and Liping Liu, editors, *Classic Works of the Dempster-Shafer Theory of Belief Functions*, volume 219 of *Studies in Fuzziness and Soft Computing*, pages 73–104. Springer Berlin Heidelberg, 2008. ISBN 978-3-540-25381-5. doi: 10.1007/978-3-540-44792-4_4. URL http://dx.doi.org/10.1007/978-3-540-44792-4_4.

[64] Jorge Arrubla, Irene Neuner, David Hahn, Frank Boers, and N. Jon Shah. Recording visual evoked potentials and auditory evoked p300 at 9.4t static magnetic field. *PLoS ONE*, 8(5):e62915, 05 2013. doi: 10.1371/journal.pone.0062915. URL http://dx.doi.org/10.1371%2Fjournal.pone.0062915.

[65] D.L. Schacter, D. T. Gilbert, and D. M. Wegner. *Psychology (2nd Edition)*. Worth, New York, 2011. URL http://www.amazon.com/Psychology-Daniel-L-Schacter/dp/1429237198/ref=sr_1_1?s=books&ie=UTF8&qid=1313937150&sr=1-1.

[66] Sarah-Jayne Blakemore. The developing social brain: Implications for education. *Neuron*, 65(6):744 – 747, 2010. ISSN 0896-6273. doi: http://dx.doi.org/10.1016/

j.neuron.2010.03.004. URL http://www.sciencedirect.com/science/article/pii/S089662731000173X.

[67] Nicole A. Lazar, Beatriz Luna, John A. Sweeney, and William F. Eddy. Combining brains: A survey of methods for statistical pooling of information. *NeuroImage*, 16(2):538 – 550, 2002. ISSN 1053-8119. doi: http://dx.doi.org/10.1006/nimg.2002.1107. URL http://www.sciencedirect.com/science/article/pii/S1053811902911079.

[68] Genaro Rebolledo-Mendez, Ian Dunwell, Erika Martínez-Mirón, María Dolores Vargas-Cerdán, Sara de Freitas, Fotis Liarokapis, and Alma Rosa García-Gaona. Assessing neurosky's usability to detect attention levels in an assessment exercise. In Julie A. Jacko, editor, *HCI (1)*, volume 5610 of *Lecture Notes in Computer Science*, pages 149–158. Springer, 2009. ISBN 978-3-642-02573-0. URL http://dblp.uni-trier.de/db/conf/hci/hci2009-1.html#Rebolledo-MendezDMVFLG09.

[69] C.K. Yuen. On the smoothed periodogram method for spectrum estimation. *Signal Processing*, 1(1):83 – 86, 1979. ISSN 0165-1684. doi: http://dx.doi.org/10.1016/0165-1684(79)90009-4. URL http://www.sciencedirect.com/science/article/pii/0165168479900094.

[70] Lawrence A. Klein. *Sensor and Data Fusion Concepts and Applications*. Society of Photo-Optical Instrumentation Engineers (SPIE), Bellingham, WA, USA, 2nd edition, 1999. ISBN 0819432318.

[71] D.L. Hall and J. Llinas. An introduction to multisensor data fusion. *Proceedings of the IEEE*, 85(1):6–23, Jan 1997. ISSN 0018-9219. doi: 10.1109/5.554205.

[72] F. E. White. Data Fusion Lexicon. Technical report, 1991.

[73] Belur V. Dasarathy. *Decision Fusion*. IEEE Computer Society Press, Los Alamitos, CA, USA, 1994. ISBN 0818644524.

[74] I. R. Goodman, Ronald P. Mahler, and Hung T. Nguyen. *Mathematics of Data Fusion*. Kluwer Academic Publishers, Norwell, MA, USA, 1997. ISBN 0792346742.

[75] Mieczyslaw M. Kokar, Jerzy A. Tomasik, and Jerzy Weyman. Formalizing classes of information fusion systems. *Information Fusion*, 5(3):189 – 202, 2004. ISSN 1566-2535. doi: http://dx.doi.org/10.1016/j.inffus.2003.11.001. URL http://www.sciencedirect.com/science/article/pii/S1566253503000939.

[76] Philippe Smets. Analyzing the combination of conflicting belief functions. *Information Fusion*, 8(4):387 – 412, 2007. ISSN 1566-2535. doi: http://dx.doi.org/10.1016/

j.inffus.2006.04.003. URL http://www.sciencedirect.com/science/article/pii/S1566253506000467.

[77] R. Joshi and A.C. Sanderson. Minimal representation multisensor fusion using differential evolution. In *Computational Intelligence in Robotics and Automation, 1997. CIRA'97., Proceedings., 1997 IEEE International Symposium on*, pages 266–273, Jul 1997.

[78] Hugh Durrant-Whyte and ThomasC. Henderson. Multisensor data fusion. In Bruno Siciliano and Oussama Khatib, editors, *Springer Handbook of Robotics*, pages 585–610. Springer Berlin Heidelberg, 2008. ISBN 978-3-540-23957-4. doi: 10.1007/978-3-540-30301-5_26. URL http://dx.doi.org/10.1007/978-3-540-30301-5_26.

[79] Didier Dubois and Henri Prade. Rough fuzzy sets and fuzzy rough sets*. *International Journal of General Systems*, 17(2-3):191–209, 1990. doi: 10.1080/03081079008935107. URL http://dx.doi.org/10.1080/03081079008935107.

[80] Arnaud Doucet, Nando De Freitas, and Neil Gordon, editors. *Sequential Monte Carlo methods in practice*. 2001. URL http://www.worldcatlibraries.org/wcpa/top3mset/839aaf32b6957a10a19afeb4da09e526.html.

[81] Bernd A. Berg. Introduction to markov chain monte carlo simulations and their statistical analysis, 2004. URL http://arxiv.org/abs/cond-mat/0410490.

[82] N. Metropolis and S. Ulam. The Monte Carlo Method. *Journal of the American Statistical Association*, 44(247):335–341, 1949. ISSN 01621459. doi: 10.2307/2280232.

[83] W.K. Hastings. *Biometrika*. ISSN 1464-3510. doi: 10.1093/biomet/57.1.97.

[84] Sushmita Mitra and Sankar K. Pal. Fuzzy sets in pattern recognition and machine intelligence. *Fuzzy Sets Syst.*, 156(3):381–386, December 2005. ISSN 0165-0114. doi: 10.1016/j.fss.2005.05.035. URL http://dx.doi.org/10.1016/j.fss.2005.05.035.

[85] D. Istrate, E. Castelli, M. Vacher, L. Besacier, and J.-F. Serignat. Information extraction from sound for medical telemonitoring. *Information Technology in Biomedicine, IEEE Transactions on*, 10(2):264–274, April 2006. ISSN 1089-7771. doi: 10.1109/TITB.2005.859889.

[86] Didier Dubois, Hélène Fargier, and Henri Prade. Possibility theory in constraint satisfaction problems: Handling priority, preference and uncertainty. *Applied Intelligence*, 6:287–309, 1996.

List of publications

Articles published in indexed journals

A brain and gaze-controlled wheelchair, Hachem A. Lamti, Mohamed Moncef Ben Khelifa, Philippe Gorce and Adel M. Alimi, Computer Methods in Biomechanics and Biomedical Engineering, 16(1): 128-129, 2013.

Emotion detection for wheelchair navigation enhancement, Hachem A. Lamti, Mohamed Moncef Ben Khelifa, Adel M. Alimi and Philippe Gorce, Robotica, In press

Effect of fatigue on SSVEP during virtual wheelchair navigation, Hachem A. Lamti, Mohamed Moncef Ben Khelifa, Adel M. Alimi and Philippe Gorce, Journal of Theoretical and Applied Information Technology, In press.

Book chapters

A Brain Eyes WHEELchair Interface for severely disabled people assistance, Hachem A. Lamti, Mohamed Moncef Ben Khelifa, Adel M. Alimi and Philippe Gorce, Everyday Technology for Independence and Care, Assistive Technology Research Series, 29:686 - 694, IOS Press Ebooks, 2011.

Articles published in international conferences

The command of a wheelchair using thoughts and gaze, Hachem A. Lamti, Mohamed Moncef Ben Khelifa, Philippe Gorce and Adel M. Alimi, published in Electrotechnical Conference (MELECON), 2012 16th IEEE Mediterranean, pages 161-166, march, 2012.

The use of brain and thought in service of handicap assistance: Wheelchair navigation, Hachem A. Lamti, Mohamed Moncef Ben Khelifa, Philippe Gorce and Adel M. Alimi, published in Individual and Collective Behaviors in Robotics (ICBR), 2013 International Conference on , pages 80-85, 15-17 Dec. 2013.